UNIVERSITAT DE BARCELONA

Department of Psychiatry and Clinical Psychobiology
School of Medicine, University of Barcelona

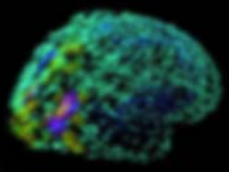

Neuroanatomical and neurofunctional brain basis of cognitive deficits in adolescent subjects who were born preterm. Structural and functional magnetic resonance study

Thesis presented by
Mónica Giménez Navarro,
to obtain the grade of Doctor by the University of Barcelona

Supervisor:
Dr. Carme Junqué i Plaja, University of Barcelona

Neurosciences Doctorate Program

Barcelona, july 2006

ELSEVIER

NeuroImage

www.elsevier.com/locate/ynimg
NeuroImage 23 (2004) 869–877

Hippocampal gray matter reduction associates with memory deficits in adolescents with history of prematurity

Mónica Giménez,[a] Carme Junqué,[a,*] Ana Narberhaus,[a] Xavier Caldú,[a] Pilar Salgado-Pineda,[a] Núria Bargalló,[b] Dolors Segarra,[a] and Francesc Botet[c]

[a]*Department of Psychiatry and Clinical Psychobiology, Institut d'Investigacions Biomèdiques August Pi i Sunyer (IDIBAPS), University of Barcelona, 08036, Barcelona, Spain*
[b]*Neuroradiology Section, Radiology Department, Centre de Diagnòstic per la Imatge (CDI), Hospital Clínic, Faculty of Medicine, University of Barcelona, 08036, Barcelona, Spain*
[c]*Pediatrics Section, Department of Obstetrics and Gynecology, Pediatrics, Radiology and Physics Medicine, Hospital Clínic, Casa Maternitat, 08028, Barcelona, Spain*

Received 15 December 2003; revised 30 June 2004; accepted 7 July 2004

Using optimized voxel-based morphometry (VBM), we compared the relationship between hippocampal and thalamic gray matter loss and memory impairment in 22 adolescents with history of prematurity (HP) and 22 normal controls. We observed significant differences between groups in verbal learning and verbal recognition, but not in visual memory. VBM analysis showed significant left hippocampal and bilateral thalamic reductions in HP subjects. Using stereological methods, we also observed a reduction in hippocampal volume, with left posterior predominance. We found correlations between left hippocampal gray matter reductions (assessed by VBM) and verbal memory (learning and percentage of memory loss) in the premature group. The stereological analysis showed a correlation between verbal learning and the left posterior hippocampus. Our results suggest that left hippocampal tissue loss may be responsible for memory impairment and is probably related to the learning disabilities that HP subjects present during schooling.

Keywords: Hippocampus; Memory deficits; Prematurity; Voxel-based morphometry

Introduction

Prematurity and very low birth weight are risk factors for brain abnormalities (Bhutta and Anand, 2001; Stewart et al., 1999; Ward and Beachy, 2003). The main MRI structural findings in prematurity that can be identified by visual inspection are ventricular enlargement (Cooke and Abernethy, 1999; Felderhoff-Mueser et al., 1999; Isaacs et al., 2000; Stewart et al., 1999), periventricular lucencies (Cooke and Abernethy, 1999; Inder et al., 2003; Krägeloh-Mann et al., 1999), and corpus callosum atrophy (Cooke and Abernethy, 1999; Santhouse et al., 2002; Stewart et al., 1999).

Brain volumetric studies are able to identify subtle changes that cannot be evaluated by the standard clinical radiological approach. In subjects with history of prematurity, decreased volumes have been described in the whole brain (Nosarti et al., 2002), cortical gray matter (Nosarti et al., 2002; Peterson et al., 2000), cerebellum (Peterson et al., 2000), basal ganglia (Abernethy et al., 2002; Peterson et al., 2000), and hippocampus (Isaacs et al., 2000, 2003; Peterson et al., 2000).

Neuropsychological studies of premature children have reported deficits in global intelligence, learning, attention, visuoperceptual memory, and frontal lobe functions (Anderson et al., 2003; Bhutta and Anand, 2001; Rushe et al., 2001). The relationship between neuropsychological deficits and their cerebral substrate is not always clear (Rushe et al., 2001). Patients with substantial MRI lesions that can be identified by visual inspection have cerebral palsy, mental retardation, and also attention and hyperactivity symptoms (Krägeloh-Mann et al., 1999). However, Rushe et al. (2001) were unable to relate MRI findings with cognitive status. They reported that premature children with and without MRI lesions did not differ in terms of long-term neuropsychological outcome.

Few studies have correlated volumetric MRI data and neuropsychological performance. Peterson et al. (2000) found strong correlations of regional gray matter with global intelligence quotient and several subtests of the Wechsler Intelligence Scale. Isaacs et al. (2000) found that decreased

* Corresponding author. Department of Psychiatry and Clinical Psychobiology, Institut d'Investigacions Biomèdiques August Pi i Sunyer (IDIBAPS), University of Barcelona, C/Casanova 143, 08036 Barcelona, Spain. Fax: +34 93 403 52 94.
E-mail address: cjunque@ub.edu (C. Junqué).
Available online on ScienceDirect (www.sciencedirect.com.)

1053-8119/$ - see front matter © 2004 Elsevier Inc. All rights reserved.
doi:10.1016/j.neuroimage.2004.07.029

hippocampal volume was related to everyday memory deficits.

Visual inspection and manual delineation of cerebral regions of interest inevitably reduce reproducibility due to intraobserver variations. In contrast, voxel-based morphometry (VBM) allows whole or regional brain analysis by comparing regional gray or white matter volumes using standardized *t* test models on a voxel-by-voxel basis. One of its major advantages is that data processing is almost completely user independent, and inter- and intraobserver variations are avoided. VBM has become an established instrument in morphometry and is the most appropriate tool for detecting differences in gray matter density of neuronal networks (Ashburner and Friston, 2001; Wilke et al., 2003).

Memory impairment is one of the most important cognitive deficits because in the immature brain it may be responsible for learning disabilities during schooling. We selected two brain structures, the hippocampus and thalamus, which have previously been found to be impaired in premature children and are clearly related to declarative learning (Squire and Knowlton, 1995; Squire and Zola, 1996).

To our knowledge, no previous studies have used VBM to analyze the possible structural correlates of memory deficits in a young sample of subjects with a history of prematurity.

Materials and methods

Subjects

The sample of subjects with history of prematurity (HP) composed 22 adolescents (8 girls and 14 boys). Gestational age ranged from 25 to 35 weeks (mean = 29.41, SD = 2.91). All 22 subjects had perinatal complications (anoxia, periventricular hemorrhage, or fetal suffering). Six subjects had low weight for their gestational age. The age at the time of neuropsychological and neuroimaging study ranged from 10 to 18 years (mean = 13.32, SD = 2.19). Five subjects were left handed. Exclusion criteria were history of focal traumatic brain injury, cerebral palsy, or neurological diagnosis and presence of global mental disabilities. We used the Wechsler Intelligence Scales to obtain an estimation of global intellectual functioning. Either the WAIS-III or the WISC-R was used, depending on the age of the subjects. The Full Intelligence Quotient (FIQ) of subjects with HP was 91.23 (SD = 16.14). All the subjects follow normal schooling. A normal gestation control group (11 girls and 11 boys; GA mean = 39.41, SD = 1.46; range from 36 to 42) were matched to HP subjects by age and handedness. The Full Intelligence Quotient (FIQ) of the control sample was 113.50 (SD = 12.41). The study was approved by the ethical committee of the University of Barcelona and a national research committee. All the subjects or their family gave written informed consent before participation in the study.

Memory assessment

To assess verbal memory function, we selected a modified version of the Rey Auditory Verbal Learning Test (RAVLT), a test with well-known sensitivity for declarative memory impairment (Lezak, 1995). The sum of the recall of the five 15-word list trials was taken as a measure of learning, and recognition was tested by asking the respondent to indicate which words from a set of 30 were from the 15-word list and which were not. Finally, verbal long-term retention (percentage of memory loss) was evaluated as the percentage of words lost after 20 min of interference. The formula used to create this variable was (presentation of trial 6 − presentation of trial 5/sum of words recalled across the five presentations × 100). This test is described in detail in Lezak (1995). We also evaluated visual memory with the classical Rey's (1941) Complex Figure Test. The Rey's Complex Figure Test was administered in two parts. First, subjects were asked to copy the figure on a blank piece of paper, which was the same size as the model. As each section was finished, the subject was handed a different colored pencil and a note was made of the color sequence. There was no time limit. Second, once the copy was finished, both the figure and the copy were removed from sight. A 3-min delay interval between copy and reproduction was established by a distraction task. After the 3 min, subjects were asked to draw the figure from memory onto a blank sheet of paper using a pencil with no color change. Participants were not forewarned of the task. We took the raw score of the reproduction as a measure of visual retention.

MRI acquisition and processing

Data were obtained during a experimental MRI examination routine on a GE Signa 1.5 T scanner (General Electric, Milwaukee, WI). A set of high-resolution T1-weighted images was acquired with an FSPGR 3d sequence (TR/TE = 12/5.2; TI 300 1 nex; FOV = 24 × 24 cm; 256 × 256 matrix); the whole-brain data were acquired in an axial plane yielding contiguous slices with slice thickness of 1 mm.

The original MR images were registered in DICOM format (one two-dimensional file per slice). MRI data were processed in a SUN workstation provided by Solaris 8. The two-dimensional DICOM files were organized into volumetric three-dimensional files of each brain by means of the ANALYZE 5.0 software (Biomedical Resource, Mayo Foundation, Rochester, MN); the images were saved in an ANALYZE 7.5 format, compatible with the SPM99 software (Statistical Parametric Mapping, Wellcome Department of Cognitive Neurology, University College London, UK).

VBM protocol (Good et al., 2001)

The automated image processing was done using SPM99, running in Matlab (MathWorks, Natick, MA). A single investigator performed the prior manual steps in image preparation (anterior–posterior commissure line determination and image reorienting).

An anatomical template was first created from the 44 subjects, so that each MRI was transformed into a standardized coordinate system. This was achieved by registering each of the images to the same template image (T1 SPM99 template) by minimizing the residual sum of squared differences between them (Ashburner and Friston, 2000). The normalized data were smoothed with an 8-mm full-width at half-maximum (FWHM) isotropic Gaussian kernel, and a mean image (the T1 template) was created. All the 44 structural images (in a native space) were then transformed to the same stereotactic space using the template created. The spatially normalized images were automatically partitioned into separate images representing probability maps for gray matter (GM), white matter (WM), and cerebrospinal fluid (CSF) using the combined pixel intensity and a priori knowledge approach integrated in

SPM99. The tissue classification method is exhaustively described in Ashburner and Friston (1997). The partitions were completed by the "lots of inhomogeneity correction" option (Ashburner and Friston, 2000). The normalized, segmented images were smoothed using an 8-mm FWHM isotropic Gaussian kernel. A separate gray matter template was created by averaging all the 44 smoothed normalized GM images.

All the original images (in a native space) were segmented into gray and white matter images, followed by a series of fully automated morphological operations for removing nonbrain voxels from the segmented images by the evaluated function:

$$\mathrm{GM}/(\mathrm{GM}+\mathrm{WM}+\mathrm{CSF})\times \quad \mathrm{BrainMask}$$

The GM images extracted were normalized to the GM template, preventing any contribution of nonbrain voxels and affording optimal spatial normalization of GM. But since the initial segmentation was performed on a nonnormalized image and since we applied probability maps that are designed for normalized images, the optimized (for GM) normalization parameters were reapplied to the original structural images. The results were normalized (by optimal normalization parameters). These images were then segmented into gray and white matter. The GM images were cleaned following the procedure described previously.

To compensate for the possible volume changes due to the spatial normalization procedure, the segmented images were modulated by the Jacobian determinants derived from the spatial normalization step. The analysis of modulated data tests for regional differences in gray matter volume, whereas analysis of unmodulated data tests for regional differences in concentration (density) of gray matter.

Stereology protocol

To provide complementary volumetric analysis in support of the VBM hippocampal results, we performed stereological measurements of this structure. Measures were carried out in a SUN workstation provided by Solaris 8, using ANALYZE 5.0 software. First, images were interpolated from 1.5 mm slices to 0.5 mm slices to achieve better resolution; a voxel size of 0.5 mm^3 was generated. Afterwards, images were aligned in accordance with the anterior commissure–posterior commissure orientation. The hippocampus volume was measured using a 7×7 mm^2 rigid grid with random starting position and angle of deviation from horizontal. The grid was superimposed on every third coronal slice. The coronal orientation was chosen to work with slices oriented perpendicular to the long axis of the hippocampus, a procedure reported to improve measurements (Sheline et al., 1996). The interslice increment and grid size chosen yielded a CE in the 0.01–0.03 range. The orthogonals tool provided by ANALYZE 5.0 makes it possible to view every grid point in three orthogonal views simultaneously, which helps to decide whether a point is contained by the measured structure or not. With stereology, we can exclude adjacent parahippocampal cortices. We obtained direct values from hippocampal volumes. To evaluate anterior–posterior volume differences in the hippocampus, we carried out a complementary analysis. We defined two hippocampal regions: the anterior and the caudal portions of hippocampus. Given the characteristics of stereological grid definition, we used an approximate, arbitrary division system of hippocampus. For each subject and each hippocampus, we defined the grid extension along the structure and we established a medial division depending on this grid extension; the grid size extension along the hippocampus ranged from 54 to 81 slices. All stereological measures were corrected by the intracranial volume (ICV).

Statistical analysis

The processed images for GM were analyzed using an SPM99 *t* test group comparison. Specifically, we performed two one-sided comparisons (patients > controls and patients < controls) in the GM study. Guided by previous studies and the VBM results, we focused the VBM analysis on possible hippocampal and thalamus changes; for this purpose, we used the WFU-Pickatlas toolbox software for SPM, version 1.02 (Joseph Maldjian, Functional MRI Laboratory, Wake Forest University School of Medicine). We created two ROIs that included (a) hippocampal and parahippocampal area and (b) thalamus, both bilaterally. We used the convention that group comparison results should survive at family-wise false-positive error (FWE)-corrected *P* value ($P < 0.05$). Only clusters larger than 15 contiguous voxels were considered in the analysis. With the use of FWE-corrected *P* value in SPM, thresholded maps are displayed in which the chance of a false-positive anywhere in the image is less than 0.05. Therefore, the threshold is useful for focussing on either strong effects or weak but consistent effects. The FWE value is the multiple comparison family-wise error type I error, which eliminates false-positives.

In addition, we report GM changes covariated for IQ, with the same statistical conventions presented above.

We also performed a "simple regression" (correlation) SPM99 analysis to evaluate the relationship between GM hippocampal and thalamus volume changes and different neuropsychological memory measures, separately for the patient and the control subjects. Again, results of these analyses were thresholded at FWE-corrected *P* value ($P < 0.05$), and only the clusters larger than 15 contiguous voxels were introduced into the statistical model.

Hippocampal volumes and memory performance in the two groups were compared by means of Student's *t* test using the SPSS 11.0 version. Pearson correlation analysis between memory measures and corrected stereological measures of hippocampus was also conducted.

Results

Memory performance

Results from RAVLT showed that the groups significantly differed in learning ($t = -2.429$; $P = 0.020$) and recognition ($t = -3.007$; $P = 0.005$). We also observed a trend towards statistical significance in percentage of verbal memory loss ($t = 1.925$; $P = 0.061$). In contrast, the groups did not differ in visual memory, as assessed by the Rey Complex Figure retention ($t = -1.208$; $P = 0.234$) (see Table 1).

VBM results

Hippocampal ROI analysis showed that local left gray matter volume was decreased in premature sample. In the contrast patients < controls, we obtained a corrected $P < 0.0001$ (see Table 2 and Fig. 1). With the reversed analysis (patients > controls), no gray matter volume decreases were observed.

Table 1
Memory performance

	Premature group (mean + SD)	Control group (mean + SD)	*t* tests (*P* value)
Rey Auditory Verbal Learning Test			
Learning	49.77 + 8.55	55.36 + 6.59	−2.429 (0.020)
Percentage of memory loss	14.46 + 4.12	12.41 + 2.80	1.925 (0.061)
Recognition	13.64 + 1.50	14.68 + 0.65	−3.007 (0.005)
Rey's Complex Figure			
Visual retention	21.73 + 6.84	24.00 + 5.58	−1.208 (0.234)

For the thalamus, we observed bilateral regional GM volume decreases in subjects with antecedents of prematurity in a region that involves the pulvinar nuclei (corrected $P < 0.0001$) (see Table 2 and Fig. 2).

To remove the possible effects of intelligence on memory performance, we performed an analysis of covariance. For the hippocampus, we also found a left hippocampal decrease in the premature sample (cluster size 528 mm^3; Talairach coordinate −33 −31−10; corrected $P = 0.023$). Thalamic ROIs, covariated for FIQ, showed regional GM volume decreases also bilaterally in HP subjects (right pulvinar nucleus: cluster size 1616 mm^3, Talairach Coordinate 9 −28 12, corrected $P < 0.0001$; left pulvinar nucleus: cluster size 440 mm^3, Talairach coordinate −9 −28 12, corrected $P = 0.012$).

GM correlations with memory performance

Hippocampal ROI analysis revealed a positive significant correlation between verbal learning and GM volume in a left hippocampal cluster (cluster size: 246 mm^3; Talairach coordinates −34 −15 −12; corrected $P = 0.001$) for the premature group (see Fig. 3).

We also observed a significant positive correlation between percentage of memory loss and GM volume loss in a left anterior hippocampal cluster (cluster size: 68 mm^3; Talairach coordinates −29 −12 −18; corrected $P = 0.033$) for the premature group (see Fig. 4); the greater the volume loss, the lower the level of long-term retention.

No other correlations were observed for memory measures between the HP group and controls; no significant correlation was obtained between GM volume and learning.

Thalamic ROI analysis revealed no significant correlations between any memory measures.

Table 2
VBM: gray matter volume decreases in hippocampus and thalamus by ROI analysis in premature sample compared to controls

	P (corrected)	Talairach coordinate (*x*,*y*,*z*)	Cluster size (mm^3)
Hippocampal ROIs			
Left hippocampus	<0.0001	−33 −30 −8	140
Thalamic ROIs			
Left thalamus (pulvinar nucleus)	<0.0001	−9 −28 10	518
Right thalamus (pulvinar nucleus)	<0.0001	13 −30 11	374

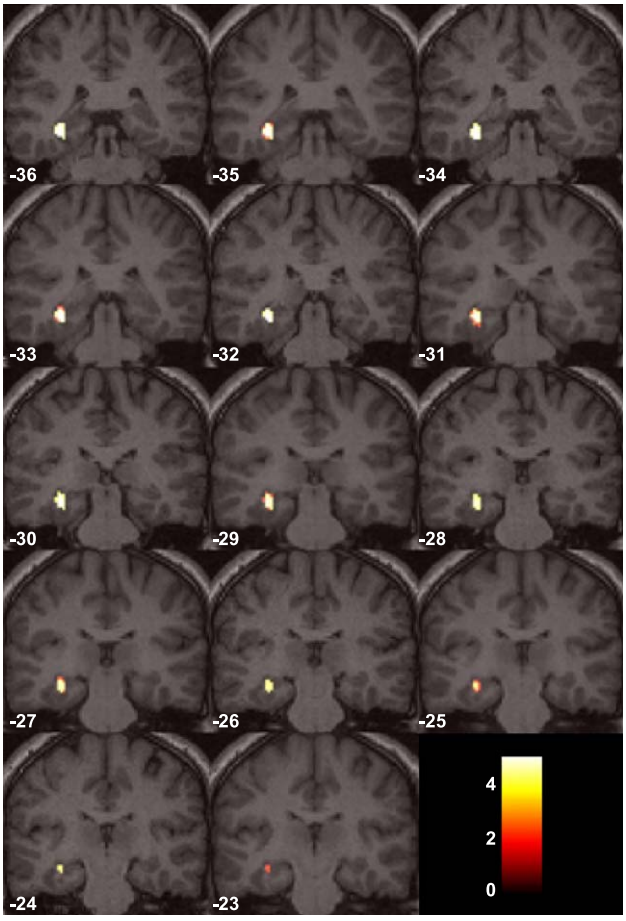

Fig. 1. Hippocampal ROIs showing gray matter loss in this area in premature sample compared to controls: Statistical parametric maps (SPMs) with left as left according to neurological convention (coronal view). ROI results are superimposed on a T1 standard control brain.

Hippocampal stereology

We estimated the left and right hippocampal volumes in premature and control groups. Both left and right hippocampus showed a significant volume loss in the premature group (direct values) compared to controls (left: $t = -5.034$, $P < 0.0001$; right: $t = -4.643$, $P < 0.0001$).

The whole brain volume of the premature sample differed from that of the controls (prematures mean: 1453934 mm^3, SD: 151422.06; controls mean: 1579708 mm^3, SD: 123160.36, $t = -3.030$, $P = 0.004$). After standardization of hippocampal direct values by ICV, only the left hippocampal volume presented a statistically significant loss ($t = -2.137$; $P = 0.038$). There was a trend towards significance in right hippocampus ($t = -1.839$; $P = 0.073$) (see Table 3).

Analyzing the anterior and posterior parts of hippocampus (direct values), we found significant differences between group for all the regions (left anterior hippocampus: $t = -3.924$, $P < 0.0001$; left posterior hippocampus: $t = -4.490$, $P < 0.0001$; right anterior hippocampus: $t = -3.794$, $P < 0.001$; right posterior hippocampus: $t = -4.224$, $P < 0.0001$). Corrected volumetric values by ICV showed that only the left posterior hippocampus achieved significance ($t = -2.230$; $P = 0.031$).

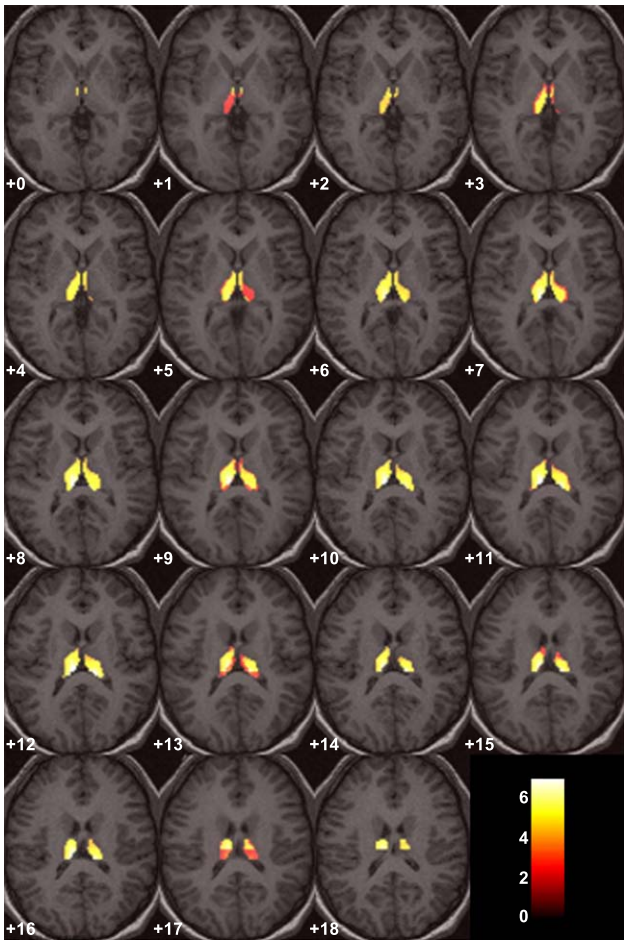

Fig. 2. Thalamic ROIs showing gray matter loss in this area in premature sample compared to controls: Statistical parametric maps (SPMs) with left as left according to neurological convention (axial view). ROI results are superimposed on a T1 standard control brain.

Pearson correlation analysis between memory measures and corrected stereological values (by ICV) showed a significant positive correlation in the premature sample between verbal learning and the left posterior hippocampus ($r = 0.428$; $P = 0.047$): The lower the volume, the lower the level of learning. No other correlations were observed for memory measures either in the premature group and/or in controls.

Discussion

This optimized VBM study found significantly lower gray matter levels in the premature sample than in controls in two brain regions: in the left hippocampus, and bilaterally in the thalamus. In addition, significant positive correlations between left hippocampal gray matter changes and verbal memory were found in premature subjects but not in controls.

To our knowledge, VBM has not been used before to investigate the possible role of the thalamus and hippocampal reductions in memory impairment in subjects with history of prematurity.

Like previous manual volumetric studies (Isaacs et al., 2000, 2003; Nosarti et al., 2002; Peterson et al., 2000), we observed hippocampal volume reductions in HP subjects, and the neuroimaging data were in agreement with neuropathological studies that clearly demonstrated the existence of necrotic processes in the hippocampus in preterm samples (Felderhoff-Mueser et al., 1999). Postmortem studies probably report the most complicated cases. Neuroimaging data investigating the long-term cerebral consequences of prematurity and their cognitive correlates are more clinically relevant because they can provide useful information on the basis of learning disabilities of children with history of prematurity and without clear neurological impairment or mental retardation.

Interestingly, we found the abnormalities to be bilateral, with left-sided predominance. Only the left hemisphere achieved

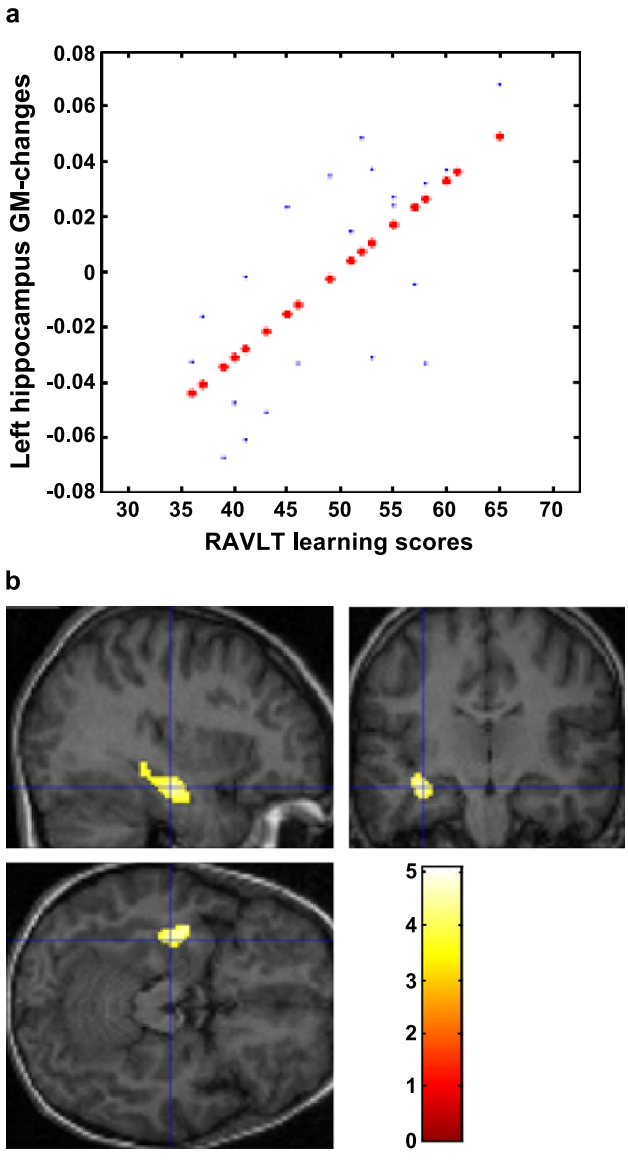

Fig. 3. Correlation between GM volume and verbal learning. Hippocampal ROI analysis: (a) Plot of hippocampal gray matter value against learning RAVLT measure in left hippocampus of premature group (red points: data adjusted to the theoretical model; blue points: real data). (b) Gray matter loss in premature sample. ROI results are superimposed on a T1 standard control brain. (For interpretation of the references to colour in this figure legend, the reader is referred to the web version of this article.)

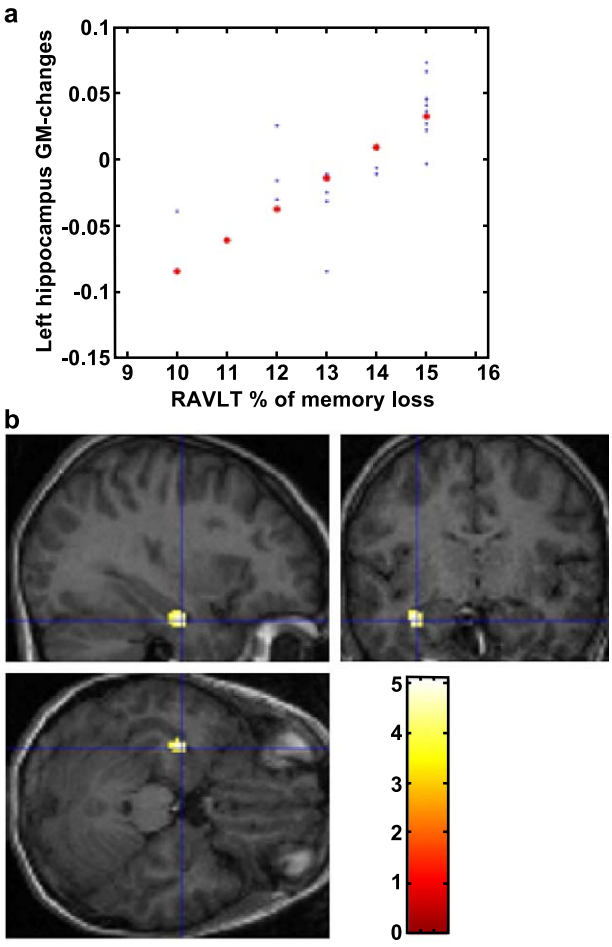

Fig. 4. Correlation between GM volume and percent of memory loss. Hippocampal ROI analysis: (a) Plot of hippocampal gray matter value against percent of memory loss. RAVLT measure in left hippocampus of premature group (red points: data adjusted to the theoretical model; blue points: real data). (b) Gray matter loss in premature sample. ROI results are superimposed on a T1 standard control brain. (For interpretation of the references to colour in this figure legend, the reader is referred to the web version of this article.)

significance at a corrected level of $P < 0.05$; the right hippocampus was significantly decreased at uncorrected $P < 0.001$ but lost significance after correction. The left predominance has also been observed in other conditions in which bilateral reductions would be expected. For example, in Alzheimer's disease and mild cognitive impairment, the E4 Apoe gene seems to be related to a greater reduction of the left hippocampus (Lehtovirta et al., 2000); and in the fetal alcoholic syndrome, white matter reduction is greater on the left side than on the right (Sowell et al., 2001). Two other studies of premature samples report the same trend (lower left hippocampal volume), though the results were not statistically significant (Isaacs et al., 2003; Peterson et al., 2000).

Our premature sample showed a significant global brain volume reduction (approximately about 8.0%) compared to controls. This finding agrees with previous studies. Nosarti et al. (2002) reported a 6.0% whole brain volume reduction in adolescents who were born very preterm. Despite this global cerebral reduction, the hippocampal atrophy remained significant after the intracranial volume correction.

Our study provides evidence of high consistency between the results obtained by VBM and stereological methods. Similar findings have been reported by Keller et al. (2002), studying the hippocampal atrophy in subjects with temporal lobe epilepsy. We found that both hippocampi were decreased using VBM and stereology. Moreover, stereological standardized values showed the same results as those obtained by P-corrected VBM values: a predominantly left-sided decrease. The agreement between techniques is also observed in the correlation analysis. With both data analyses, we observed a correlation between the left hippocampus and verbal learning, but VBM also showed a correlation between left hippocampus and percentage of memory loss (long-term retention).

The volumetric analysis by stereology allowed us to analyze a possible dissociation of anterior and posterior parts of hippocampus. After correcting hippocampus volume for whole brain size, we found a posterior predominance of atrophy, in which only the left hemisphere achieved significance. The predominance of damage in the posterior part can be related to the fact that CA1 field is located in this region and CA1 is very vulnerable to neurotoxic factors (Cavaglia et al., 2001). In a functional magnetic resonance study in normal subjects, Fernández et al. (1998) reported a positive correlation between recalled words and the left posterior hippocampus. Our results corroborate these findings, that is, that the left posterior hippocampus correlates with verbal memory impairment in premature subjects. The

Table 3
Stereological analysis: hippocampal volume in premature sample compared to controls

	Premature sample (mean; SD)	Control sample (mean; SD)	*t* test value (*P*)
Direct values			
Left hippocampus	2477.28 (366.78)	2972.57 (280.05)	−5.034 (<0.0001)
Right hippocampus	2525.73 (354.43)	2987.61 (303.45)	−4.643 (<0.0001)
Left anterior hippocampus	1396.50 (240.52)	1654.58 (193.17)	−3.924 (<0.0001)
Left posterior hippocampus	1080.78 (174.65)	1317.99 (175.81)	−4.490 (<0.0001)
Right anterior hippocampus	1420.72 (250.88)	1668.78 (176.40)	−3.794 (0.001)
Right posterior hippocampus	1105.01 (151.56)	1317.15 (180.34)	−4.224 (<0.0001)
Standardized values by intracranial volume × 100			
Left hippocampus	0.1721 (0.030)	0.1892 (0.023)	−2.137 (0.038)
Right hippocampus	0.1755 (0.030)	0.1899 (0.022)	−1.839 (0.073)
Left anterior hippocampus	0.0971 (0.020)	0.1052 (0.014)	−1.580 (0.122)
Left posterior hippocampus	0.0750 (0.013)	0.0840 (0.013)	−2.230 (0.031)
Right anterior hippocampus	0.0987 (0.019)	0.1061 (0.012)	−1.512 (0.139)
Right posterior hippocampus	0.0768 (0.013)	0.0837 (0.012)	−1.785 (0.081)

reduction of this region leads to lower efficiency in recalling words. However, we did not find this correlation in normal subjects.

In addition to the left hippocampal reduction, we also observed a bilateral gray matter loss in the thalamus. No studies to date have provided quantitative volumetric data of this structure in subjects with history of prematurity, but visual inspection of abnormal MRI findings showed thalamic atrophy associated with severe periventricular lesions (Krägeloh-Mann et al., 1999). In addition, the histopathological study by Felderhoff-Mueser et al. (1999) noted histological abnormalities in basal ganglia and thalami that were not associated with visually abnormal MRI in a small preterm sample.

As regards the neuropsychological findings and in agreement with the hippocampal left predominance, our HP sample showed a verbal learning impairment, with preserved visual memory. These verbal–visual discrepancies were also obtained in the sample of Isaacs et al. (2003). In the RAVLT, we did not observe a dissociation between verbal recall and recognition. This dissociation has previously been reported in amnesic subjects due to hypoxic ischemic encephalopathy and is a characteristic of the syndrome of developmental amnesia (Düzel et al., 2001; Vargha-Khadem et al., 2001).

We observed a selective correlation of verbal memory with hippocampal atrophy in the HP sample but not in controls. Indeed, we found a positive correlation between GM hippocampal changes and two memory scores (learning and percentage of memory loss), and this correlation was only significant in the left hemisphere in the premature sample. Isaacs et al. (2000) reported verbal memory dysfunctions accompanied by bilateral hippocampal atrophy, but they did not find a brain–behavior correlation.

Though the thalamus is a part of the neural memory circuitry involved in memory functions (Van der Werf et al., 2003a,b), we did not find significant correlations between this structure and any memory measure. The group comparison showed a clear bilateral gray matter loss in our sample, but this was unrelated to memory deficits. Probably our negative results in the correlations are due to the particular region of the thalamus that demonstrated a GM volume loss. We observed reductions in the region that corresponds mainly to the pulvinar nucleus, and the anterior and dorsomedial thalamic nuclei are the thalamic regions involved in memory functions (Parent and Carpenter, 1996). The pulvinar nucleus is a region of the thalamus that is related to attentional and visuospatial functions and projects to the occipital region (Parent and Carpenter, 1996).

Our study has some limitations. One is implicit in the VBM procedures; though the algorithms in SPM are considered robust, this software was not initially designed to evaluate structural abnormalities, and so imperfect registration may lead to inaccuracy (Bookstein, 2001). We addressed this problem by using an optimized version of the VBM, creating a common customized template for both premature and control samples (Good et al., 2001; Karas et al., 2003; Toga and Thompson, 2001). Though the authors or designers of SPM recommended the creation of a single template combining both patient and control subjects, we cannot ignore the probable deformations in the normalized common template that may have affected individual control normalizations. To evaluate gray matter changes, we used the modulation by the Jacobian determinants derived from spatial normalization. This procedure attempts to correct for the effects of volume changes, but it cannot be considered a direct measure of regional volumes and the results should be interpreted with caution. Recent approaches to the correct use of an optimized VBM protocol consider the importance of complementary volumetric measures by volume definitions based on automatic labeling parcellation procedures (Tzourio-Mazoyer et al., 2002), which can provide guidance for human investigator (Wilke et al., 2001). Moreover, we cannot avoid the fact that spatial normalization of pediatric brains is influenced by standard adult references. This optimized VBM protocol uses a prior SPM T1 image in the first stage (with adult references). To minimize the problems arising from this stage, we created a customized template as well as a prior map for our complete sample (Ashburner and Friston, 1997; Good et al., 2001). We conducted the entire first normalization subject by subject, ensuring that all subjects were well adapted to the T1 template, minimizing the contribution of nonbrain and nongray matter tissue to spatial normalization and segmentation.

The proportion of left-handedness in our sample of premature subjects was higher than normal. Previous studies in premature samples have also found high numbers of left handers (Marlow et al., 1989; O'Callaghan et al., 1993a). For example, Marlow's study reported a large sample (240 subjects) similar to ours (subjects without major neurological impairment) with a left-handedness percentage of about 27%. In our sample, 22% of the children were left handed. The reason for this high proportion is unknown, though O'Callaghan et al. (1993b) suggested that brain injury could be considered as a mechanism that increases left hand preference. A possible role of cerebral lesions has been suggested for "pathological left handedness" (Carlsson et al., 1992; Soper and

Satz, 1984), but our MRI data showed that none of the premature subjects had a cortical injury that could explain a hand preference change.

In summary, the present study provides evidence of left hippocampal and bilateral thalamic gray matter reductions. The posterior region of the hippocampus was more atrophic than the anterior one. The left hippocampal gray matter loss involved poor verbal memory. These impaired regions may be related to learning disabilities in subjects with antecedents of prematurity.

Acknowledgments

This study was supported by grants SAF2002-00836 (Ministerio de Ciencia y Tecnología), 2001SGR 00139 (Generalitat de Catalunya), a 2003F100191 (Generalitat de Catalunya) to X. Caldú, a research grant from the University of Barcelona to A. Narberhaus, and the grant AP2002-0737 (Ministerio de Educación, Cultura y Deporte) to M. Giménez. The assistance of Dr. Carles Falcón during data analysis is gratefully acknowledged.

References

Abernethy, L.J., Palaniappan, M., Cooke, R.W.I., 2002. Quantitative magnetic resonance imaging of the brain in survivors of very low birth weight. Arch. Dis. Child. 87, 279–283.

Anderson, P., Doyle, L.W., The Victorian Infant Collaborative Study Group, 2003. Neurobehavioral outcomes of school-age children born extremely low birth weight or very preterm in the 1990s. J. Am. Med. Assoc. 289, 3264–3272.

Ashburner, J., Friston, K.J., 1997. Multimodal image coregistration and partitioning. A unified framework. NeuroImage 6, 209–217.

Ashburner, J., Friston, K.J., 2000. Voxel-based morphometry—The methods. NeuroImage 11, 805–821.

Ashburner, J., Friston, K.J., 2001. Why voxel-based morphometry should be used. NeuroImage 14, 1238–1243.

Bhutta, A.T., Anand, K.J.S., 2001. Abnormal cognition and behaviour in preterm neonates linked to smaller brain volumes. Trends Neurosci. 24, 129–130.

Bookstein, F.L., 2001. Voxel-based morphometry should not be used with imperfectly registered images. NeuroImage 14, 1454–1462.

Carlsson, G., Hugdahl, K., Uvebrant, P., Wiklund, L.M., von Wendt, L., 1992. Pathological left-handedness revisited: dichotic listening in children with left vs. right congenital hemiplegia. Neuropsychologia 30, 471–481.

Cavaglia, M., Dombrowski, S.M., Drazba, J., Vasanji, A., Bokesch, P.M., Janigro, D., 2001. Regional variation in brain capillary density and vascular response to ischemia. Brain Res. 910, 81–93.

Cooke, R.W.I., Abernethy, L.J., 1999. Cranial magnetic resonance imaging and school performance in very low birth weight infants in adolescence. Arch. Dis. Child., Fetal Neonatal 81, F116–F121.

Düzel, E., Vargha-Khadem, F., Heinze, H.J., Mishkin, M., 2001. Brain activity evidence for recognition without recollection after early hippocampal damage. Proc. Natl. Acad. Sci. 98, 8101–8106.

Felderhoff-Mueser, U., Rutherford, M.A., Squier, W.V., Cox, P., Maalouf, E.F., Counsell, S.J., Bydder, G.M., Edwards, A.D., 1999. Relationship between MR imaging and histopathologic findings of the brain in extremely sick preterm infants. Am. J. Neuroradiol. 20, 1349–1357.

Fernández, G., Weyerts, H., Scheader-Bölsche, M., Tendolkar, I., Smid, H., Tempelmann, C., Hinrichs, H., Scheich, H., Elger, C.E., Mangun, G.R., Heinze, H.J., 1998. Successful verbal encoding into episodic memory engages the posterior hippocampus: a parametrically analyzed functional magnetic resonance imaging study. J. Neurosci. 18, 1841–1847.

Good, C.D., Johnsrude, I.S., Ashburner, J., Henson, R.N.A., Friston, K.L., Frackowiak, S.J., 2001. A voxel-based morphometric study of ageing in 465 normal adult human brains. NeuroImage 14, 21–36.

Inder, T.E., Anderson, N.J., Spencer, C., Wells, S., Volpe, J.J., 2003. White matter injury in the premature infant: a comparison between serial cranial sonographic and MR findings at term. Am. J. Neuroradiol. 24, 805–809.

Isaacs, E.B., Lucas, A., Chong, W.K., Word, S.J., Johnson, C.L., Marshall, C., Vargha-Khadem, F., Gadian, D.G., 2000. Hippocampal volume and everyday memory in children of very low birth weight. Pediatr. Res. 47, 713–720.

Isaacs, E.B., Vargha-Khadem, F., Watkins, K.E., Lucas, A., Mishkin, M., Gadian, D.G., 2003. Developmental amnesia and its relationship to degree of hippocampal atrophy. Proc. Natl. Acad. Sci. 100, 13060–13063.

Karas, G.B., Burton, E.J., Rombouts, S.A.R.B., van Schijndek, R.A., O'Brien, J.T., Scheltens, P., McKeith, I.G., Williams, D., Ballard, C., Barkhof, F., 2003. A comprehensive study of gray matter loss in patients with Alzheimer's disease using optimized voxel-based morphometry. NeuroImage 18, 895–907.

Keller, S.S., Mackay, C.E., Barrick, T.R., Wieshmann, U.C., Howard, M.A., Roberts, N., 2002. Voxel-based morphometric comparison of hippocampal and extrahippocampal abnormalities in patients with left and right hippocampal atrophy. NeuroImage 16, 23–31.

Krägeloh-Mann, I., Toft, P., Lunding, J., Andresen, J., Pryds, O., Lou, H.C., 1999. Brain lesions in preterms: origin, consequences and compensation. Acta Paediatr. 88, 897–908.

Lehtovirta, M., Laakso, M.P., Frisoni, G.B., Soininen, H., 2000. How does the apolipoprotein E genotype modulate the brain in aging and in Alzheimer's disease? A review of neuroimaging studies. Neurobiol. Aging 21, 293–300.

Lezak, M.D. (Ed.), 1995. Neuropsychological Assessment. Oxford Univ. Press, New York.

Marlow, N., Roberts, B.L., Cooke, R.W., 1989. Laterality and prematurity. Arch. Dis. Child. 64, 1713–1716.

Nosarti, C., Al-Asady, M., Frangou, S., Stewart, A., Rifkin, L., Murray, R., 2002. Adolescents who were born very preterm have decreased brain volumes. Brain 125, 1616–1623.

O'Callaghan, M.J., Burn, Y.R., Mohay, H.A., Rogers, Y., Tudehope, D.I., 1993a. The prevalence and origins of left hand preference in high risk infants, and its implications for intellectual, motor and behavioural performance at four and six years. Cortex 29, 617–627.

O'Callaghan, M.J., Burn, Y.R., Mohay, H.A., Rogers, Y., Tudehope, D.I., 1993b. Handedness in extremely low birth weight infants: aetiology and relationship to intellectual abilities, motor performance and behaviour at four and six years. Cortex 29, 629–637.

Parent, A., Carpenter, M.B. (Eds.), 1996. Carpenter's Human Neuroanatomy. Williams and Wilkins, Baltimore.

Peterson, B.S., Vohr, B., Staib, L.H., Cannistraci, C.J., Dolberg, A., Schneider, K.C., Katz, K.H., Westerveld, M., Sparrow, S., Anderson, A., Duncan, C., Makuch, R.W., Gore, J., Ment, L.R., 2000. Regional brain volume abnormalities and long-term cognitive outcome in preterm infants. J. Am. Med. Assoc. 284, 1939–1947.

Rey, A., 1941. L'examen psychologique dans les casd'encéphalopathie traumatique. Arch. Psychol. 28, 286–340.

Rushe, T.M., Rifkin, L., Stewart, A.L., Townsend, J.P., Roth, S.C., Wyatt, J.S.W., Murria, R.M., 2001. Neuropsychological outcome at adolescence of very preterm birth and its relation to brain structure. Dev. Med. Child Neurol. 43, 226–233.

Santhouse, A.M., Ffytche, D.H., Howard, R.J., Wiliams, S.C.R., Stewart, A.L., Rooney, M., Wyatt, J.S., Rifkin, L., Murray, R.M., 2002. The functional significance of perinatal corpus callosum damage: an fMRI study in young adults. Brain 125, 1782–1792.

Sheline, Y.I., Wang, P.W., Gado, M.H., Csernansky, J.G., Vannier, M.W., 1996. Hippocampal atrophy in recurrent major depression. Proc. Natl. Acad. Sci. 93, 3908–3913.

Soper, H.V., Satz, P., 1984. Pathological left-handedness and ambiguous handedness: a new explanatory model. Neuropsychologia 22, 511–515.

Sowell, E.R., Thompson, P.M., Mattson, S.N., Tessner, K.D., Jernigan, T.J., Riley, E.P., Toga, A.W., 2001. Voxel-based morphometric analyses of the brain in children and adolescents prenatally exposed to alcohol. NeuroReport 12, 515–523.

Squire, L.R., Knowlton, B.J., 1995. Learning about categories in the absence of memory. Proc. Natl. Acad. Sci. 92, 12470–12474.

Squire, L.R., Zola, S.M., 1996. Structure and function of declarative and nondeclarative memory systems. Proc. Natl. Acad. Sci. 93, 13515–13522.

Stewart, A.L., Rifkin, L., Amess, P.N., Kirkbride, V., Townsend, J.P., Miller, S.W., Kingsley, D.P.E., Moseley, I.F., Foster, O., Murray, R.M., 1999. Brain structure and neurocognitive and behavioural function in adolescents who were born very preterm. Lancet 353, 1653–1657.

Toga, A.W., Thompson, P.M., 2001. The role of image registration in brain mapping. Image Vis. Comput. 19, 3–24.

Tzourio-Mazoyer, N., Landeau, B., Papathanassiou, D., Crivello, F., Etard, O., Delcroix, N., Mazoyer, B., Joliot, M., 2002. Automated anatomical labeling of activations in SPM using a macroscopic anatomical parcellation of the MNI MRI single-subject brain. NeuroImage 15, 273–289.

Van der Werf, Y.D., Jolles, J., Witter, M.P., Uylings, H.B., 2003a. Contributions of thalamic nuclei to declarative memory functioning. Cortex 39, 1047–1062.

Van der Werf, Y.D., Scheltens, P., Lindeboom, J., Witter, M.P., Uylings, H.B., Jolles, J., 2003b. Deficits of memory, executive functioning and attention following infarction in the thalamus; a study of 22 cases with localised lesions. Neuropsychologia 41, 1330–1344.

Vargha-Khadem, F., Gadian, D.G., Mishkin, M., 2001. Dissociation in cognitive memory: the syndrome of developmental amnesia. Philos. Trans. R. Soc. Lond., B Biol. 356, 1435–1440.

Ward, R.M., Beachy, J.C., 2003. Neonatal complications following preterm birth. Br. J. Obstet. Gynaecol. 110, 8–16.

Wilke, M., Kaufmann, C., Grabner, A., Pütz, B., Wetter, T.C., Auer, D.P., 2001. Gray matter-changes and correlates of disease severity in schizophrenia: a statistical parametric mapping study. NeuroImage 13, 814–824.

Wilke, M., Kassubeck, J., Ziyeh, S., Schulze-Bonhage, A., Huppertz, H.J., 2003. Automated detection of gray matter malformations using optimized voxel-based morphometry: a systematic approach. NeuroImage 20, 330–343.

Correlations of thalamic reductions with verbal fluency impairment in those born prematurely

Mónica Giménez[a,d], Carme Junqué[a,d], Ana Narberhaus[a], Francesc Botet[b,d], Núria Bargalló[c] and Josep Maria Mercader[c,d]

[a]Department of Psychiatry and Clinical Psychobiology, [b]Pediatrics Section, Department of Obstetrics & Gynecology, Pediatrics, Radiology and Physics Medicine, [c]Neuroradiology Section, Radiology Department, Centre de Diagnòstic per la Imatge (CDI), Hospital Clínic, Faculty of Medicine, University of Barcelona and [d]Institute of Biomedical Research August Pi i Sunyer (IDIBAPS), Barcelona, Spain

Correspondence and requests for reprints to Dr Carme Junqué, Department of Psychiatry and Clinical Psychobiology, University of Barcelona, Institut d'Investigacions Biomèdiques August Pi i Sunyer (IDIBAPS), C/Casanova, 143, CP 08036 Barcelona, Spain
Tel: +34 93 403 44 46; fax: +34 93 403 52 94; e-mail: cjunque@ub.edu

Sponsorship: This study was supported by grants SAF2002-00836 (Ministerio de Ciencia y Tecnología), 2001SGR 00139 (Generalitat de Catalunya), the grant 2005FIR 00095 (Generalitat de Catalunya) to A. Narberhaus and the grant AP2002-0737 (Ministerio de Educación, Cultura y Deporte) to M. Giménez.

Received 19 January 2006; accepted 27 January 2006

Prematurity is associated with reduced brain volume, and the thalamus is among the structures most affected. We used a voxel-based morphometry analysis of gray matter to map regional atrophy in the thalamus in a sample of 30 adolescents with antecedents of very preterm birth. The preterm sample was compared with 30 controls matched by age, sex, handedness and sociocultural status. Individuals with very preterm birth differed from controls in several thalamic nuclei, and semantic and phonetic fluency showed different correlation patterns with brain volume. Semantic fluency achieved significant correlations with more thalamic nuclei than phonetic fluency. These results agree with functional magnetic resonance imaging studies showing that semantic fluency involves more cerebral regions than phonetic fluency. *NeuroReport* 17:463–466 © 2006 Lippincott Williams & Wilkins.

Keywords: prematurity, thalamus, verbal fluency

Introduction

Preterm birth and very low birth weight are risk factors for brain and behavior abnormalities [1–3]. An earlier voxel-based morphometry study by our group showed bilateral volume reductions in the hippocampus and thalamus in a sample of adolescents with antecedents of prematurity, and that memory impairment correlated with hippocampal but not thalamic reductions [4].

In addition to memory deficits, preterm individuals have language, attentional and frontal lobe dysfunctions [5–9]. Impairment of verbal fluency is a frequent sequelae of thalamic lesions [10–12]; in normal individuals, the thalamus is activated during verbal fluency [13,14]. To our knowledge, only one study has evaluated this verbal ability in preterm samples in relationship with corpus callosum thinning [15], finding that verbal fluency presented significant correlations with the mid-sagittal callosal area and with the size of the posterior corpus callosum quarter.

Our purpose was to map possible volume reductions in regions of the thalamus and to investigate the relationship between volumetric changes in different thalamic nuclei and verbal fluency in a sample with very preterm birth antecedents.

Methods

Study participants

The sample comprised 30 adolescents (15 girls and 15 boys; mean age=14.3+2.0 years) with very preterm birth (<33 weeks of gestation; mean gestational age=29.1+2.0 weeks) and very low birth weight (<1500 g, mean gestational weight=1107.8+240.3 g) antecedents. Exclusion criteria for participants were (1) history of focal traumatic brain injury, (2) cerebral palsy or neurological diagnosis and (3) presence of global mental disabilities. Six participants were left handed. A control group was matched to preterm participants by age (mean age=14.1+2.0 years), sex, handedness and sociocultural status. All the participants were in normal schooling. The study was approved by the Ethics Committee of the University of Barcelona, and all the participants or their families gave written informed consent.

Neuropsychological assessment

Verbal fluency was evaluated using two tasks: (1) a phonetic fluency task comprising a modified version of the Controlled Oral Word Association Test [16]. Participants were instructed to verbally generate words that began with the letters P, M and R in three separate, 1-min trials; (2) a semantic fluency task, generating words when cued with a particular category. Participants were instructed to name as many animals as possible in 1 min. We also administrated the vocabulary subtest from the Wechsler intelligence scales.

Magnetic resonance imaging acquisition and analysis

Data were obtained by a General Electric Signa 1.5-T scanner (Milwaukee, Wisconsin, USA). A set of high-resolution

T1-weighted images was acquired with a fast spoiled gradient-recalled three-dimensional sequence (time of repetition/time of echo=12/5.2; time of inversion=300 1 nex; field of view=24 cm; 256 × 256 matrix); the whole-brain data were acquired in an axial plane yielding contiguous slices with a slice thickness of 1 mm. Magnetic resonance images were analyzed using the voxel-based morphometry approach [17] by SPM2 software (Statistical Parametric Mapping, Wellcome Department of Cognitive Neurology, University College London, London, UK, http://www.fil.ion.ucl.ac.uk/spm) running in Matlab (MathWorks, Natick, Massachusetts, USA) (see Table 1 for the voxel-based morphometry protocol). For the image preparation, a single investigator (M.G.) performed the prior manual steps (line determination of the anterior–posterior commissures and image reorienting).

Statistical analysis

Thalamic reduction: a global thalamic region of interest

Changes in thalamic volume were analyzed using an SPM2 *t*-test group comparison. We performed two one-sided comparisons of modulated images (preterms > controls and preterms < controls) by region of interest analyses focused on the thalamus, bilaterally. With this procedure, we could observe gray matter reductions in both thalami.

As the thalamus projects into the frontal cortex, a separate complementary region of interest analysis was conducted to evaluate the possible impairment of frontal regions in the preterm sample (using an SPM2 *t*-test group comparison). The frontal region of interest included the inferior frontal gyrus, the middle frontal gyrus and the superior frontal gyrus.

Correlations between thalamic nuclei volume and verbal fluency: thalamic nuclei regions of interest

To further investigate the relationship between gray matter reductions in the thalamic nuclei and verbal fluency, we performed separate correlation SPM2 analyses for each group and nucleus. We analyzed the 11 thalamic regions of interest contained in the Pickatlas toolbox software for SPM version 1.02 (Joseph Maldjian, Functional MRI Laboratory, Wake Forest University School of Medicine, Winston-Salem, North Carolina, USA). The regions of interest were lateral dorsal nucleus, lateral geniculate nucleus, lateral posterior nucleus, medial dorsal nucleus, medial geniculate nucleus, midline nucleus, pulvinar, ventral anterior nucleus, ventral lateral nucleus, ventral posterior lateral nucleus and ventral posterior medial nucleus, bilaterally. As the groups differed in the vocabulary subtest, we controlled for the effects of this variable in the correlation analyses.

All results were thresholded at uncorrected voxel level $P < 0.001$ and only clusters larger than five contiguous voxels were considered in the statistical model. All frontal and thalamic regions of interest were based on stereotactically normalized brains.

Total intracranial volume and the three types of brain tissue (gray matter, white matter and cerebrospinal fluid) were compared using the Student's *t*-test, using SPSS version 12.0. The values for brain tissues (in dm^3) were obtained through the segmentation function. A between-group neuropsychological comparison was carried out using the Student's *t*-test.

Table 1 Optimized voxel-based morphometry procedure: steps

1.	Reorientation of the original TI images, attending to the anterior–posterior commissure orientation
2.	Non-linear normalization of the reoriented images by the TI SPM template
3.	Smoothing of the normalized images (kernel=8 mm)
4.	Mean image of the previous images → *TI study-specific template*
5.	Non-linear normalization of the original reoriented TI images by the study-specific template
6.	Segmentation (into gray and white matter and cerebrospinal fluid) of the previous normalized images
7.	Smoothing of the previous segmented images (kernel=8 mm)
8.	Mean image of the segmented, normalized and smoothed images → *gray matter study-specific template*
9.	Segmentation of the original TI images
10.	Determination of the normalization parameters in the previous gray matter images using our gray matter study-specific template
11.	Application of the previous normalization parameters (non-linear normalization) to the original TI images
12.	Segmentation of the original and normalized TI images
13.	Application of the Jacobean's determinants
14.	Smoothing of the unmodulated and modulated normalized gray matter files (kernel=8 mm)

Results

The preterm group performed significantly worse than the controls in both semantic [preterm mean=16.6 ± 3.6; control mean=21.1 ± 4.7; t=4.07 ($P < 0.0001$)] and phonetic [preterm mean=28.0 ± 8.5; control mean=32.6 ± 8.8; t=2.06 (P=0.044)] fluency. The groups also differed in the vocabulary subtest [preterm mean=10.8 ± 3.3; control mean=14.0 ± 2.7; t=4.08 ($P < 0.0001$)].

Segmentation analysis revealed that preterm participants had significantly less white matter and cerebrospinal fluid, and their total intracranial volume was lower than that of controls. In contrast, there was no significant difference between groups in gray matter (see Table 2).

Voxel-based morphometry found larger volume reductions in the preterm group than in controls in both thalami (left cluster: size=528 mm^3; local maxima Talairach coordinates=−21, −27, 1, cluster-corrected P=0.001; right cluster: size=368 mm^3, local maxima Talairach coordinates=21, −24, 3, cluster-corrected P=0.002) (see Fig. 1).

A complementary region of interest analysis was conducted to evaluate the possible reduction of the frontal thalamic-related gray matter areas in the preterm group. We found no significant volume differences in the frontal regions between groups.

Correlations between gray matter volume changes in each thalamic nucleus and verbal fluency values revealed positive relationships in the preterm group between semantic and phonetic fluency and a bilateral gray matter decrease in the thalamus: that is, the lower the thalamic volume, the poorer the verbal fluency (see Fig. 1 and Table 3).

Table 2 Brain and cerebral tissues volume comparison

	Premature (Mean ± SD)	Controls (Mean ± SD)	Student's *t*-test (*P* value)
Gray matter (dm^3)	0.78 ± 0.07	0.81 ± 0.06	1.39 (0.170)
White matter (dm^3)	0.36 ± 0.05	0.40 ± 0.04	3.21 (0.002)
Cerebrospinal fluid (dm^3)	0.31 ± 0.05	0.34 ± 0.04	2.46 (0.017)
Brain volume (dm^3)	1.46 ± 0.14	1.55 ± 0.01	2.54 (0.014)

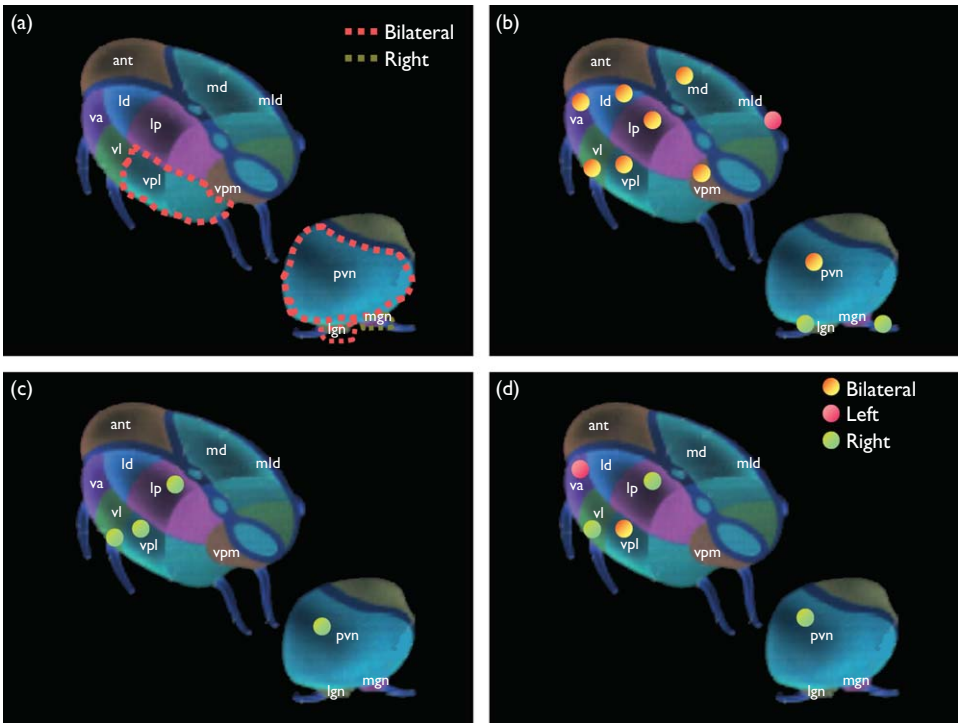

Fig. 1 Thalamic nuclei and verbal fluency. (a) Gray matter decreases in the preterm group compared with that in the controls, (b) correlations between gray matter and semantic fluency in premature individuals, (c) correlations between gray matter and phonetic fluency in controls and (d) correlations between gray matter and phonetic fluency in premature individuals. Results were thresholded at voxel $P < 0.001$. ant, anterior; va, ventral anterior; ld, lateral dorsal; vl, ventral lateral; lp, lateral posterior; vpl, ventral posterior lateral; md, medial dorsal; vpm, ventral posterior medial; mld, midline; pvn, pulvinar; lgn, lateral geniculate; mgn, medial geniculate.

In the control group, we only found a significant correlation between gray matter changes in the right thalamus and phonetic fluency. The cluster included the pulvinar, the lateral posterior nucleus, the ventral lateral nucleus and the ventral posterior lateral nucleus (global cluster size including all the nuclei=416 mm^3, local maxima Talairach coordinates=20, −26, 16, r=0.65, cluster-corrected P=0.001) (see Fig. 1).

Discussion

As in our preliminary study with a smaller sample [4], we found significant thalamic volume reductions in a premature group compared with controls. In the preterm group, the pulvinar showed a significant volume reduction, as did the lateral and medial geniculate nuclei and the ventral posterior lateral nucleus. In addition, significant positive correlations between thalamic volume and both verbal fluency tasks were found in both groups; some partial overlapping was observed between regions, but also some specificity.

Luders *et al.* [18] reported sex-dependent differences in gray matter volume. Despite the fact that our groups were matched by sex, they differed significantly in total brain size, but global brain gray matter volume was similar. So, there is no influence of global gray matter in the reported regional differences.

In the thalamic nuclei that presented significant volume reduction, we also observed a positive correlation between the gray matter changes and semantic fluency only in the preterm group: the lower the volume of the nuclei, the poorer the fluency. In addition, other volume changes in the ventral, lateral and medial nuclei showed relationships with semantic impairment in the preterm sample. The thalamus is involved in language processing and its lesions produce verbal fluency impairment [12]. The main clusters were found in the pulvinar (mainly the right side), in the ventral lateral nuclei and in the medial dorsal nuclei. The medial dorsal nucleus is known to be involved in memory processes [19] and thus probably supports the evocation of learned words. In a recent functional study, Maguire and Frith [20] showed activation of the medial dorsal nucleus in a verbal memory task in a healthy sample. The pulvinar of the thalamus may operate by integrating and coordinating visual attention [21], a function necessary for semantic fluency. On the other hand, the ventral lateral nucleus has connections to the supplementary motor regions [22], and may be involved in language production. A study of laterothalamic infarcts demonstrated that lesions in the ventral lateral nucleus impair verbal fluency [10].

The right lateral and medial geniculate bodies also correlated with semantic fluency. These two relay regions connect with visual and auditory cortical areas, respectively, and are reported to be involved in language processing tasks [23]. This gives rise to the possibility that both posterior nuclei are involved in preserving the mental representation of the category.

In phonetic fluency, both groups showed significant correlations between the scores and some thalamic nuclei, but the pattern of correlations was less extensive than that of semantic fluency. Most of the nuclei that correlated with phonetic scores in both groups belong to the lateral ventral nuclear group, associated classically with motor functions [24].

Table 3 Correlation analysis in premature group between thalamic nuclei volume changes and verbal fluency

Thalamic nucleus (region of interest analysis)	Cluster size (mm^3)	Local maxima Talairach coordinate (*x*, *y*, *z*)	*r*
Semantic fluency			
Left thalamic nuclei			
Lateral dorsal	96	−10, −17, 17	0.64
Lateral posterior	48	−14, −19, 16	0.56*
Medial dorsal	944	−2, −13, 3	0.68
Midline	64	−6, −17, 17	0.72
Pulvinar	248	−8, −27, 12	0.61
Ventral anterior	592	−13, −8, 14	0.68
Ventral lateral	856	−13, −11, 6	0.70
Ventral posterior lateral	304	−18, −17, 6	0.61
Ventral posterior medial	120	−13, −19, 4	0.58
Right thalamic nuclei			
Lateral dorsal	96	9, −17, 16	0.61
Lateral geniculate	48	22, −23, −2	0.58
Lateral posterior	240	16, −19, 16	0.63
Medial dorsal	976	2, −13, 3	0.69
Medial geniculate	56	16, −25, −4	0.59
Pulvinar	1456	13, −31, 2	0.68
Ventral anterior	552	14, −7, 10	0.68
Ventral lateral	896	13, −9, 10	0.67
Ventral posterior lateral	304	18, −17, 3	0.62
Ventral posterior medial	144	13, −19, 4	0.61
Phonetic fluency			
Left thalamic nuclei			
Ventral anterior	56	−13, −7, 14	0.59
Ventral posterior lateral	96	−17, −17, 6	0.63
Right thalamic nuclei			
Lateral posterior	104	17, −19, 16	0.60
Pulvinar	112	17, −23, 16	0.60
Ventral lateral	272	18, −15, 17	0.60
Ventral posterior lateral	128	18, −17, 3	0.60

All significant at *P* uncorrected level <0.0001, except for $*P=0.001$. All remained significant at *P* corrected level <0.05.

Semantic and phonetic fluencies coincided in part with the same regions, but certain thalamic nuclei correlated only with semantic fluency in the preterm group. A recent functional study in a pathological sample reported that semantic fluency required a greater activation of cortical areas than phonetic fluency [25]. Similar and overlapping semantic–phonetic brain patterns have been reported previously [12,14].

Conclusion

Thalamic volume reductions seem to contribute to verbal fluency impairment in adolescents with antecedents of very preterm birth, and the overlapping but differential correlational patterns for semantic and phonetic fluency reflects the presence of different networks for these two language functions.

References

1. Peterson BS, Vohr B, Staib LH, Cannistraci CJ, Dolberg A, Schneider KC, *et al*. Regional brain volume abnormalities and long-term cognitive outcome in preterm infants. *JAMA* 2000; **284**:1939–1947.
2. Stewart AL, Rifkin L, Amess PN, Kirkbride V, Townsend JP, Miller SW, *et al*. Brain structure and neurocognitive and behavioural function in adolescents who were born very preterm. *Lancet* 1999; **353**:1653–1657.
3. Skranes JS, Martinussen M, Smevik O, Myhr G, Indredavik M, Vik T, *et al*. Cerebral MRI findings in very-low-birth-weight and small-for-gestational-age children at 15 years of age. *Pediatr Radiol* 2005; **35**:758–765.
4. Giménez M, Junqué C, Narberhaus A, Caldú X, Salgado P, Bargalló N, *et al*. Hippocampal gray matter reduction associates with memory deficits in adolescents with history of prematurity. *Neuroimage* 2004; **23**:869–877.
5. Taylor HG, Minich NM, Klein N, Hack M. Longitudinal outcomes of very low birth weight: neuropsychological findings. *J Int Neuropsychol Soc* 2004; **10**:149–163.
6. Olsen P, Vainionpaa L, Paakko E, Korkman M, Pyhtinen J, Jarvelin MR. Psychological findings in preterm children related to neurologic status and magnetic resonance imaging. *Pediatrics* 1998; **102**:329–336.
7. Briscoe J, Gathercole SE, Marlow N. Short-term memory and language outcomes after extreme prematurity at birth. *J Speech Lang Hear Res* 1998; **41**:654–666.
8. Anderson P, Doyle LW, the Victorian Infant Collaborative Study Group. Neurobehavioral outcomes of school-age children born extremely low birth weight or very preterm in the 1990s. *JAMA* 2003; **289**:3264–3272.
9. Foulder-Hughes LA, Cooke RW. Motor, cognitive, and behavioural disorders in children born very preterm. *Dev Med Child Neurol* 2003; **45**:97–103.
10. Annoni JM, Khateb A, Gramigna S, Staub F, Carota A, Maeder P, *et al*. Chronic cognitive impairment following laterothalamic infarcts: a study of 9 cases. *Arch Neurol* 2003; **60**:1439–1443.
11. Kuljic-Obradovic DC. Subcortical aphasia: three different language disorder syndromes? *Eur J Neurol* 2003; **10**:445–448.
12. Crosson B. Subcortical mechanisms in language: lexical–semantic mechanisms and the thalamus. *Brain Cogn* 1999; **40**:414–438.
13. Ravnkilde B, Videbech P, Rosenberg R, Gjedde A, Gade A. Putative tests of frontal lobe function: a PET-study of brain activation during Stroop's test and verbal fluency. *J Clin Exp Neuropsychol* 2002; **24**:534–547.
14. Vitali P, Abutalebi J, Tettamanti M, Rowe J, Scifo P, Fazio F, *et al*. Generating animal and tool names: an fMRI study of effective connectivity. *Brain Lang* 2005; **93**:32–45.
15. Nosarti C, Rushe TM, Woodruff PW, Stewart AL, Rifkin L, Murray RM. Corpus callosum size and very preterm birth: relationship to neuropsychological outcome. *Brain* 2004; **127**:2080–2089.
16. Artiola i Fortuny L, Hermosillo Romo D, Heaton RK, Pardee RE 3rd. *Manual de normas y procedimientos para la batería neuropsicológica en español (Handbook of norms and procedures for the neuropsychological battery in Spanish) [in Spanish]*. Tucson, Arizona: m Press; 1999; pp. 33–34.
17. Good CD, Johnsrude IS, Ashburner J, Henson RNA, Friston KL, Frackowiak SJ. A voxel-based morphometric study of ageing in 465 normal adult human brains. *Neuroimage* 2001; **14**:21–36.
18. Luders E, Steinmetz H, Jäncke L. Brain size and grey matter volume in the healthy human brain. *Neuroreport* 2002; **13**:2371–2374.
19. Edelstyn NM, Hunter B, Ellis SJ. Bilateral dorsolateral thalamic lesions disrupts conscious recollection. *Neuropsychologia* (in press).
20. Maguire EA, Frith CD. The brain network associated with acquiring semantic knowledge. *Neuroimage* 2004; **22**:171–178.
21. Kastner S, Pinsk MA. Visual attention as a multilevel selection process. *Cogn Affect Behav Neurosci* 2004; **4**:483–500.
22. McFarland NR, Haber SN. Thalamic relay nuclei of the basal ganglia form both reciprocal and nonreciprocal cortical connections, linking multiple frontal cortical areas. *J Neurosci* 2002; **22**:8117–8132.
23. Cestnick L, Coltheart M. The relationship between language-processing and visual-processing deficits in developmental dyslexia. *Cognition* 1999; **71**:231–255.
24. Asanuma C, Thach WT, Jones EG. Distribution of cerebellar terminations and their relation to other afferent terminations in the ventral lateral thalamic region of the monkey. *Brain Res* 1983; **286**:237–265.
25. Kubota Y, Toichi M, Shimizu M, Mason RA, Coconcea CM, Findling RL, *et al*. Prefrontal activation during verbal fluency tests in schizophrenia: a near-infrared spectroscopy (NIRS) study. *Schizophr Res* 2005; **77**:65–73.

ELSEVIER

NeuroImage

www.elsevier.com/locate/ynimg
NeuroImage 32 (2006) 1485 – 1498

White matter volume and concentration reductions in adolescents with history of very preterm birth: A voxel-based morphometry study

Mónica Giménez,[a,b] Carme Junqué,[a,b,*] Ana Narberhaus,[a] Núria Bargalló,[c] Francesc Botet,[b,d] and Josep Maria Mercader[b,c]

[a] *Department of Psychiatry and Clinical Psychobiology, Faculty of Medicine, University of Barcelona, Institut d'Investigacions Biomèdiques August Pi i Sunyer (IDIBAPS), C/Casanova, 143, CP: 08036 Barcelona, Spain*
[b] *Institut d'Investigacions Biomèdiques August Pi i Sunyer (IDIBAPS), Spain*
[c] *Neuroradiology Section, Radiology Department, Centre de Diagnòstic per la Imatge (CDI), Hospital Clínic, Faculty of Medicine, University of Barcelona, Spain*
[d] *Pediatrics Section, Department of Obstetrics and Gynecology, Pediatrics, Radiology and Physics Medicine, Hospital Clínic, Spain*

Received 8 September 2005; revised 22 December 2005; accepted 3 May 2006
Available online 30 June 2006

Very preterm birth (VPTB) is an important risk factor for white matter (WM) damage. We used voxel-based morphometry (VBM) to examine regional WM brain abnormalities in 50 adolescents with antecedents of very preterm birth (VPTB) without evidence of WM damage on T2-weighted MRI. This group was compared with a group of 50 subjects born at term and matched for age, handedness and socio-cultural status. We also examined the relationship between WM changes and gestational age (GA) and weight (GW) at birth in VPTB subjects. Both modulated and unmodulated VBM analyses showed significant abnormalities in several WM brain regions in the VPTB group, involving all the cerebral lobes. However, density analyses (unmodulated data) mainly identified periventricular damage and the involvement of the longitudinal fascicles while volume analyses (modulated data) detected WM decreases in regions distant from the ventricular system, located at the origin and end of the long fascicles. A significant correlation was found between WM decreases and both GA and GW in various brain regions: the lower the GA and GW, the lower the WM integrity. This study supports the current view that widespread white matter impairment is associated with immature birth.

Introduction

Preterm newborns are particularly vulnerable to cerebral white matter (WM) damage, and this vulnerability is dependent on the stage of brain maturation (Blumenthal, 2004; Deguchi et al., 1999; Larroque et al., 2003; McQuillen and Ferriero, 2004; Rezaie and Dean, 2002; Volpe, 2001). Several studies have demonstrated WM abnormalities in preterm newborns, the most common finding being periventricular WM damage (Counsell et al., 2003; Hüppi et al., 2001; Inder et al., 2003a,b, 2005; Miller et al., 2002). Recent neuroimaging studies suggest that, in addition to a periventricular WM injury characterized by cell necrosis, axonal injury and/or microglia activation, there is a more diffuse myelination disturbance in other brain areas (Counsell et al., 2003).

Diffusion tensor imaging (DTI) is a technique that assesses early stages of white matter damage in vivo and provides an indirect measure of neural connectivity and the presence of myelinated brain tracts. DTI has mainly been used in premature infants and children (Arzoumanian et al., 2003; Counsell et al., 2003; Miller et al., 2002; Partridge et al., 2004). In normal subjects, DTI studies report slow WM maturation until early adulthood, characterized by increases in WM density and organization (Schmithorst et al., 2002; Snook et al., 2005) that indicate a long-term period of WM maturation and then a possible restructuring after early brain injury. The only long-term DTI study of WM in a group of adolescents with antecedents of prematurity performed to date (Nagy et al., 2003) described persistent disturbances in WM microstructure.

The DTI approach provides quantitative information about the orientation and integrity of WM tracts in terms of the apparent diffusion coefficient and the fractional anisotropy (Kubicki et al., 2002; Melhem et al., 2000). In long-term studies, magnetic resonance imaging (MRI) T1-weighted sequences appear to be sensitive for the detection of WM lesions by a tissue contrast. The voxel-based morphometry (VBM) approach allows whole or regional brain analysis by comparing regional gray or WM changes in terms of indirect measures of density and volume in

* Corresponding author. Fax: +34 93 403 52 94.
E-mail address: cjunque@ub.edu (C. Junqué).
Available online on ScienceDirect (www.sciencedirect.com).

1053-8119/$ - see front matter © 2006 Elsevier Inc. All rights reserved.
doi:10.1016/j.neuroimage.2006.05.013

all brain areas through structural MRI scans and allows the study of the entire brain at a small voxel level in minute detail. VBM uses standardized *t* test models on a voxel-by-voxel basis. One of its major advantages is that data processing is almost completely user-independent, and inter- and intraobserver variations are avoided (Ashburner and Friston, 2000).

The aim of the present study was to investigate regional WM abnormalities using a VBM approach in subjects with antecedents of very preterm birth (VPTB) and without evidence of WM injury on conventional MRI visual inspection of T2-weighted images. This is the first long-term report establishing a WM comparison analysis in an adolescent sample with VPTB using the VBM technique, combining both WM concentration (unmodulated data) and volume (modulated data) results. We hypothesize that periventricular WM injury may be accompanied by other distal subtle WM brain abnormalities not detected by visual inspection. We also investigated the correlation between gestational age (GA), and gestational weight (GW) at birth, and the WM changes to examine their influence in the WM integrity loss.

Methods

Subjects

The sample of subjects with VPTB antecedents comprised 50 adolescents (26 girls and 24 boys), taken from the archives of the Pediatric Service at the Hospital Clinic in Barcelona. The sample was selected from the population born between 1982 and 1994. Inclusion criteria for this study were: current age between 12 and 18 years, and GA equal to or less than 32 weeks for the VPTB group and equal to or more than 38 weeks for controls. Exclusion criteria for the whole sample were: (a) history of focal traumatic brain injury, (b) cerebral palsy or neurological diagnosis (including seizure and motor disorders) and (c) presence of global mental disabilities. Conventional T2-weighted images showed no evidence of WM injury in the preterm sample. A normal gestation control group (28 girls and 22 boys) was matched to VPTB subjects by age, handedness (7 left-handers in each group) and socio-cultural status. The total sample thus comprised 100 adolescents with a mean age of 14 years. Seven of the fifty VPTB subjects had low weight for their GA. We used the Wechsler intelligence scales to estimate the intelligence quotient (either the WAIS-III or the WISC-R, depending on subjects' age). All subjects attended normal school. Characteristics of the groups are summarized in Table 1. The study was approved by the ethics committee of the University of Barcelona and by a national research committee. All the subjects or their family gave written informed consent prior to participation in the study.

MRI acquisition and processing

Data were obtained from a GE Signa 1.5 T scanner (General Electric, Milwaukee, WI). A set of high-resolution inversion recovery T1-weighted images was acquired with an FSPGR 3D sequence (TR/TE = 12/5.2; TI 300 1 nex; FOV = 24 × 24 cm; 256 × 256 matrix). The whole-brain data were acquired in an axial plane yielding contiguous slices 1.5 mm thick. Axial T2-weighted images were obtained from a fast spin echo sequence (TR/TE = 4000/102; echo train 10; matrix 256 × 256, thickness 5 mm, gap 1.5 mm).

All MRI acquisitions were evaluated by two expert neuroradiologists (NB, JMM). From the original sample of 54 subjects with VPTB, four subjects with visible WM abnormalities were excluded.

The original MR images were recorded in DICOM format (one two-dimensional file per slice). MRI data were processed in a SUN workstation using the Solaris 8 operating system. The two-dimensional DICOM files were organized into volumetric three-dimensional files of each brain by means of the ANALYZE 5.0 software (Biomedical Resource, Mayo Foundation, Rochester, MN). The images were saved in an ANALYZE 7.5 format, compatible with the SPM2 software (Statistical Parametric Mapping, Wellcome Department of Cognitive Neurology, University College London, UK, http://www.fil.ion.ucl.ac.uk/spm).

Table 1
Demographic, clinical, neuropsychological variables and global volumetric measures of the sample

	Very preterm birth group ± SD	Control group ± SD	*t* and χ^2 statistic (*P* value)
Demographic data			
Age	14.5 ± 1.7	14.5 ± 2.2	$t = 0.05$ (0.960)
Gender (M/F)	24/26	22/28	$\chi^2 = 0.16$ (0.688)
Clinical data			
Gestational age (weeks)	29.9 ± 1.9	39.5 ± 1.6	$t = -27.98$ (<0.0001)
Weight at birth (mg)	1327 ± 414	3453 ± 419	$t = -25.54$ (<0.0001)
Intelligence			
Verbal IQ	107.3 ± 18.8	117.3 ± 12.9	$t = -3.09$ (0.003)
Performance IQ	97.9 ± 13.0	106.0 ± 10.4	$t = -3.42$ (0.001)
Full IQ	103.0 ± 15.7	113.5 ± 11.4	$t = -3.82$ (<0.0001)
Volumetrical data (mm^3)			
Cerebral spinal fluid	323,867 ± 46,042	334,858 ± 46,042	$t = -1.24$ (0.218)
Gray matter	787,796 ± 80,810	815,708 ± 68,052	$t = -1.87$ (0.065)
White matter	377,178 ± 47,396	397,781 ± 40,498	$t = -2.34$ (0.021)
Global intracranial volume	1,488,841 ± 148,755	1,548,347 ± 130,322	$t = -2.13$ (0.036)

VBM protocol

The automated image processing by VBM from both controls and VPTB subjects was done using SPM2 software, running in Matlab 6.5 (MathWorks, Natick, MA). For the image preparation, a single investigator (MG) performed the prior manual steps (line determination of the anterior–posterior commissures and image reorienting). The VBM applied to images was based on the optimized method proposed by Good et al. (2001) and was used only with WM brain images.

Image pre-processing

Applying the methodology of Good et al. (2001), the pre-processing of structural images followed defined processing stages (see Table 2). First, this methodology incorporates the creation of a prior anatomical study-specific template. In our case, this template was obtained from all 100 subjects (prematures and controls), so that each MRI was transformed into the same standardized coordinate system. Specifically, we registered each of the individual T1 images to the same template (T1 SPM2) by minimizing the residual sum of squared differences between them (Ashburner and Friston, 2000). The normalized structural data from the 100 subjects were smoothed with an 8 mm full-width at half-maximum (FWHM) isotropic Gaussian kernel, and an optimized mean image was performed with the previous smoothed files, including all the subjects in our whole sample (N = 100). This mean image was the study-specific template used for the pre-processing steps. SPM experts recommend the use of a single template that includes both types of subjects (controls and patients), if numbers are sufficient, in order to achieve the most consistent spatial normalization. Otherwise, we would be comparing the effects of two templates against each other. All the 100 original T1 structural images (in a native space) were then registered to the new study-specific template. The spatially normalized images were automatically partitioned into separate images representing probability maps for gray matter (GM), WM, and cerebrospinal fluid (CSF), using the combined pixel intensity and a priori probabilistic knowledge approach of the spatial distribution of tissues (Ashburner and Friston, 1999) integrated in SPM2. The tissue classification method was exhaustively described in Ashburner and Friston (1997). The segmentation procedure involves the calculation for each voxel of a Bayesian probability of its belonging to each brain tissue type (GM, WM, and CSF). The SPM2 version implements an updated segmentation process to improve the bias correction step and the misclassification as brain of non-brain tissue (ftp://ftp.fil.ion.ucl.ac.uk/spm/spm2_updates/). Specifically, this new segmentation model in SPM2 improves the segmentation of abnormal brains that can contain non-brain tissue (for example, voxels containing CSF). The segmentation procedure in SPM2 includes an automatic "clean-up" procedure whereby small regions of non-brain tissue that are misclassified as brain are removed. The normalized segmented images were smoothed using an 8-mm FWHM isotropic Gaussian kernel. A separate WM template was created by averaging all the 100 smoothed normalized WM images. Again, all the original T1 images (in a native space) were segmented into GM, WM and CSF images. The extracted WM images were normalized to the WM template, affording optimal spatial normalization of WM. With this step, we normalized the individual WM files using the study-specific WM template. But since the initial segmentation was performed on a non-normalized image and since we applied probability maps that are designed for normalized images, the optimized normalization parameters were reapplied to the original T1 images. These normalized images were then segmented into GW, WM and CSF. Normalized WM images were smoothed with an isotropic Gaussian kernel 8 mm in FWHM. In each registration step, we used a non-linear normalization and in each segmentation step we used the SPM2 segmentation process. In addition, to compensate for the possible volume changes due to the spatial normalization procedure, the segmented WM images were modulated by the Jacobian determinants derived from the spatial normalization step (these modulated images were also smoothed with the same kernel). The analysis of modulated data tests for regional differences in absolute WM volume (Good et al., 2001), whereas the analysis of unmodulated data can be taken to represent regional differences in concentration (density) of WM.

Table 2
Optimized voxel-based morphometry protocol

1. Reorientation of the original T1 images, attending to the AC–P orientation
2. Normalization of the reoriented images by the T1 SPM template
3. Smoothing of the normalized images (FHWM = 8 mm)
4. Mean image of the previous images → T1 study-specific template
5. Normalization of the original reoriented T1 images by the study-specific template
6. Segmentation (into gray and white matter (WM) and cerebral spinal fluid) of the previous normalized images
7. Smoothing of the previous segmented images (FHWM = 8 mm)
8. Mean image of the segmented, normalized and smoothed images → white matter study-specific template
9. Segmentation of the original images
10. Determination of the normalization parameters in the previous WM images using our WM template
11. Application of the previous normalization parameters to the original T1 images
12. Segmentation of the original and normalized T1 images
13. Application of the Jacobean's determinants
14. Smoothing of the unmodulated and modulated normalized WM files

Statistical analysis

The processed images for WM were analyzed using the SPM2 t test group comparison. We performed two one-sided comparisons to evaluate both WM cerebral concentration and volume changes in the premature sample compared to controls (contrast: control group > VPTB group). For this purpose, we used the WFU-PickAtlas toolbox software for SPM, version 1.02 to create a whole-brain WM Region of Interest (ROI), excluding the hindbrain (the area of the brain comprising the pons, medulla and cerebellum) (see Maldjian et al., 2003 for a description of the WFU-PickAtlas).

Moreover, "simple regression" (correlation) analyses were performed in the premature group, testing for a possible relationship between whole-brain WM concentration and volume changes and two clinical variables: GA and GW. Specifically, four correlational analyses were performed in the group of adolescents with antecedents of VPTB: 1—unmodulated data and GA; 2—

unmodulated data and GW; 3—modulated data and GA; 4—modulated data and GW. Just to illustrate the relationship between WM changes and the clinical variables, correlation results between WM changes in the fascicular regions and both clinical variables were plotted.

To display the results, we used a threshold at an uncorrected voxel P value of <0.001. But, for statistical purposes, we only report clusters that were significant at a corrected cluster P level. The corrected P values for clusters are related to false positive rates.

Intracranial volume and the three types of brain tissue (GM, WM and CSF) were compared in the two groups with the Student's t test, using the SPSS 11.0 version. The values for GM, WM and CSF were obtained through the segmentation function in SPM2. We segmented the original files obtaining a partition in GM, WM and CSF for each subject. We obtained a concrete value in mm^3 for each tissue. Intracranial volume was calculated by the sum of the three values.

Results

Optimized VBM statistical map comparison of unmodulated data demonstrated significantly lower WM concentrations in VPTB subjects than in controls in both hemispheres. The areas and levels of significance of WM decreases are shown in Table 3. Fig. 1 shows that many WM concentration differences were visible in frontal (bilateral medial and inferior gyrus), parietal (left superior region), temporal (right superior gyrus), insular (bilateral areas) and occipital lobes (bilateral medial gyrus), the bilateral cingulate region, and in periventricular areas, bordering both lateral ventricles. Moreover, WM concentration in regions that involve fiber tracts appeared to be affected in premature subjects: the superior and inferior longitudinal fasciculus and the superior occipitofrontal fasciculus showed bilateral abnormalities. Other areas with significant WM reductions were the left uncinate fascicle, the right optic radiation complex and the commissural tracts of the corpus callosum.

Modulated data group comparison showed WM volume decreases in VPTB subjects in the frontal (bilateral inferior gyrus, left precentral gyrus and right medial gyrus), parietal (bilateral precuneus area, left postcentral gyrus and left superior region), temporal (bilateral superior gyrus and right fusiform area), insular (left hemisphere), occipital lobes (right cuneus area), the bilateral cingulate region and in the periventricular areas. Regional volume differences in WM indicated a bilateral involvement of the superior and inferior longitudinal fasciculus. In the left hemisphere, there was a volume reduction in the superior occipitofrontal and uncinate fascicles (see Fig. 1). In contrast to unmodulated data, the corpus callosum did not show significant reductions nor did the occipital–medial gyrus, the right insular region, the right optic radiation complex or the right superior occipitofrontal fasciculus. For the modulated analysis, statistical significance, Talairach coordinates and cluster size values for each region are given in Table 4.

A complementary VBM GM analysis was conducted to evaluate the possible relationship between WM changes and injury in the immediately GM adjacent areas. As Figs. 2 and 3 show, the WM decreases in VPTB group were not directly related to GM changes in adjacent areas.

WM correlations with clinical variables

In the 50 adolescents with VPTB, statistically significant correlations were observed between WM regions and both GA and GW. Correlation analysis of WM concentration (unmodulated data) showed a significant relationship between WM changes and the GA in regions involving the left and right inferior longitudinal fasciculus (left: $r = 0.542$, $P < 0.0001$; right: $r = 0.511$, $P < 0.0001$), the superior longitudinal fasciculus (left: $r = 0.493$, $P < 0.0001$; right: $r = 0.508$, $P < 0.0001$) and the superior occipitofrontal fasciculus (left: $r = 0.564$, $P < 0.0001$; right: $r = 0.533$, $P < 0.0001$). Other areas showing significant correlations were frontal regions, bilaterally, left parietal superior area, left cingulate region and various corpus callosum regions ($P < 0.0001$, in all cases). Table 5 gives the results of the correlation analysis in VPTB group between WM changes and the two clinical variables. Global brain correlation results between WM values (concentration) and GA are also displayed in Fig. 4. The GA relationship with WM concentration changes is illustrated in Fig. 5 for the six representative WM fascicular areas.

Similar findings were obtained in the correlation analysis between the modulated data and the GA in different brain regions. The areas presenting significant correlations were the left superior longitudinal fasciculus ($r = 0.563$, $P < 0.0001$), the left uncinate fasciculus ($r = 0.531$, $P < 0.0001$) and the right inferior longitudinal fasciculus ($r = 0.503$, $P < 0.0001$). Again, bilateral parietal and frontal areas and the left cingulate region showed significant positive correlations (see Table 5).

Regarding the GW, we found significant correlations between WM concentration changes and this clinical variable in the inferior longitudinal fasciculus (left: $r = 0.550$, $P < 0.0001$; right: $r = 0.501$, $P < 0.0001$) and the superior occipital fasciculus (left: $r = 0.598$, $P < 0.0001$; right: $r = 0.561$, $P < 0.0001$) (see Fig. 6).Table 5 shows significant correlations for three other areas: the cingulate region (bilaterally) and the right temporal medial gyrus.

As in the case of the unmodulated results, correlation analysis with modulated data (volume) showed a significant correlation between the right inferior longitudinal fasciculus and the GW ($r = 0.600$, $P < 0.0001$). There was also a significant relationship between WM volume reduction and GW in the left uncinate fasciculus ($r = 0.627$, $P < 0.0001$). Other regions that showed significant correlations were bilateral frontal and parietal areas and the right cingulate region (see Table 5).

Discussion

The present investigation used VBM to describe the regional distribution of WM damage in a sample of adolescents with VPTB antecedents. Our results support the current concept that immature birth is associated with extensive WM damage rather than with isolated periventricular involvement, as was classically postulated.

Our results demonstrate that VPTB adolescents are characterized by the presence of WM concentration and volume reductions in several WM brain areas, including frontal, parietal, temporal and occipital lobes. The location of WM decreases suggests the

Table 3
Areas of white matter concentration decrease in the very preterm birth group compared to controls

Anatomical region (Brodmann area)	Cluster size (mm^3)	Cluster *P* (corrected)	Talairach coordinates			*t* statistic
			x	*y*	*z*	
Left hemisphere						
Frontal lobe						
Frontal-inferior gyrus (47)	344	<0.0001	−40	27	−5	3.97
Frontal-medial gyrus (8)	112	0.003	−34	15	38	3.63
Cingulate region (31)	4760✓	<0.0001	−4	−29	35	5.84
Occipital lobe						
Occipital-medial gyrus (19)	200	<0.0001	−42	−78	20	4.96
Parietal lobe						
Superior area (4)	1480	<0.0001	−32	−23	36	4.69
Insular lobe	296	<0.0001	−42	2	5	5.02
Periventricular areas						
Lateral ventricle	9344▲	<0.0001	−30	−40	8	4.75
White matter fiber tracts						
Superior longitudinal fasciculus	1000	<0.0001	−36	28	15	5.25
Inferior longitudinal fasciculus	9344▲	<0.0001	−37	−58	8	4.88
Superior occipitofrontal fasciculus	120	0.002	−18	−8	24	3.49
Uncinate fasciculus	344	<0.0001	−28	11	−11	3.83
	672	<0.0001	−34	−2	−15	4.56
Right hemisphere						
Frontal lobe						
Frontal-inferior gyrus (47)	224	<0.0001	42	27	−3	4.17
Frontal-medial gyrus (10)	88	0.016	6	50	−9	3.70
(10)	632	<0.0001	40	34	11	4.81
(6,8)	1400	<0.0001	30	−10	32	3.72
Cingulate region (31)	104	0.005	6	−54	41	4.47
	128	0.001	6	−2	37	3.84
	1880	<0.0001	8	−25	36	6.57
Temporal lobe						
Temporal-superior gyrus (38)	528	<0.0001	46	−2	−7	4.21
Fusiform area (20)	688	<0.0001	42	−22	−19	4.41
Occipital lobe						
Occipital-medial gyrus (19)	664	<0.0001	44	−73	20	4.23
Insular lobe	240	<0.0001	42	6	5	4.98
Periventricular areas						
Lateral ventricle	11,216●	<0.0001	28	−29	0	6.37
White matter fiber tracts						
Superior longitudinal fasciculus	11,216●	<0.0001	32	−36	17	5.36
Inferior longitudinal fasciculus	584	<0.0001	32	1	−22	4.50
Superior occipitofrontal fasciculus	616	<0.0001	16	1	29	3.70
	656▲▼	<0.0001	20	22	17	3.27
Optic radiation complex optica	176	<0.0001	32	−67	14	3.96
	376	<0.0001	20	−79	4	5.09
Corpus callosum						
Rostral body	4760✓	<0.0001	−8	5	26	4.30
Genu	656▲▼	<0.0001	14	31	8	4.26

▲▼●▲✓: each symbol indicates clusters including different areas. Referring to the brain position, Talairach coordinates indicate: *x* increases from left (−) to right (+); *y* increases from posterior (−) to anterior (+); and *z* increases from inferior (−) to superior (+).

impairment of several associative tracts. Reductions in both WM concentration and volume were found in the VPTB sample in the superior and inferior longitudinal fasciculus and in the left superior occipitofrontal and uncinate fasciculi. We also observed differences in concentration, though not in volume, in the right superior occipitofrontal fasciculus, the right optic radiation complex and in the corpus callosum.

The WM abnormalities observed in the premature group are very interesting since they seem to involve intrahemispheric association fibers (Mori et al., 2005; Wakana et al., 2004) and may therefore be related to the impairment in complex neuropsychological functions described in these subjects (Giménez et al., 2004; Peterson et al., 2000). Our results suggested a loss of the bilateral integrity of the WM association tracts, parallel to more diffuse WM damage in the adjacent brain areas. We observed WM decreases in the longitudinal fascicles (both superior and inferior) and in the inferior occipitofrontal fascicles. In addition, extensive clusters of WM loss were observed in the regions into which these fibers project.

The abnormalities in the inferior occipitofrontal and uncinate fasciculi merit special consideration. These two fascicles form the

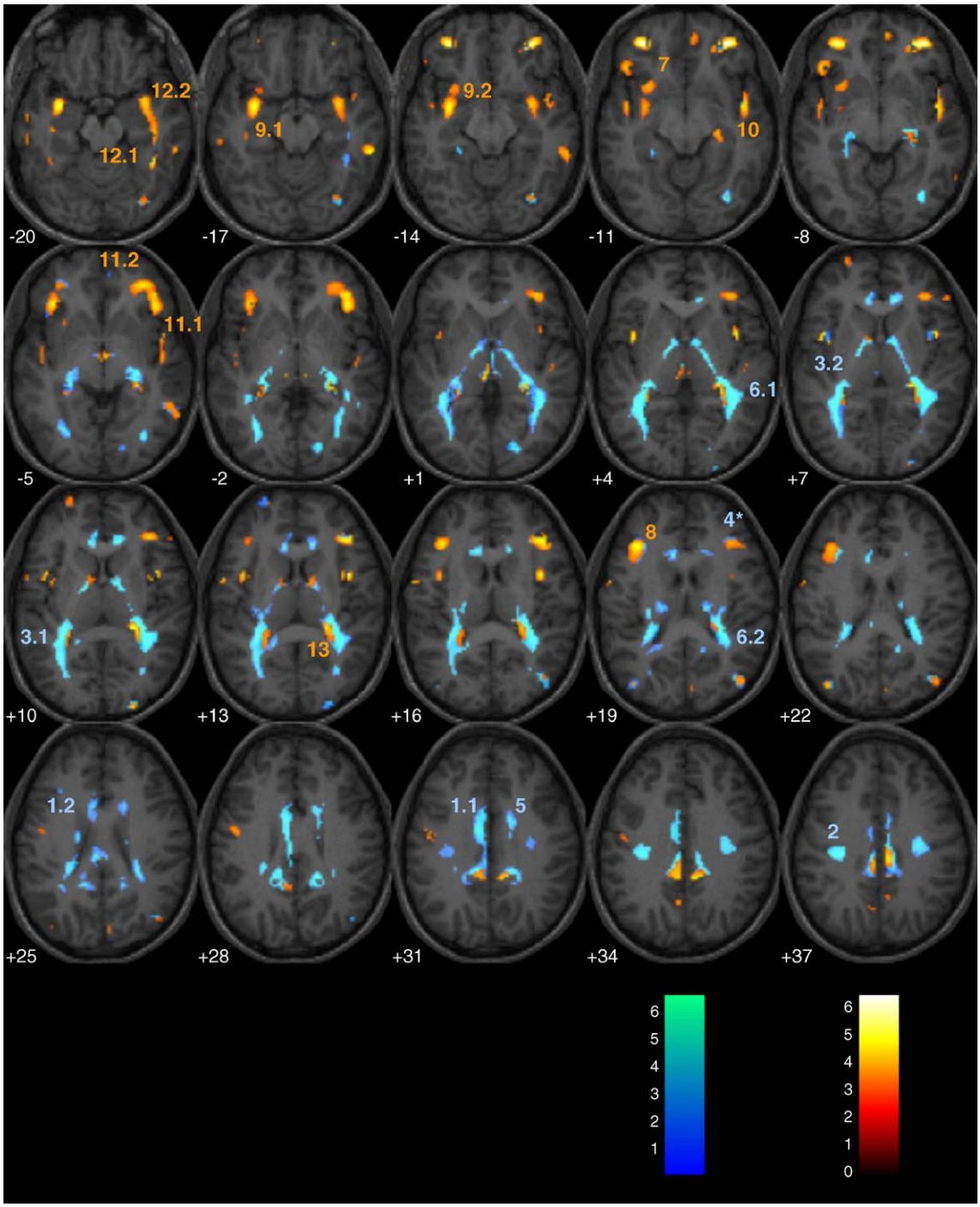

Fig. 1. Axial sections of images illustrating both unmodulated and modulated WM decreases in VPTB sample compared to controls. The unmodulated decreases are shown in winter colors; and modulated reductions are displayed in hot colors. Images are representative slices at 3 slice interval. Differences are mapped on a brain from a control subject from our sample. The color bar represents the *t* scores. Results are displayed at an uncorrected voxel *P* value threshold of <0.001. Statistical Parametric Maps (SPMs) are represented according to neurological convention (left corresponding to the left hemisphere). Number codes: unmodulated data: 1.1. left cingulate region; 1.2. corpus callosum rostral body; 2. left parietal superior area; 3.1. left periventricular area: lateral ventricle; 3.2. left inferior longitudinal fasciculus; 4* (overlapped). right frontal–medial area; 5. right cingulate region; 6.1. right periventricular area: lateral ventricle; 6.2 right superior longitudinal fasciculus. Modulated data: 7. left frontal–inferior gyrus; 8. left superior longitudinal fasciculus; 9.1. left inferior longitudinal fasciculus; 9.2. left uncinate fasciculus; 10. right temporal superior area; 11.1. right frontal–inferior gyrus; 11.2. right superior longitudinal fasciculus; 12.1. right fusiform area; 12.2 right inferior longitudinal fasciculus; 13. right periventricular area: lateral ventricle.

Table 4
Areas of white matter volume reduction in the very preterm birth group compared to controls

Anatomical region (Brodmann area)	Cluster size (mm^3)	Cluster *P* (corrected)	Talairach coordinates			*t* statistic
			x	*y*	*z*	
Left hemisphere						
Frontal lobe						
Frontal-inferior gyrus (47)	2248	<0.0001	−40	29	−5	4.66
Precentral gyrus (4)	256	<0.0001	−6	−34	57	3.64
Temporal lobe						
Temporal-superior gyrus (38)	392	<0.0001	−46	−4	−8	3.91
Cingulate region (31)	544	<0.0001	−4	−31	35	4.47
Parietal lobe						
Superior area (7)	160	<0.0001	−20	−54	45	3.46
Postcentral gyrus (12)	192	<0.0001	−34	−31	49	3.83
Precuneus area (7)	208	<0.0001	−4	−64	42	4.33
Insular lobe	592	<0.0001	−42	4	5	5.20
Periventricular areas						
Lateral ventricle	736 ▲▼	<0.0001	−28	−40	8	4.17
White matter fiber tracts						
Superior longitudinal fasciculus	1128	<0.0001	−38	28	15	5.21
Inferior longitudinal fasciculus	2936 ▲	<0.0001	−34	−3	−17	5.29
Superior occipitofrontal fasciculus	736 ▼	<0.0001	−24	−40	15	3.77
Uncinate fasciculus	2936 ▲	<0.0001	−28	11	−11	4.04
Right hemisphere						
Frontal lobe						
Frontal-inferior gyrus (47)	4680 ✓	<0.0001	42	27	−3	4.78
Frontal-medial gyrus (10)	216	<0.0001	6	50	−9	4.10
Temporal lobe						
Temporal-superior gyrus (38)	1080	<0.0001	48	−4	−8	4.55
Fusiform area (19)	224	<0.0001	32	−72	−8	3.75
(20)	4088 ●	<0.0001	42	−24	−22	4.66
Cingulate region (31)	304	<0.0001	10	−41	33	4.96
	232	<0.0001	8	−25	36	4.66
Parietal lobe						
Precuneus area (31)	208	<0.0001	6	−54	41	4.71
Occipital lobe						
Cuneus (18)	72	0.050	6	−80	28	3.56
Periventricular areas						
Lateral ventricle	1640	<0.0001	28	−35	2	5.14
White matter fiber tracts						
Superior longitudinal fasciculus	4680 ✓	<0.0001	37	44	−11	5.08
Inferior longitudinal fasciculus	4088 ●	<0.0001	32	1	−22	5.08

▲▼ ● ▲ ✓: each symbol indicates clusters including different areas. Referring to the brain position, Talairach coordinates indicate: *x* increases from left (−) to right (+); *y* increases from posterior (−) to anterior (+); and *z* increases from inferior (−) to superior (+).

temporal stem (Kier et al., 2004), a temporal WM region that interconnects the temporal region with other brain structures. In a previous DTI analysis, Hanyu et al. (1998) reported abnormalities of water diffusion in Alzheimer's disease in the temporal stem and suggested an association with GM degenerative processes in the temporal lobe. Previous GM findings in premature samples demonstrate GM medial temporal lobe decreases, especially in the hippocampus (Giménez et al., 2004; Isaacs et al., 2000, 2003; Peterson et al., 2000).

The involvement of the uncinate fasciculus has been described in a sample of adults with history of very low birth weight (Allin et al., 2004). Our VBM also demonstrated WM impairment of a region involving the superior occipitofrontal fascicle. In a tractographic DTI study, Catani et al. (2002) reported that this fascicle connects mainly the dorsolateral prefrontal cortex with the superior parietal gyrus. In our study, unmodulated and modulated WM data showed that on the brain side with the greater parietal WM decrease there is a WM damage of the respective superior occipitofrontal fascicle.

In addition, the WM concentration involving the right optic radiation complex fibers (arising from the lateral geniculate body and ending in the cortex of the calcarine fissure [BA17]) was altered in the VPTB group. This adds support to previous findings about the possible risk of visual impairment in preterm and very low birth weight samples (Rudanko et al., 2003). Allin et al. (2004)'s study of adults with very low birth weight antecedents also demonstrated deficits in WM in optic radiation.

Despite the fact that associative pathways were the mainly injured tracts, some projection pathways may also be affected. Some of the clusters reported involved small regions that contained different projections tracts, such as the corticopontine tract and the posterior thalamic radiation. We did not expect to find major impairment of motor and sensorial tracts because in our VPTB

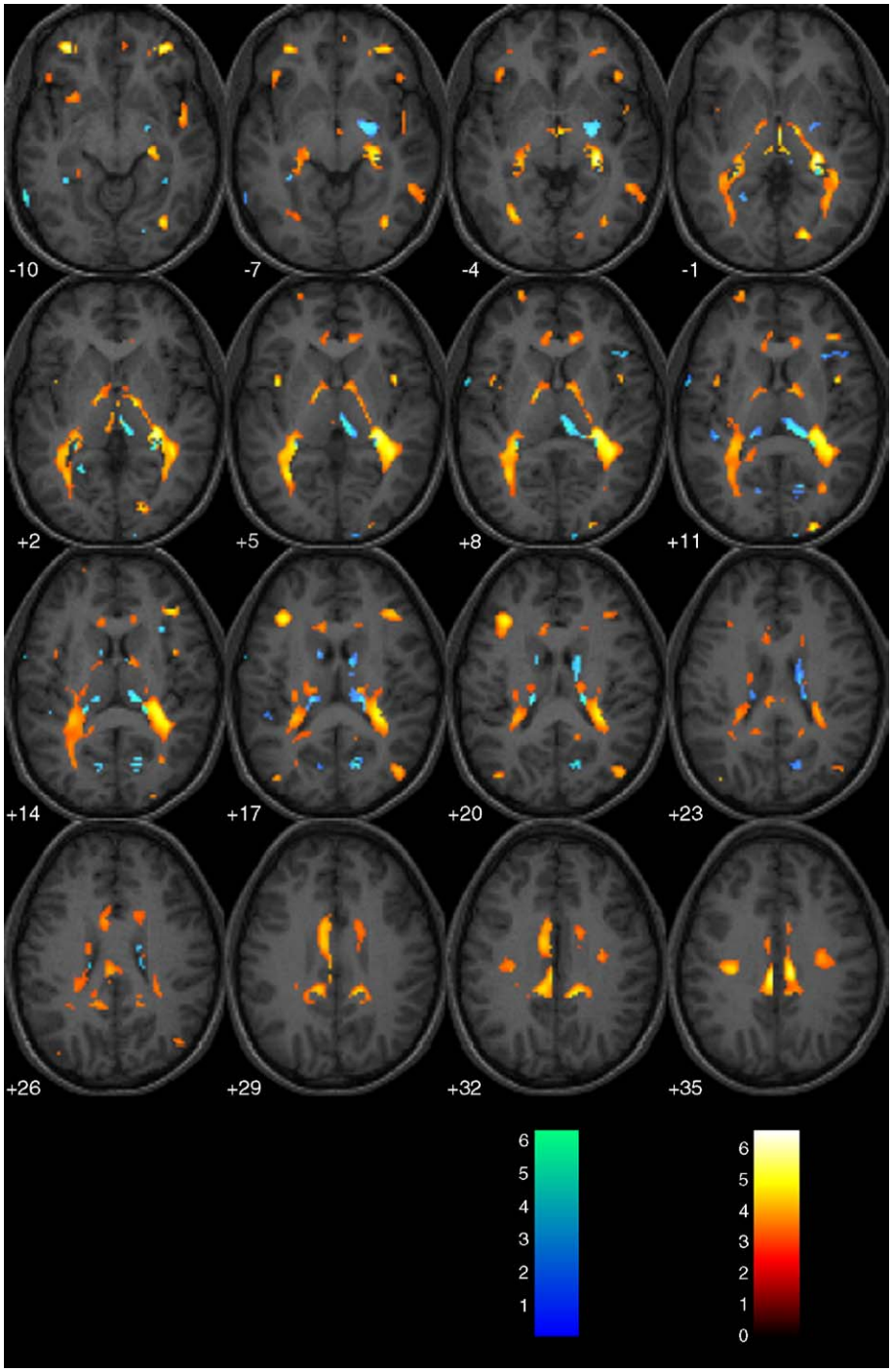

Fig. 2. Axial sections of images illustrating both unmodulated GM and WM decreases in VPTB sample compared to controls. The GM decreases are shown in winter colors; and WM reductions are displayed in hot colors. Images are representative slices at 3 slice interval. Differences are mapped on a brain from a control subject from our sample. The color bar represents the *t* scores. Results are displayed at an uncorrected voxel *P* value threshold of <0.001. Statistical Parametric Maps (SPMs) are represented according to neurological convention (left corresponding to the left hemisphere).

sample we excluded subjects with antecedents of severe motor and sensorial disorders.

Concentration and volumetric VBM data seem to be sensitive to various WM changes associated to premature birth. The concentration analysis detected periventricular WM impairment and involvement of the major association fibers. In contrast, the volume analysis (modulated data) supported recent findings of more diffuse WM impairment in premature birth, probably due to injury to the oligodendrocyte progenitors (Back and Rivkees, 2004). The WM in premature infants of less than 32 weeks gestation is poorly vascularized and contains oligodendrocyte progenitors (pre-oligodendrocytes) which are sensitive to the effects of ischemia and infection (Blumenthal, 2004).

The modulated analysis showed clusters of WM decreases in frontal, temporal and parietal regions very distant from the ventricular system, corresponding to the starting and ending

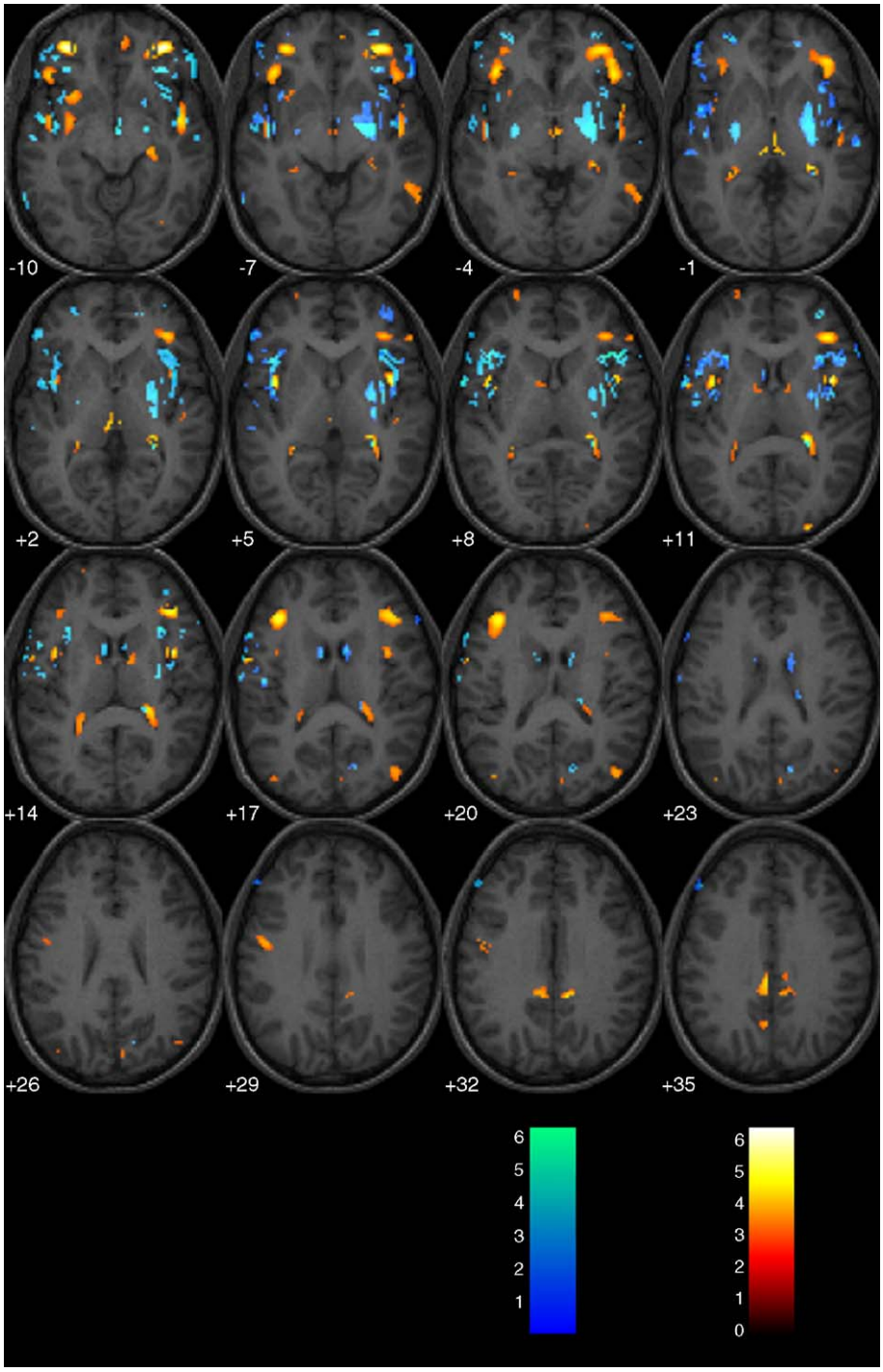

Fig. 3. Axial sections of images illustrating both modulated GM and WM decreases in VPTB sample compared to controls. The GM decreases are shown in winter colors; and WM reductions are displayed in hot colors. Images are representative slices at 3 slice interval. Differences are mapped on a brain from a control subject from our sample. The color bar represents the *t* scores. Results are displayed at an uncorrected voxel *P* value threshold of <0.001. Statistical Parametric Maps (SPMs) are represented according to neurological convention (left corresponding to the left hemisphere).

regions of the superior and inferior longitudinal fascicles. These data provide further support for the notion that WM injury is more generalized and more common in immature infants than previously realized (Blumenthal, 2004) and favor the use of the term cerebral "leucoencephalopathy" in place of the classical "periventricular leucomalacy" such as it has been proposed by Volpe (2003).

Recent reports demonstrate that the vulnerability of immature brains to hypoxic–ischemic insults provokes damage earlier in the WM than in the GM (Meng et al., 2005). However, hypoxic–ischemic insults can also produce GM damage (Vannucci and Vannucci, 2005). So, WM abnormalities may not only reflect damage to WM precursor cells, but may also be due to damage to cells originating in the cortex. In Alzheimer's disease, changes in

Table 5
Correlation analysis: relationship between white matter changes in the very preterm birth group and clinical variables (whole-brain white matter analysis)

Anatomical region (Brodmann area)	Cluster size (mm^3)	Talairach coordinates			Correlation coefficients
		x	*y*	*z*	
Unmodulated images (concentration)					
Gestation age					
L frontal superior gyrus (9)	568	−8	35	31	0.587**
L parietal superior area (7)	1216	−30	−53	32	0.608**
L cingulate region (31)	1176	−4	−37	33	0.568**
L superior longitudinal fasciculus	1088	−36	30	19	0.493**
L inferior longitudinal fasciculus and uncinate fasciculus	3008	−42	−28	−10	0.542**
		−34	−2	−8	
L superior occipitofrontal fasciculus	4416	−20	−30	20	0.564**
R frontal superior gyrus (6)	512	14	14	47	0.624**
(9)	456	16	46	22	0.549**
R frontal medial gyrus (44)	552	44	3	15	0.578**
R superior longitudinal fasciculus	608	36	−10	29	0.508**
R inferior longitudinal fasciculus	3600	40	−10	−5	0.511**
	992	38	−56	6	0.536**
R superior occipitofrontal fasciculus	488	20	−12	25	0.533**
Corpus callosum					
Genu	1176	−8	25	10	0.555**
	392	14	32	13	0.505**
Rostral body and anterior midbody	424	−14	7	24	0.451*
		−14	−1	26	0.452*
Isthmus	464	−2	−18	23	0.523**
Gestational weight					
L cingulate region (31)	1104	−6	−20	36	0.599**
L inferior longitudinal fasciculus	3328	−42	−28	−10	0.550**
L superior occipitofrontal fasciculus	11,688	−21	−16	25	0.598**
R temporal medial gyrus (20)	1912	38	−18	−9	0.541**
R cingulate region (31)	680	6	−33	40	0.682**
R inferior longitudinal fasciculus and	1064	38	−56	8	0.501**
R optic radiation complex Optica		34	−65	14	
R superior occipitofrontal fasciculus	1688	20	−8	26	0.561**
Modulated images (volume)					
Gestation age					
L precentral gyrus (6)	656	−8	−23	53	0.596**
L parietal superior area (7)	768	−32	−53	36	0.545**
L cingulate region (31)	568	−6	−37	33	0.611**
L superior occipitofrontal fasciculus	984	−20	−28	23	0.563**
L uncinate fasciculus	3576	−34	−2	−8	0.531**
R frontal medial gyrus (45)					
(6)	616	42	3	15	0.578**
	536	6	−21	53	0.573**
R parietal superior area (7)	424	14	−52	43	0.532**
R inferior longitudinal fasciculus	2712	36	−1	−15	0.503**
Gestational weight					
L parietal superior area (7)	2024	−12	−58	36	0.631**
L precentral gyrus (4)	720	−6	−28	61	0.476**
L uncinate fasciculus	9144	−32	12	−5	0.627**
R frontal medial gyrus (10)	1544	42	41	0	0.558**
R parietal superior area (7)	2304	12	−62	43	0.610**
R cingulate region (31)	616	6	−37	37	0.687**
R inferior longitudinal	8736	33	−5	−20	0.600**
fasciculus and uncinate fasciculus		30	0	−7	

L: left, R: right.
* Significant at P level = 0.001.
** Significant at P level < 0.0001.

corpus callosum have been related to degeneration of cortical neurons in the association cortex (Hampel et al., 1998). We observed some GM reductions in our VPTB sample, but these reductions cannot explain the whole WM damage.

Our investigation showed that WM integrity positively correlated with gestational age (GA) and gestational weight (GW) in a group of adolescents with VPTB in several brain areas: the lower the GA and GW, the lower the WM integrity.

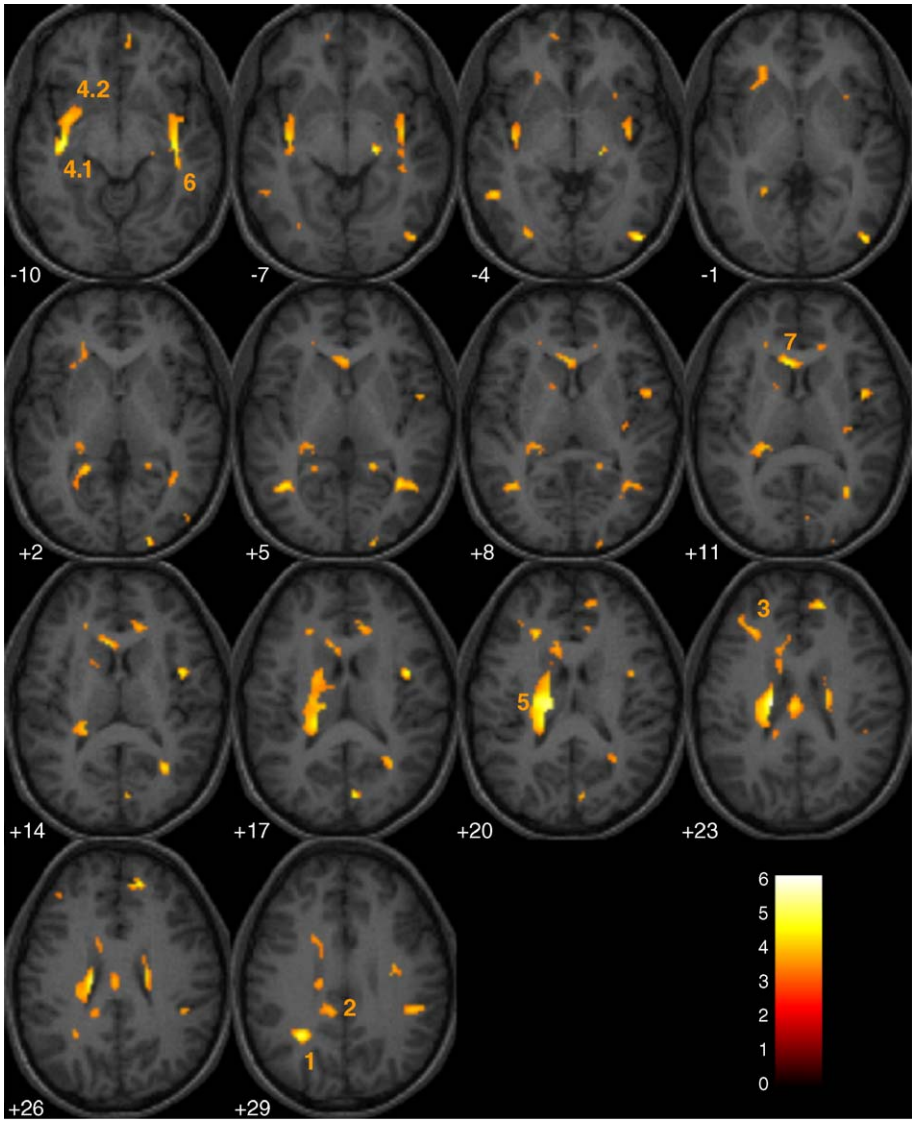

Fig. 4. Axial slices display showing the correlation between WM concentration (unmodulated data) decreases and GA: the lower the GA, the lower the WM integrity. Images are representative slices at 3 slice interval. Differences are mapped on a brain from a control subject from our sample. The color bar represents the *t* scores. Results are displayed at an uncorrected voxel *P* value threshold of <0.001. Statistical Parametric Maps (SPMs) are represented according to neurological convention (left corresponding to the left hemisphere). Number codes: 1. left parietal superior area; 2. left cingulated region; 3. left superior longitudinal fasciculus; 4.1. left inferior longitudinal fasciculus; 4.2. left uncinate fasciculus; 5. left superior occipitofrontal fasciculus; 6. right inferior longitudinal fasciculus; 7. corpus callosum genu.

The relationship between the presence of WM injury and GA has been reported in previous research using a range of approaches. Our results are in agreement with a cranial ultrasound investigation in newborns with GA of up to 32 weeks (Larroque et al., 2003). Evaluating the presence of WM damage, those authors observed that the incidence of WM injury was highest in subjects with the lowest GA. Moreover, Inder et al. (2003b) demonstrated that lower GA appeared to be a predictor for the appearance of WM abnormalities in conventional clinical MRI studies. Finally, a recent DTI study in preterm newborns by Partridge et al. (2004) indicated that fractional anisotropy (a measure used to evaluate the degree of alignment of cellular structures with fiber tracts and the structural integrity of these tracts) and water diffusivity values (related to tissue water loss) in WM presented the same correlations with GA as those found in our study, namely an increase in fractional anisotropy and a decrease in water diffusivity values with increasing GA in the limb internal capsula areas, the centrum semiovale, the external capsule and the splenium of the corpus callosum. GW also influences WM disturbances (Iwata et al., 2004). The relationship between regional WM changes and GA and GW in adolescence of subjects with VPTB suggests that the disturbances in brain development depend on the immaturity of the newborn and that the relationship persists until adolescence. Unfortunately, our study cannot separate the specific contribution of low weight in WM injury; though low weight was clearly related to low GA, the sample size does not allow investigating the differences between subjects with normal or abnormal weight according to their GA.

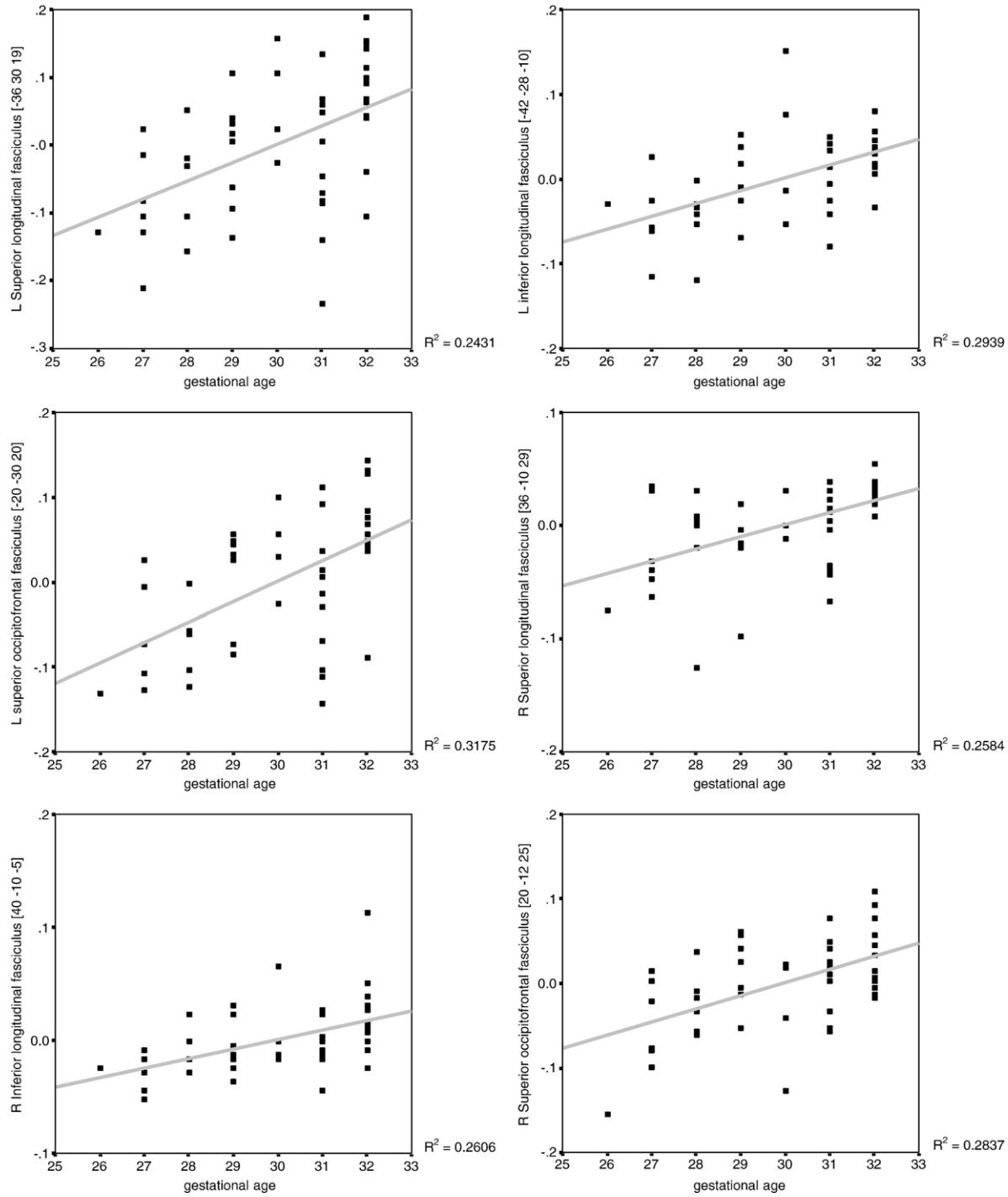

Fig. 5. Correlations between WM density changes (unmodulated data) and GA in weeks in the VPTB group in the fascicular areas. Plots of WM density values against GA: points indicate real data; the line indicates data adjusted to the theoretical model. Abbreviations: L: left; R: right.

We should mention a methodological issue concerning the VBM approach in our study. We cannot avoid the fact that the spatial normalization of brains was adapted to the T1 SPM adult space. Spatial normalization is an important tool for direct voxel comparison of data sets between subjects. This optimized VBM approach uses an adult-derived template for spatial normalization of the adolescent brain in the first stage of the VBM. To minimize the problems arising from this procedure, we conducted the entire first normalization subject by subject, ensuring that all subjects were well adapted to the T1 template. To do so, a single investigator (M.G.) checked nine different referential anatomical points to see their visual correspondence and coincidence in the T1 SPM template and in each individual brain. This verification was also carried out comparing the T1 SPM template and the study-specific template. The new template was properly adapted to the T1 SPM coordinates to take advantage of the SPM classification priors in the segmentation process.

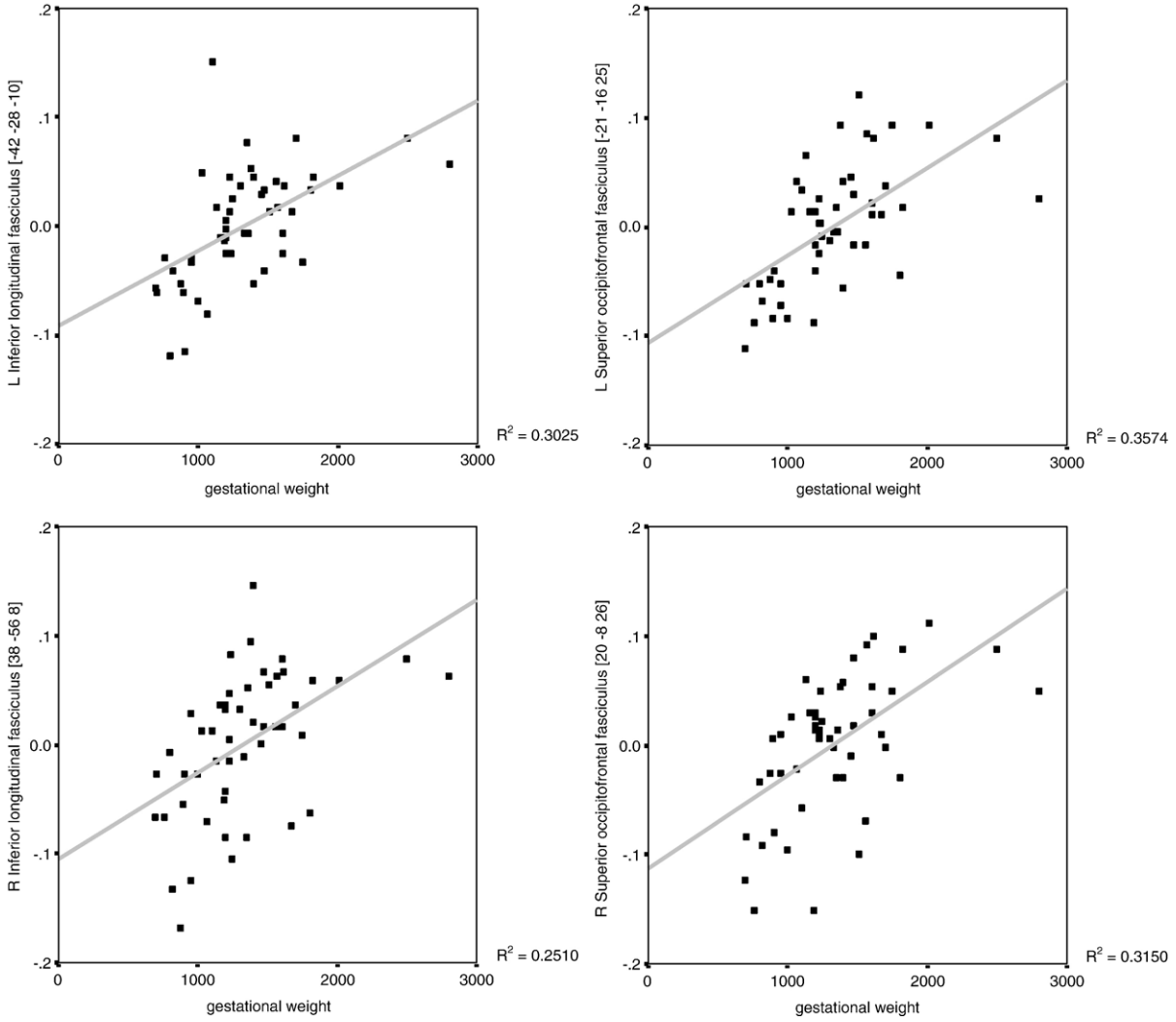

Fig. 6. Correlations between WM density changes (unmodulated data) and GW in kilograms in the VPTB group in areas involving the long fascicles. Plots of WM density values against GW: points indicate real data; the line indicates data adjusted to the theoretical model. Abbreviations: L: left; R: right.

In summary, VPTB antecedents seem to be associated with WM concentration and volumetric abnormalities in different brain regions that may underlie the cognitive and functional deficits observed in premature samples. The pattern of cerebral alterations presented in prematures is significantly related to the degree of immaturity at birth. The WM damage observed here in a sample of adolescents with VPTB antecedents demonstrates that the brain disturbances observed in other newborns samples do not normalize in adolescence and supports the use of the recently coined term "cerebral leucoencephalopathy" in association with premature birth.

Acknowledgments

This study was supported by grants SAF2005-07340 (Ministerio de Ciencia y Tecnología), 2005SGR 00855 (Generalitat de Catalunya), the grant 2005FIR 00095 (Generalitat de Catalunya) to A. Narberhaus, and the grant AP2002-0737 (Ministerio de Educación, Cultura y Deporte) to M. Giménez. The assistance of Dr. Carles Falcón during data analysis is gratefully acknowledged.

References

Allin, M., Henderson, M., Suckling, J., Nosarti, C., Rushe, T., Fearon, P., Stewart, A.L., Bullmore, E.T., Rifkin, L., Murray, R., 2004. Effects of very low birthweight on brain structure in adulthood. Dev. Med. Child Neurol. 46, 46–53.

Arzoumanian, Y., Mirmiran, M., Barnes, P.D., Wooley, K., Ariagno, R.L., Moseley, M.E., Fleisher, B.E., Atlas, S.W., 2003. Diffusion tensor brain imaging findings at term-equivalent age may predict neurologic abnormalities in low birth weight preterm infants. Am. J. Neuroradiol. 24, 1646–1653.

Ashburner, J., Friston, K.J., 1997. Multimodal image coregistration and partitioning—A unified framework. NeuroImage 6, 209–217.

Ashburner, J., Friston, K.J., 1999. Nonlinear spatial normalization using basis functions. Hum. Brain Mapp. 7, 254–266.

Ashburner, J., Friston, K.J., 2000. Voxel-based morphometry—The methods. NeuroImage 11, 805–821.

Back, S.A., Rivkees, S.A., 2004. Emerging concepts in periventricular white matter injury. Semin. Perinatol. 28, 405–414.

Blumenthal, I., 2004. Periventricular leucomalacia: a review. Eur. J. Pediatr. 163, 435–442.

Catani, M., Howard, R.J., Pajevic, S., Jones, D.K., 2002. Virtual in vivo interactive dissection of white matter fasciculi in the human brain. NeuroImage 17, 77–94.

Counsell, S.J., Allsop, J.M., Harrison, M.C., Larkman, D.J., Kennea, N.L., Kapellou, O., Cowan, F.M., Hajnal, J.V., Edwards, A.D., Rutherford, M.A., 2003. Diffusion-weighted imaging of the brain in preterm infants with focal and diffuse white matter abnormality. Pediatrics 112, 1–7.

Deguchi, K., Oguchi, K., Matsuura, N., Armstrong, D.D., Takashima, S., 1999. Periventricular leukomalacia: relation to gestational age and axonal injury. Pediatr. Neurol. 20, 370–374.

Giménez, M., Junqué, C., Narberhaus, A., Caldu, X., Salgado-Pineda, P., Bargalló, N., Segarra, D., Botet, F., 2004. Hippocampal gray matter reduction associates with memory deficits in adolescents with history of prematurity. NeuroImage 23, 869–877.

Good, C.D., Johnsrude, I.S., Ashburner, J., Henson, R.N., Friston, K.J., Frackowiak, R.S., 2001. A voxel-based morphometric study of ageing in 465 normal adult human brains. NeuroImage 14, 21–36.

Hampel, H., Teipel, S.J., Alexander, G.E., Horwitz, B., Teichberg, D., Schapiro, M.B., Rapoport, S.I., 1998. Corpus callosum atrophy is a possible indicator of region- and cell type-specific neuronal degeneration in Alzheimer disease: a magnetic resonance imaging analysis. Arch. Neurol. 55, 193–198.

Hanyu, H., Sakurai, H., Iwamoto, T., Takasaki, M., Shindo, H., Abe, K., 1998. Diffusion-weighted MR imaging of the hippocampus and temporal white matter in Alzheimer's disease. J. Neurol. Sci. 156, 195–200.

Hüppi, P.S., Murphy, B., Maier, S.E., Zientara, G.P., Inder, T.E., Barnes, P.D., 2001. Microstructural brain development after perinatal cerebral white matter injury assessed by diffusion tensor magnetic resonance imaging. Pediatrics 107, 455–460.

Inder, T.E., Anderson, N.J., Spencer, C., Wells, S., Volpe, J.J., 2003a. White matter injury in the premature infant: a comparison between serial cranial sonographic and MR findings at term. Am. J. Neuroradiol. 24, 805–809.

Inder, T.E., Wells, S.J., Mogridge, N.B., Spencer, C., Volpe, J.J., 2003b. Defining the nature of the cerebral abnormalities in the premature infant: a qualitative magnetic resonance imaging study. J. Pediatr. 143, 171–179.

Inder, T.E., Warfield, S.K., Wang, H., Hüppi, P.S., Volpe, J.J., 2005. Abnormal cerebral structure is present at term in premature infants. Pediatrics 115, 286–294.

Isaacs, E.B., Lucas, A., Chong, W.K., Wood, S.J., Johnson, C.L., Marshall, C., Vargha-Khadem, F., Gadian, D.G., 2000. Hippocampal volume and everyday memory in children of very low birth weight. Pediatr. Res. 47, 713–720.

Isaacs, E.B., Vargha-Khadem, F., Watkins, K.E., Lucas, A., Mishkin, M., Gadian, D.G., 2003. Developmental amnesia and its relationship to degree of hippocampal atrophy. Proc. Natl. Acad. Sci. U. S. A. 100, 13060–13063.

Iwata, O., Iwata, S., Tamura, M., Nakamura, T., Hirabayashi, S., Fueki, N., Kondou, Y., Hizume, E., Kihara, H., 2004. Periventricular low intensities on fluid attenuated inversion recovery imaging in the newborn infant: relationships to the clinical data and long-term outcome. Pediatr. Int. 46, 150–157.

Kier, E.L., Staib, L.H., Davis, L.M., Bronen, R.A., 2004. MR imaging of the temporal stem: anatomic dissection tractography of the uncinate fasciculus, inferior occipitofrontal fasciculus, and Meyer's loop of the optic radiation. Am. J. Neuroradiol. 25, 677–691.

Kubicki, M., Westin, C.F., Maier, S.E., Mamata, H., Frumin, M., Ersner-Hershfield, H., Kikinis, R., Jolesz, F.A., McCarley, R., Shenton, M.E., 2002. Diffusion tensor imaging and its application to neuropsychiatric disorders. Harv. Rev. Psychiatry 10, 324–336.

Larroque, B., Marret, S., Ancel, P.Y., Arnaud, C., Marpeau, L., Supernant, K., Pierrat, V., Roze, J.C., Matis, J., Cambonie, G., Burguet, A., Andre, M., Kaminski, M., Breart, G.EPIPAGE Study Group, 2003. White matter damage and intraventricular hemorrhage in very preterm infants: the EPIGAGE study. J. Pediatr. 143, 477–483.

Maldjian, J.A., Laurienti, P.J., Kraft, R.A., Burdette, J.H., 2003. An automated method for neuroanatomic and cytoarchitectonic atlas-based interrogation of fMRI data sets. NeuroImage 19, 1233–1239.

McQuillen, P.S., Ferriero, D.M., 2004. Selective vulnerability in the developing central nervous system. Pediatr. Neurol. 30, 227–235.

Melhem, E.R., Itoh, R., Jones, L., Barker, P.B., 2000. Diffusion tensor MR imaging of the brain: effect of diffusion weighting on trace and anisotropy measurements. Am. J. Neuroradiol. 21, 1813–1820.

Meng, S., Qiao, M., Foniok, T., Tuor, U.I., 2005. White matter damage precedes that in gray matter despite similar magnetic resonance imaging changes following cerebral hypoxia–ischemia in neonatal rats. Exp. Brain Res. 166, 56–60.

Miller, S.P., Vigneron, D.B., Henry, R.G., Bohland, M.A., Ceppi-Cozzio, C., Hoffman, C., Newton, N., Partridge, J.C., Ferriero, D.M., Barkovich, A.J., 2002. Serial quantitative diffusion tensor MRI of the premature brain: development in newborns with and without injury. J. Magn. Reson. Imaging 16, 621–632.

Mori, S., Wakana, S., Nagae-Poetscher, L.M., van Zijl, P.C.M., 2005. MRI Atlas of Human White MatterElsevier, Amsterdam.

Nagy, Z., Westerberg, H., Skare, S., Andersson, J.L., Lilja, A., Flodmark, O., Fernell, E., Holmberg, K., Bohm, B., Forssberg, H., Lagercrantz, H., Klingberg, T., 2003. Preterm children have disturbances of white matter at 11 years of age as shown by diffusion tensor imaging. Pediatr. Res. 54, 672–679.

Partridge, S.C., Mukherjee, P., Henry, R.G., Miller, S.P., Berman, J.I., Jin, H., Lu, Y., Glenn, O.A., Ferriero, D.M., Barkovich, A.J., Vigneron, D.B., 2004. Diffusion tensor imaging: serial quantitation of white matter tract maturity in premature newborns. NeuroImage 22, 1302–1314.

Peterson, B.S., Vohr, B., Staib, L.H., Cannistraci, C.J., Dolberg, A., Schneider, K.C., Katz, K.H., Westerveld, M., Sparrow, S., Anderson, A.W., Duncan, C.C., Makuch, R.W., Gore, J.C., Ment, L.R., 2000. Regional brain volume abnormalities and long-term cognitive outcome in preterm infants. J. Am. Med. Assoc. 284, 1939–1947.

Rudanko, S.L., Fellman, V., Laatikainen, L., 2003. Visual impairment in children born prematurely from 1972 through 1989. Ophthalmology 110, 1639–1645.

Rezaie, P., Dean, A., 2002. Periventricular leukomalacia, inflammation and white matter lesions within the developing nervous system. Neuropathology 22, 106–132.

Schmithorst, V.I., Wilke, M., Dardzinski, B.J., Holland, S.K., 2002. Correlation of white matter diffusivity and anisotropy with age during childhood and adolescence: a cross-sectional diffusion-tensor MR imaging study. Radiology 222, 212–218.

Snook, L., Paulson, L.A., Roy, D., Phillips, L., Beaulieu, C., 2005. Diffusion tensor imaging of neurodevelopment in children and young adults. NeuroImage 26, 1164–1173.

Vannucci, R.C., Vannucci, S.J., 2005. Perinatal hypoxic–ischemic brain damage: evolution of an animal model. Dev. Neurosci. 27, 81–86.

Volpe, J.J., 2001. Neurobiology of periventricular leukomalacia in the premature infant. Pediatr. Res. 50, 553–562.

Volpe, J.J., 2003. Cerebral white matter injury of the premature infant—More common than you think. Pediatrics 112, 176–180.

Wakana, S., Jiang, H., Nagae-Poetscher, L.M., van Zijl, P.C.M., Mori, S., 2004. Fiber tract-based atlas of human white matter anatomy. Radiology 230, 77–87.

Abnormal orbitofrontal development due to prematurity

(Accepted)

Mónica Giménez MsC [1,2], Carme Junqué PhD [1,2,CA], Pere Vendrell PhD [1,2], Ana Narberhaus MsC [1], Núria Bargalló PhD [2,3], Francesc Botet MD, PhD [2,4], Josep M Mercader MD, PhD [2,3]

[1]Department of Psychiatry and Clinical Psychobiology, Faculty of Medicine, University of Barcelona.
[2]Institut d'Investigacions Biomèdiques August Pi i Sunyer (IDIBAPS).
[3]Neuroradiology Section, Radiology Department, Centre de Diagnòstic per la Imatge (CDI), Hospital Clínic.
[4]Pediatrics Section, Department of Obstetrics & Gynecology, Pediatrics, Radiology & Physics Medicine, Hospital Clínic.

***Objective*: To investigate the effects of prematurity on sulcal formation. *Methods*: We evaluated the depth and volume of the primary olfactory sulcus (developed at 16 weeks' gestation) and the secondary orbital sulci (which start to develop at 28 weeks' gestation) in a sample of 22 adolescents with history of very preterm birth (VPTB). We compared this preterm sample to a sample of subjects born at term and matched by age, gender and sociocultural status. The *"Anatomist/BrainVISA 3.0.1"* package was used to identify and to quantify the sulci. In addition, voxel based morphometry (VBM) was used to analyze possible reductions of gray and white matter in the orbitofrontal area. *Results*: Compared to controls, we found a significant reduction in the secondary sulci depth but not in the primary sulcus in the VPTB. VBM analysis showed reduced gray matter volume in VPTB in the orbital region. *Conclusions:* Prematurity affects cerebral gyrification and this impairment is not reversible during childhood. Identification of the specific factors involved in abnormal brain maturation may lead to effective interventions.**

[CA]Corresponding author: Dr. Carme Junqué, Department of Psychiatry and Clinical Psychobiology, University of Barcelona. Institut d'Investigacions Biomèdiques August Pi i Sunyer (IDIBAPS), C/ Casanova, 143, CP: 08036 Barcelona, Spain.
Phone: +34 93 403 44 46; Fax: +34 93 403 52 94
e-mail: cjunque@ub.edu

Acknowledgments of support
This work was supported by grants from the *Ministerio de Ciencia y Tecnología* (SAF2005-007340), and the *Generalitat de Catalunya* (2005 SGR 00855). M. Giménez holds a grant from the *Ministerio de Educación, Cultura y Deporte* (AP2002-0737).

Introduction

In full-term infants the surface of the brain at birth resembles the adult brain because the sulci are well developed. In contrast, the preterm cortex appears lissencephalic at birth[1]. The data on sulci development patterns in fetuses come mainly from neuropathological[2] and sonographical[3-5] studies. However, MRI has become an important source for identifying sulci and gyral abnormalities.[6-15]

MR studies demonstrated that brain maturation starts in the central area and proceeds toward the parieto-occipital cortex. The frontal cortex develops last[15]. The last areas to develop sulci are the frontobasal, frontolobar and anterior part of the temporal lobe.[16] In the human orbitofrontal cortex, the gestational age (GA) of sulci and gyrus maturation ranges from 16 to 44 weeks,[2] with medial-lateral and posterior-anterior development trends.

We hypothesized that prematurity would affect the sulci that were more immature at birth. Accordingly, we investigated structural abnormalities in orbitofrontal cortical folding in adolescents with history of very preterm birth (VPTB) in two different

sulcus types: a) the olfactory sulcus (primary sulcus) which appears early (≥16 gestational weeks), and b) the rest of the orbitofrontal sulci including the medial, lateral and transverse sulcus (secondary sulci).

Methods

Subjects

This study is a part of a larger project on cognitive and cerebral abnormalities associated to prematurity. The preterm children are a subgroup of a cohort enrolled in previous MRI studies,[17-19] recruited at the Pediatric Service of the Hospital Clinic in Barcelona. Inclusion criteria for this study were: current age between 12 and 17 years, and GA less than 32 weeks for preterm and GA of 37 weeks or more for controls. Exclusion criteria were: a) history of focal traumatic brain injury, b) cerebral palsy or other neurological diagnosis, c) motor or sensory impairments, and d) presence of global mental disabilities (IQ below 70). Twenty-two adolescents with a GA < 31 weeks participated. In the retrospective clinical files, five preterm subjects had history of intraventricular hemorrhage identified by ultrasonography. These 5 subjects had ventricular dilatation with posterior predominance. Five out of the 22 VPTB subjects had low weight for their GA. Preterm adolescents were matched by age, sex, and sociocultural status to 22 controls born at term. Controls had no brain abnormalities on the MRI and no history of neurological or psychiatric diseases. We used the Wechsler intelligence scales to obtain a global measure of intellectual functioning. Either the WAIS-III or the WISC-R was used, depending on the age of the subjects. Only 2 subjects had an IQ below 85 (borderline range). All subjects followed normal schooling, though 5 VPTB subjects had received extra educational support in the past and 5 were receiving extra educational support during the study period. Table 1 summarizes the main demographic and clinical characteristics of the groups.

The study was approved by the ethics committee of the University of Barcelona. All families gave written informed consent prior to participation.

Image Acquisition

MR images of each subject were acquired in a GE-Signa LX 1.5 Tesla scanner (General Electric, Milwaukee, Wisconsin). A set of high-resolution inversion recovery T1-weighted images was obtained with a fast spoiled gradient-recalled 3d sequence (TR/TE = 12/5.2 ms; TI 300 1 nex; field of view = 24 cm; 256x256 matrix); the whole-brain data were acquired in an axial plane yielding contiguous 1.5 mm slices. The inversion recovery T1 sequence parameter has been reported to be the best image type for creating a representation of the cortical topography using "*Anatomist/BrainVisa 3.0.1*".[20]

Sulci Measurements

To folding identification and to quantify the sulci we used the "*Anatomist/BrainVISA 3.0.1*" package (http://brainvisa.info/). This approach adapts the T1-weighted MR images in a structure which summarizes the main information about the cortical folding patterns. The program filters the huge amount of information in the gray levels in order to build a simplified graph formed by information nodes. Each

Table 1. Demographic and clinical characteristics of the sample

	Very Preterm Birth group Mean ± SD	Control group Mean ± SD	t statistic
Demographic data			
Age	14.8 ± 1.6	14.9 ± 1.5	t = -0.09
Gender (Males/Females)	10/12	10/12	
Clinical data			
Gestational age (weeks)	29.0 ± 1.6	39.8 ± 1.6	t = -21.81**
Weight at birth (grams)	1160.9 ± 297.5	3453.6 ± 398.0	t = -21.64**
IQ			
Verbal IQ	106.2 ± 17.8	115.3 ± 14.6	t = -1.84
Performance IQ	95.6 ± 12.3	105.7 ± 10.6	t = -2.90*
Full IQ	101.6 ± 14.8	112.2 ± 12.1	t = -2.60*
Early neurodevelopmental outcome			
Beginning of walking (months)	13.1 ± 3.3	11.7 ± 2.0	t = 1.47
Beginning of speech (months)	15.9 ± 5.5	17.5 ± 6.2	t = -0.72

*<0.05
**<0.001

node corresponds to elementary cortical folds, and the links correspond to the relative topographies of these folds.[20,21]

The sulci automatically detected by the program were inspected visually by two investigators (MG, PV) in order to correct misclassified sulci segments. To do so, they followed the patterns for the orbitofrontal sulci described by the Atlas of the Cerebral Sulci.[22] Figure 1 shows an example of sulci identification in two subjects. We obtained the depth for each sulcus: the primary sulcus and the secondary sulci (including the medial, lateral and transverse sulcus as a whole). The volume (mm^3) and the maximum depth of sulci (mm) were calculated (see Figure 2). The maximum depth of the primary and secondary sulci was calculated as the average of each maximum depth in each sulcus segment. In Figure 2, the maximum depth for the primary sulcus (B) was obtained through the two maximum depth values for each segment.

Voxel Based Morphometry Protocol

Since sulci characteristics are related to the adjacent gyri, a separate complementary volumetric analysis was conducted using the voxel based morphometry (VBM) approach to evaluate the possible gray and white matter volume reductions in the orbitofrontal gyri in the preterm group. The automatic image processing from both controls and VPTB subjects was done using *Statistical Parametric Mapping* (SPM2) software, running in Matlab 6.5 (MathWorks, Natick, MA). See Table 2 for the VBM protocol.

Table 2. Voxel Based Morphometry Protocol

1.- Reorientation of the original T1 images (N=44), attending to the anterior-posterior commissure orientation.
2.- Segmentation of the original images.
3.- Determination of the normalization parameters in the previous segmented gray matter images using a *standard gray matter template* from our laboratory including a sample of N=127 adolescents (68 preterms and 59 controls, mean age: 14.3 y $\pm$ 2.0). The template is adapted to the Montreal Neurological Institute-SPM coordinates.
8.- Application of the previous gray matter normalization parameters to the original T1 images.
9.- Segmentation of the original and normalized T1 images.
13.- Application of the Jacobean's determinants→ MODULATED IMAGES= **Volume**
14.- Smoothing of the modulated normalized gray matter files: Full-Width at Half-Maximum Gaussian Kernel= 8mm.
We repeated the same procedure for the white matter (we also had a standard white matter template from the same large sample. N=127)

Data Analysis

Sulci

We performed two 2x2x2 repeated measures ANOVA analyses (one for the depth and one for the volume) with hemispheric laterality and sulcus type as intra-subject factors, and group as inter-subject factor. The ANOVA for depth accounts for the differences between groups in the primary sulcus versus the secondary sulci, taking the hemispheric laterality into account. The ANOVA for volume accounts for the intra-sulci differences between groups.

Voxel Based Morphometry

Two separate regions of interest (ROI) analyses were conducted to evaluate the possible volume reductions in the orbitofrontal gyral region in the preterm sample. We selected two ROIs contained in the WFU-Pickatlas toolbox software for SPM, version 1.02 (Joseph Maldjian, Functional MRI Laboratory, Wake Forest University School of Medicine)[23]: a) the olfactory gyrus and b) the orbital gyrus. Both ROIs were based on normalized brains, adapted to the Montreal Neurological Institute coordinates. We evaluated both gray and white matter differences between groups involved in each ROI as defined above, using the SPM2 *t*-test group comparison. The VBM protocol was applied separately to the gray and white matter images.

We used the convention that the ROI group comparison results should survive at the corrected False Discovery Rate (FDR) P value ($P < 0.05$). Moreover, only clusters larger than 10 contiguous voxels were considered in the statistical model.

Results

Neuroradiological evaluation

Visual inspection of the MRI images from the 5 subjects with intraventricular hemorrhage showed ventricular dilatation with posterior predominance. Seven other subjects also had ventricular dilation, but no subjects had active hydrocephalus or shunt. Corpus callosum reductions were clinically reported in 5 patients; in 3 of these patients corpus callosum size was two standard deviations below the control group mean.

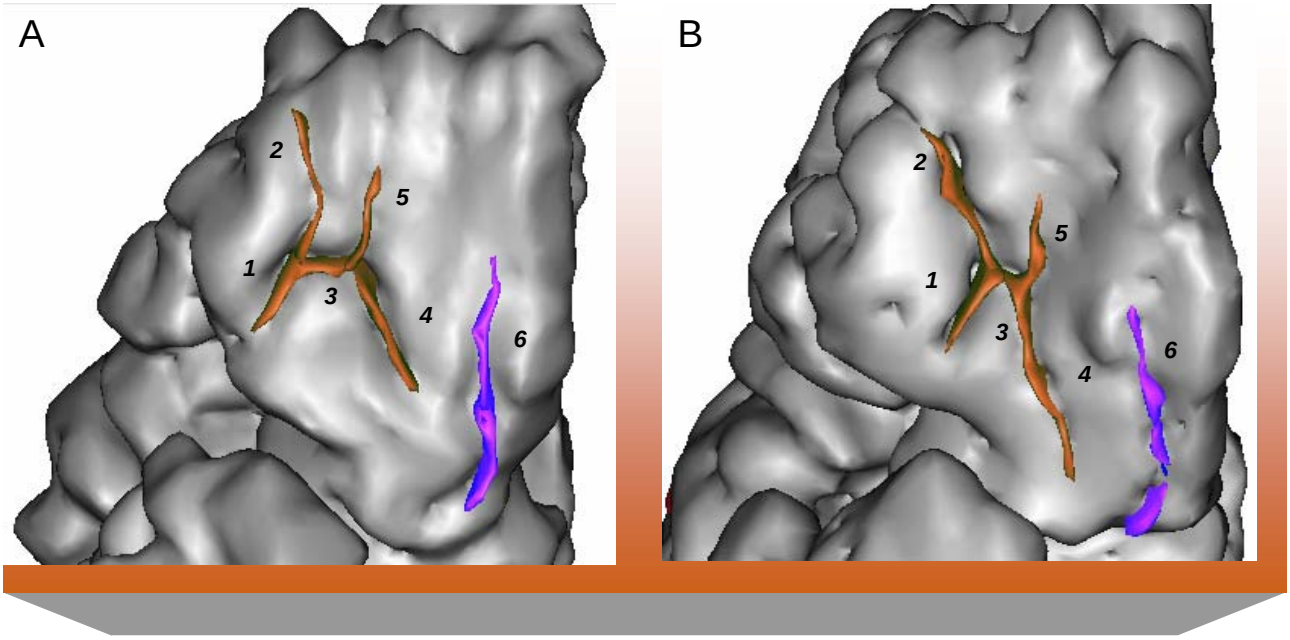

Figure 1.- Examples of the orbitofrontal sulci identification by the "Anatomist/BrainVisa 3.0.1": A) control subject; B) preterm subject. Numbers, 1: lateral orbital sulcus, caudal part; 2: lateral orbital sulcus, rostral part; 3: tranverse orbital sulcus; 4: medial orbital sulcus, caudal part; 5: medial orbital sulcus, rostral part; 6: olfactory sulcus.

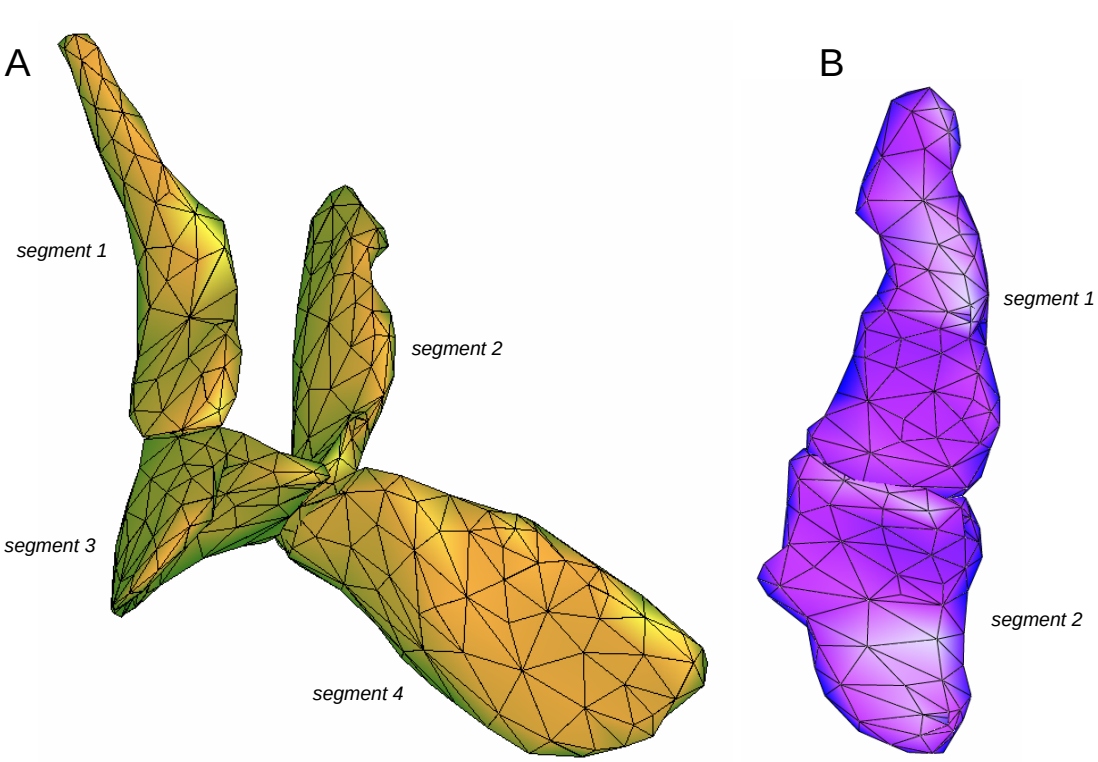

Figure 2.- Lateral view of the orbitofrontal sulci. Filled faces and wireframe appearance. A) secondary orbital sulci; B) primary sulcus (olfactory sulcus).

There were no cases of corpus callosum agenesia. In two cases T2-weighted MRI images showed mild white matter abnormalities. In addition the scores of hippocampal volumes in 8 patients were two standard deviations below the group mean (procedures for measurements of these structures were described elsewhere).[19,24]

Sulci Measurements
Descriptive data from sulcal measurements are detailed in Table 3. The ANOVA for sulcal depth showed significant interactions between type of sulcus (primary versus secondary) and group ($F_{1,42}$ = 5.492, P = 0.024) (see Figure 3). We observed significant reductions in the orbital sulci depth of the preterm group vs controls (bilateral preterm mean: 9.7 mm $\pm$ 1.0; bilateral control mean: 10.4 mm $\pm$ 0.8). Volumetric measures did not differ in the two groups ($F_{1,42}$ = 0.027, P = 0.871).

Voxel Based Morphometry: region of interest analyses
VBM showed a reduced gray matter volume in the preterm group in the orbital ROI, mainly involving the medial gyral region (cluster size = 88 mm^3, local maxima Talairach Coordinates = 4 51 -19, FDR-corrected p at voxel-level= 0.026). We found no significant gray matter volume differences between groups in the olfactory ROI. In the white matter comparison, no differences were found between groups for any gyral region.

Discussion

Consistent with our hypothesis, we observed a significant reduction in secondary sulci depth in adolescents with history of VPTB vs a term sample. In contrast, the depth of the primary sulcus was similar.

The dissociation between primary and secondary orbitofrontal sulci is consistent with the fetal stage of development of these sulci at birth. Whereas the primary olfactory sulci appear at 16 weeks of gestation and are prominent at 25 weeks, the secondary orbital sulci are not recognizable until 36 weeks.[2] All the subjects from our premature sample were born before week 32, period when the development of the secondary orbital sulci has just started.

In research into the cerebral effects of prematurity, qualitative scales of gyration have normally been used to estimate the cerebral maturation of the fetuses or the premature newborn.[7] Scales of this kind have been useful in general to identify cerebral maturation stage, to detect major neurological abnormalities, and to predict neurological outcomes of preterm newborns, but are unable to determine mild cerebral dysfunctions. Using a whole cortex convolution index a previous study found that preterm infants significantly differed from controls born at term.[1] These findings are to be expected given the difference in the groups' GA. A recent report introduced quantitative measures of cortical gyration such as the

Table 3. Measurements of the orbitofrontal sulci

	Very Preterm Birth group Mean $\pm$ SD	Control group Mean $\pm$ SD
LEFT HEMISPHERE		
Primary sulcus volume (mm^3)	242.2 $\pm$ 53.0	246.8 $\pm$ 72.6
Primary sulcus depth (mm)	11.0 $\pm$ 1.5	10.4 $\pm$ 1.1
Secondary sulci volume (mm^3)	376.0 $\pm$ 117.5	420.0 $\pm$ 114.2
Secondary sulci depth (mm)	9.8 $\pm$ 1.0	10.7 $\pm$ 1.0
RIGHT HEMISPHERE		
Primary sulcus volume (mm^3)	232.5 $\pm$ 77.8	278.9 $\pm$ 98.2
Primary sulcus depth (mm)	10.9 $\pm$ 1.9	10.8 $\pm$ 1.6
Secondary sulci volume (mm^3)	389.0 $\pm$ 117.8	385.9 $\pm$ 113.3
Secondary sulci depth (mm)	9.6 $\pm$ 1.2	10.1 $\pm$ 1.0

ratio of gyral height to width from volumetric MRI studies in premature newborns.[25] From the analysis of four cerebral regions (superior frontal, superior occipital, precentral and postcentral gyri) the authors obtained a gyral ratio which was found to be correlated with GA. These studies however cannot determine the possible persistence of gyral abnormalities after postnatal brain maturation.

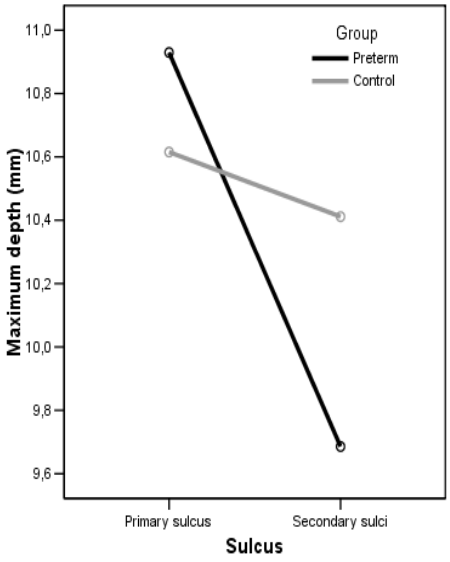

Figure 3.- Interaction effect between the sulcus type and group in the depth sulci analysis.

To our knowledge, there are no studies quantifying sulcal depth in adolescents with history of premature birth. Recently a study tested possible abnormalities in the temporal lobe associated to prematurity[26]. The authors used a gyrification index which is a measure of the degree of cortical folding, providing an estimate of gyral width. Larger values in this gyrification index suggest a higher degree of cortical folding and smaller gyral width. They reported that children born prematurely had increased gyrification in the bilateral temporal lobe at age of 8 years, but they did not explore the medial frontal lobe. These investigators demonstrated that the increase of the temporal lobe gyrification was related to decreases in the gray matter volume in the preterm sample. Sulcal depth has been previously investigated in patients with Williams's syndrome.[27,28] In these patients, in addition to bilateral reductions in sulcal depth in the intra/parietal/occipital sulcus, the authors observed a decrease in the depth of the left orbitofrontal region, and a correlation between intra/parietal/occipital sulcal depth and gray matter reduction in the same area.

In our study, we observed that sulcal depth reductions in the orbital sulci were accompanied by reduced gray matter volume in the same area using VBM analysis. This finding suggests that sulcal abnormality may be caused by gray matter reduction. The mechanisms of folding are not fully known. It is currently believed that the pattern of cortical folding depends in part on the size of the cortical area which in turn is dependent on cell migration and the cell volume (dendritic and synaptic volumes).[29] In a large cohort of 119 premature infants a significant gray matter volume reduction was observed compared to controls. The reduction was independent of evident brain injury, such as intraventricular hemorrhage.[30] The authors of the investigation suggested that gray matter damage may be due to impaired neuronal differentiation with a reduction in dendritic and axonal development or neuronal loss. In addition, periventricular white matter lesions may also contribute to gray matter reductions. The destruction of ascending and descending axons in white matter can result in damage of overlying cortical gray matter. The specific vulnerability of oligodendrocytes to the effects of ischemia and infection in the immature brain[31] could lead to a primary white matter impairment and secondary gray matter damage. There is a study that clearly demonstrated that periventricular white matter injury in the premature infant is followed by reduced cortical gray matter volume at term[32]. In our study only 2 subjects had mild white matter lesion on clinical MRI visual inspection. This low frequency compared to other samples[33] may be due to our inclusion criteria which excluded all subjects with sensory or motor impairments. However, our subjects probably had subtle white matter damage, as has been observed in voxel-based morphometry studies.[34]

The secondary orbitofrontal sulci comprise the medial and lateral orbital sulci, and the transverse sulcus.[14] Since these components have a high inter-subject variability and are difficult to separate automatically, we took the secondary orbital sulci as a whole. Future MRI procedures for the separate analysis of each secondary orbital sulcus would be of interest because they mature at different rates. The medial and lateral orbital sulci can be initially distinguished around the 28th week of gestation, but the anterior and posterior

parts of the orbital sulci are not identified until week 36.[2]

Several cortical gray matter changes occur between childhood and adolescence, and the peak of the development of the frontal lobe is around age twelve.[35,36] Since the cortical maturation in the orbital area in our sample was completed, sulcal abnormality seems to be a definitive sequela of premature birth.

An important question is whether the adverse effects on brain development are caused by prematurity per se, by other concomitant negative factors (mainly complications in the early neonatal period) or both. Identification of the specific factors involved may lead to effective interventions. An increasingly number of studies demonstrates negative effects of prematurity on brain development, in preterm infants with[32] and without brain lesions.[30] Increasingly sophisticated quantitative MR-techniques are available, as used in this study, for detecting subtle changes on brain structure, which might influence cognitive and behavioral development. Future studies are needed to show the link between those.

References

1. Ajayi-Obe M, Saeed N, Cowan FM, Rutherford MA, Edwards AD. Reduced development of cerebral cortex in extremely preterm infants. The Lancet 2000;356: 1162-1163.

2. Chi JG, Dooling EC, Gilles FH. Gyral development of the human brain. Ann Neurol 1977;1:86-93.

3. Huang CC. Sonographic cerebral sulcal development in premature newborns. Brain Dev 1991;13:27-31.

4. Monteagudo A, Timor-Tritsch IE. Development of fetal gyri, sulci and fissures: a transvaginal sonographic study. Ultrasound Obstet Gynecol 1997;9:222-228

5. Toi A, Lister WS, Fong KW. How early are fetal cerebral sulci visible at prenatal ultrasound and what is the normal pattern of early fetal sulcal development? Ultrasound Obstet Gynecol 2004;24:706-715.

6. Abe S, Takagi K, Yamamoto T, Kato T. Assessment of cortical gyrus and sulcus formation using magnetic resonance images in small-for-gestational-age fetuses. Prenat Diagn 2004;24:333-338.

7. Abe S, Takagi K, Yamamoto T, Okuhata Y, Kato T. Assessment of cortical gyrus and sulcus formation using MR images in normal fetuses. Prenat Diagn 2003;23:225-231.

8. Azoulay R, Fallet-Bianco C, Garel C, Grabar S, Kalifa G, Adamsbaum C. MRI of the olfactory bulbs and sulci in human fetuses. Pediatr Radiol 2006;36:97-107.

9. Battin MR, Maalouf EF, Counsell SJ, et al. Magnetic resonance imaging of the brain in very preterm infants: visualization of the germinal matrix, early myelination, and cortical folding. Pediatrics 1998;101: 957-962.

10. Chiavaras MM, LeGoualher G, Evans A, Petrides M. Three-dimensional probabilistic atlas of the human orbitofrontal sulci in standardized stereotaxic space. Neuroimage 2001;13:479-496.

11. Chiavaras MM, Petrides M. Orbitofrontal sulci of the human and macaque monkey brain. J Comp Neurol 2000;422:35-54.

12. Garel C, Chantrel E, Brisse H, et al. Fetal cerebral cortex: normal gestational landmarks identified using prenatal MR imaging. Am J Neuroradiol 2001;22:184-189.

13. Huttner HB, Lohmann G, von Cramon DY. Magnetic resonance imaging of the human frontal cortex reveals differential anterior-posterior variability of sulcal basins. Neuroimage 2005;25:646-651.

14. Lacerda AL, Hardan AY, Yorbik O, Keshavan MS. Measurement of the orbitofrontal cortex: a validation study of a new method. Neuroimage 2003;19:665-673.

15. Ruoss K, Lovblad K, Schroth G, Moessinger AC, Fusch C. Brain development (sulci and gyri) as assessed by early postnatal MR imaging in preterm and term newborn infants. Neuropediatrics 2001;32:69-74.

16. van der Knaap MS, van Wezel-Meijler G, Barth PG, Barkhof F, Ader HJ, Valk J. Normal gyration and sulcation in preterm and term neonates: appearance on MR images. Radiology 1996;200:389-396.

17. Gimenez M, Junque C, Narberhaus A, Botet F, Bargallo N, Mercader JM. Correlations of thalamic reductions with verbal fluency impairment in those born prematurely. Neuroreport 2006;17:463-466.

18. Gimenez M, Junque C, Narberhaus A, et al. Hippocampal gray matter reduction associates with memory deficits in adolescents with history of prematurity. Neuroimage 2004;23:869-877.

19. Gimenez M, Junque C, Vendrell P, et al. Hippocampal functional magnetic resonance imaging during a face-name learning task in adolescents with antecedents of prematurity. Neuroimage 2005;25:561-569.

20. Riviere D, Mangin JF, Papadopoulos-Orfanos D, Martinez JM, Frouin V, Regis J. Automatic recognition of cortical sulci of the human brain using a congregation of neural networks. Med Image Anal 2002;6:77-92.

21. Mangin JF, Riviere D, Cachia A, et al. A framework to study the cortical folding patterns. Neuroimage 2004;23:S129-138.

22. Ono M, Kubik S, Abernathey CD. Atlas of the Cerebral Sulci. New York: Thieme Medical Publishers, 1990.

23. Maldjian JA, Laurienti PJ, Kraft RA, Burdette JH. An automated method for neuroanatomic and cytoarchitectonic atlas-based interrogation of fMRI data sets. Neuroimage 2003;19:1233-1239.

24. Caldu X, Narberhaus A, Junque C, et al. Corpus callosum size and neuropsychologic impairment in adolescents who were born preterm. J Child Neurol 2006;21 (In press).

25. Deipolyri AR, Mukherjee P, Gill K, et al. Comparing microstructural and macrostuctural development of the cerebral cortex in premature newborns: Diffusion tensor imaging versus cortical gyration. Neuroimage 2005;27:579-586.

26. Kesler SR, Vohr B, Schneider KC, et al. Increased temporal lobe gyrification in preterm children. Neuropsychologia 2006;44:445-453.

27. Kippenhan JS, Olsen RK, Mervis CB, et al. Genetic contribution to human gyrification; sulcal morphometry in Willimas syndrome. J Neurosci 2005;25:7840-7846.

28. Thompson PM, Lee AD, Dutton RA, et al. Abnormal cortical complexity and thickness profiles mapped in Williams syndrome. J Neurosci 2005;25:4146-4158.

29. Mima T, Mikawa T. Folding of the tectal cortex by local remodeling of neural differentiation. Dev Dyn 2004;229:475-479.

30. Inder TE, Warfield SK, Wang H, Huppi PS, Volpe JJ. Abnormal cerebral structure is present at term in premature infants. Pediatrics 2005, 115, 286-294.

31. Blumenthal I. Periventricular leucomalacia: a review. Eur J Pediatr 2004;163:435-442.

32. Inder TE, Huppi PS, Warfield S, et al. Periventricular white matter injury in the premature infant is followed by reduced cerebral cortical gray matter volume at term. Ann Neurol 1999;46:755-760.

33. Stewart AL, Rifkin L, Amess PN, Kirkbridge V et al. Brain structure and neurocognitive and behavioral function in adolescents who were born very preterm. Lancet 1999;353:1653-57.

34. Gimenez M, Junqué C, Narberhaus A, Bargallo N, Botet F, Mercader JM. White matter volume and concentration reductions in adolescents with antecedents of very preterm birth: A voxel-based morphometry study. Neuroimage 2006 (In Press)

35. Paus T. Mapping brain maturation and cognitive development during adolescence. Trends Cogn Sci 2005;9:60-68.

36. Giedd JN, Blumenthal J, Jeffries NO, et al. Brain development during childhood and adolescence: a longitudinal MRI study. Nat Neurosci 1999;2:861-863.

Medial temporal MR spectroscopy is related to memory performance in normal adolescent subjects

Mónica Giménez,[1,2] Carme Junqué,[1,2,CA] Ana Narberhaus,[1] Xavier Caldú,[1,2] Dolors Segarra,[1] Pere Vendrell,[1,2] Núria Bargalló[2,3] and Josep M. Mercader[2,3]

[1]Department of Psychiatry and Clinical Psychobiology, University of Barcelona; [2]Institut d'Investigacions Biomèdiques August Pi i Sunyer (IDIBAPS), c/Casanova 143, C.P. 08036, Barcelona; [3]Neuroradiology Section, Radiology Department, Centre de Diagnóstic per la Imatge (CDI), Hospital Clínic, Faculty of Medicine, University of Barcelona, Barcelona, Spain

[2,CA]Corresponding Author: cjunque@ub.edu

Received 23 December 2003; accepted 6 January 2004

DOI: 10.1097/01.wnr.0000117645.40277.6a

In addition to the study of pathological conditions, magnetic resonance spectroscopy can provide useful information about brain–behavior relationships in normal subjects. Recently, there have been reports of correlations between *N*-acetylaspartate (NAA) values and cognitive functions in normal adults. We tested the possible specific relationship between the NAA/choline (Cho) ratio in the medial temporal lobe and memory performance in normal adolescents. The medial temporal NAA/Cho ratio was unrelated to age, gender and general intelligence but presented a clear correlation with several memory measures. In the regression analysis two memory variables (RAVLT learning and a face–name recognition task) explained 55.6% of NAA/Cho variance. We conclude that NAA values in the medial temporal lobe are related to memory abilities but not to global intelligence in normal adolescent subjects. *NeuroReport* 15:703–707 © 2004 Lippincott Williams & Wilkins.

Key words: Adolescent; Brain metabolism; Hippocampus; Medial temporal lobe; Memory; MRI; *N*-acetylaspartate; Neuropsychology

INTRODUCTION

Magnetic resonance spectroscopy (MRS) is an *in vivo* quantitative neurochemical technique that can be used to assess normal and abnormal brain functions. Proton MRS (^{1}H-MRS) provides values of *N*-acetylaspartate (NAA), which has been proposed as a marker of neuronal integrity [1]. NAA studies have been performed in psychiatric diseases mainly to increase the cumulative evidence on the neurobiological bases of illnesses such as depression or schizophrenia [2,3]. ^{1}H-MRS studies have been used to investigate the relationship between memory impairment and medial temporal NAA deficits in epilepsy [4–7] and in the elderly [8–12].

Previous investigations [13,14] provided the first evidence that MRS might identify biochemical markers of intelligence in normal subjects, finding a correlation between NAA concentration in the left occipitoparietal white matter cortex and the Full-Scale Intelligence Quotient and other cognitive abilities. Similarly, in aged normal subjects, some selectivity of neuropsychological functions and neurochemical focal data have been reported [15]. We therefore investigated the possible relationship between memory performance and NAA concentrations in the medial temporal lobe in an adolescent sample. To our knowledge, no ^{1}H-MRS studies have been carried out in normal adolescents to explore the relationship between specific memory functions and medial temporal lobe NAA levels. We selected the NAA/choline (Cho) ratio because NAA is found almost exclusively in neurons and Cho is a constituent of both neurons and glia. The ^{1}H-MRS Cho signal comprises different compounds such as glycerophosphocholine and phosphocholine. In addition, several left hippocampal single-voxel spectroscopic studies have shown that the NAA/Cho variation coefficients are minimal in this structure [16].

MATERIALS AND METHODS

Subjects: The sample comprised 21 young subjects (11 girls and 10 boys) who agreed to participate as normal controls in a project on the long-term consequences of prematurity. The study was approved by the ethics committee of the University of Barcelona and a state research committee. All the subjects or their family gave written informed consent. Exclusion criteria were: history of prematurity; a history of neurological, psychiatric or traumatic brain injury and the presence of mental or learning disabilities. The ages ranged from 10 to 18 (mean = 14.05 ± 2.46 s.d.). Two subjects were left-handed.

MRI and spectroscopy: ^{1}H-MRS was performed on a 1.5 T whole body MR scanner (General Electric Signa System; Milwaukee, WI) with a standard quadrature head coil. Proton spectra were obtained from a single-voxel ($2 \times 2 \times 2\,cm^3$) in the coronal plane. In all the subjects the voxel was placed in the left midtemporal region, covering most of the hippocampus in all the cases. The mid-brain cistern was used as the landmark to locate the voxel in all subjects, although in some cases it was necessary to move the voxel to avoid CSF contamination. This procedure was applied in the same manner in all subjects and care was taken to ensure standard placement. Water-suppressed spectra were acquired using a double-spin echo point-resolved spectroscopy sequence (PRESS) with a repetition time of 1500 ms and echo times of 35 ms for the midtemporal lobe voxel. For this location, NAA (at 2.0 p.p.m.) and Cho (at 3.15 p.p.m.) peaks were obtained, as well as the NAA/Cho ratio. The spectra were analyzed using the manufacturer-supplied spectroscopy software package for the MR system (Fig. 1). Each subject underwent ^{1}H-MRS imaging in the same month as the neuropsychological assessment.

Neuropsychological assessment: We used the Wechsler intelligence scales to obtain an estimation of global intellectual functioning. Either the WAIS-III or the WISC-R was used, depending on the age of the subject. To assess memory functions we selected a modified version of the Auditory Verbal Learning Test (RAVLT). The RAVLT was administered as follows. A list of 15 words (list A) was read aloud to the subject. The first five trials were applied as a repeated reading of the same word list, followed by asking the subject to recall as many words as possible, in any order. The next trial was the interference trial in which a new list (list B) was read aloud to the subject and free recall was requested. Trial seven was administered in the same way as trial six (no reading of list A) but after a 20-min delay. We obtained four memory measures: (a) the recall of the 15-word list immediately after the first oral presentation was taken as a measure of immediate memory; (b) the sum of the words recalled during the first five trials was taken as a measure of verbal learning; (c) recognition was tested by asking the respondent to mark (on a piece of paper showing a long list of words) which words from a set of 30 were from the 15-word list (list A) and which were not; (d) long-term retention was evaluated as the percentage of words lost after 20 min of interference. The formula used to create this variable was (presentation of trial 7−presentation of trial 5/ sum of words recalled across the 5 presentations × 100). Details of these tests are described by Lezak [20].

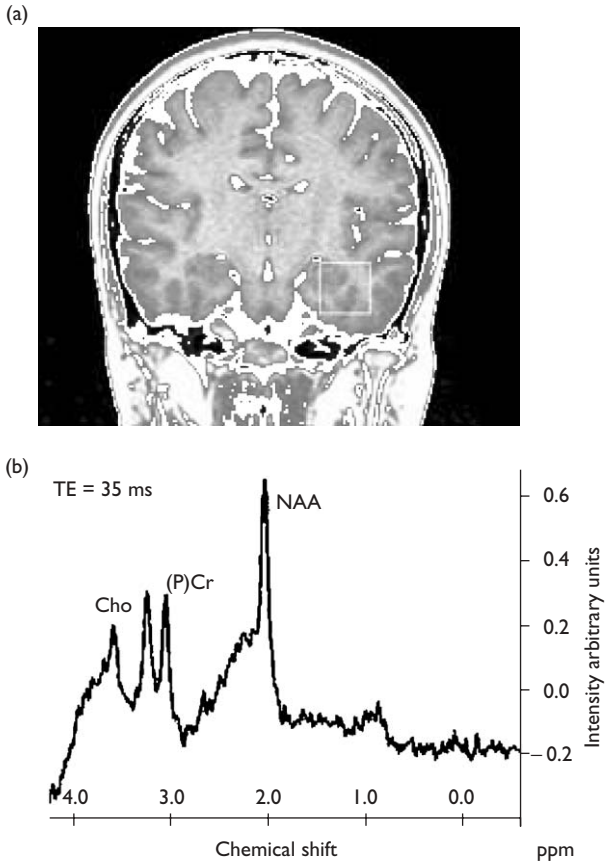

Fig. 1. Voxel placement and proton magnetic resonance spectra from the volume of interest in the sample. (**a**) Single voxel ($2 \times 2 \times 2\,cm^3$) located in the left midtemporal lobe from a coronal section. (**b**) Corresponding proton MR spectra below were acquired with TR=1500 and TE=35 ms.

Face–name memory task: The task consisted of a modified version of the design for hippocampal activation in an fMRI paradigm [21]. The two conditions were, first the target task (or novel face–name pairs), in which subjects examined 16 novel face–name pairs (eight male and eight female). Each pair was presented for 2 s with a dark background, followed by a blank screen period of 1 s; second, the control task (or repeated face–name pairs), in which subjects examined two repeated face–name pairs (one male and one female). Each pair was presented for 2 s with a dark background, followed by a blank screen period of 1 s. Sequences of alternating periods of active (48 s) and control (48 s) conditions were repeated for a total of 6 min 24 s, resulting in 192 images of 20 slices each. The series began with a control condition. All the stimuli were back-projected (by a Sanyo Multimedia Prox-III) onto a screen which subjects viewed through a mirror located on the scanner's head coil. Stimuli were generated in a Hewlett Packard computer by the Presentation 0.45 program (Neurobehavioral Systems, USA). Participants were administered a checked memory test to assess the number of novel face–name pairs remembered just after MRI acquisition. Two measures were obtained: free recall (by asking the name of each face directly without any clue) and recognition (by providing the 16 names on independent cards). This task has proved to be a consistent predictor of hippocampal activation [17]. ^{1}H-MRS imaging acquisition was obtained just after the fMRI memory task.

RESULTS

The statistical descriptive values of regional NAA/Cho metabolite concentrations, memory scores and IQ performance from all subjects are shown in Table 1.

Pearson correlation analysis was used to test the possible relationship between the NAA/Cho ratio and neuropsychological performance (Table 2). We found a strong positive correlation between the NAA/Cho ratio and the RAVLT list A immediate recall (r=0.579, p=0.006), and learning (r=0.590, p=0.005). We also found a negative correlation

Table 1. Memory and NAA/Cho results.

	Mean	s.d.	Range
Auditory Verbal Learning Test memory results (RAVLT)			
Immediate recall	6.95	1.99	3–10
Learning sum of trials 1–5	56.29	6.02	44–67
Long-term retention	11.88	2.86	6.90–19.55
Recognition	14.71	0.64	13–16
Face–Name task			
Free recall	10.52	4.06	3–16
Recognition	13.19	3.46	3–16
Intelligence quotient (IQ)			
Global IQ	116.43	7.98	100–133
Verbal IQ	120.43	7.64	111–138
Manipulative IQ	108.19	10.24	88–125
NAA/Cho ratio	1.70	0.22	1.41–2.23

Table 2. Correlations of NAA/Cho values with memory performance.

	Medial temporal NAA/Cho ratio
Auditory Verbal Learning Test memory (RAVLT)	
Immediate recall	0.579; p=0.006**
Learning sum of trials 1–5	0.590; p=0.005**
Long-term retention	−0.567; p=0.007**
Recognition	0.358; p=0.973
Face–Name task	
Free recall	0.559; p=0.008**
Recognition	0.511; p=0.018*
Intelligence Quotient (IQ)	
Global IQ	−0.017; p=0.942
Verbal IQ	0.009; p=0.968
Manipulative IQ	−0.008; p=0.973

*Significant at 0.05 level (bilateral).
**Significant at 0.01 level (bilateral).

between long-term memory loss and NAA/Cho ratio (r=−0.567, p=0.007): the higher the memory loss, the lower the NAA/Cho concentration. The plots of the significant correlations are depicted in Fig. 2. We also tested possible NAA/Cho relationships with age or gender. We did not find any significant difference for these variables (for age, r=0.377, p=0.092; for gender, t=0.947, p=0.356).

Correlation analysis between midtemporal NAA/Cho values and the face–name memory task showed a significant correlation between metabolite values and both memory measures, free recall and recognition (r=0.559, p=0.008; r=0.511; p=0.018, respectively; Fig. 3). In contrast, intelligence quotients were unrelated to the NAA/Cho ratio (r=−0.017, p=0.942). Step-wise linear regression was used to check the independent contribution to the model of each memory test measure. Specifically, the variables introduced as constants were: immediate memory, learning memory, long-term retention, the two face–name fMRI measures and age. Only two measures, RAVLT learning as the first step (R^2=0.348, F(1,19)=10.159; p=0.005) and face–name recognition as the second added variable (R^2=0.556, F(2,18)=11.293; p=0.001), entered the model, in this order, explaining 55.6% of the global variance.

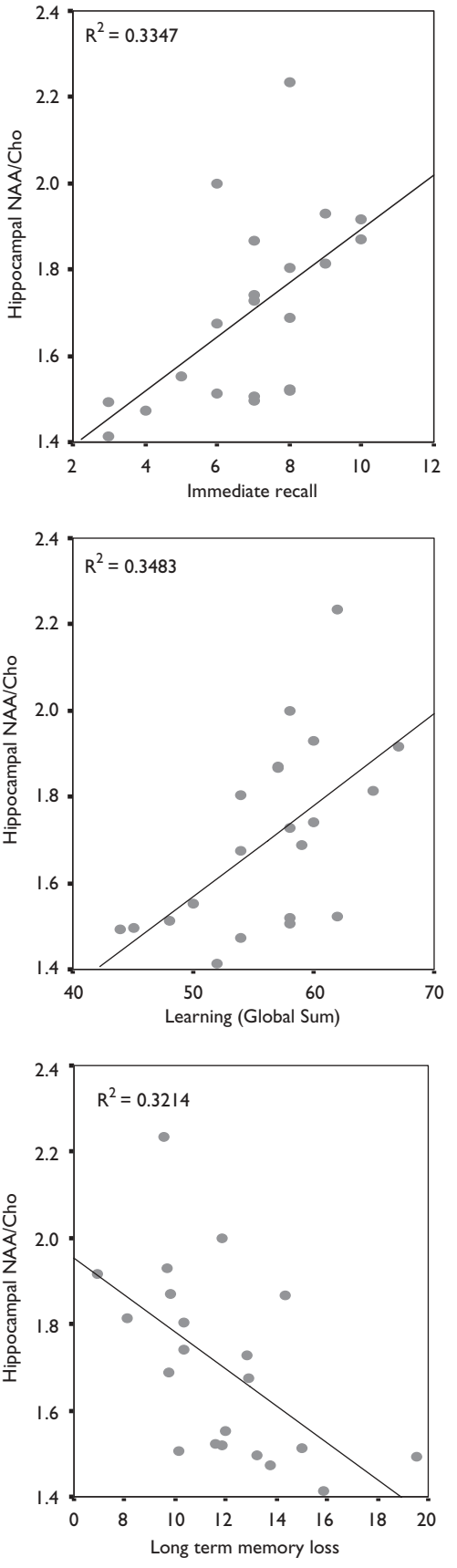

Fig. 2. Scatter plots showing the correlations between verbal memory variables and NAA/Cho ratio.

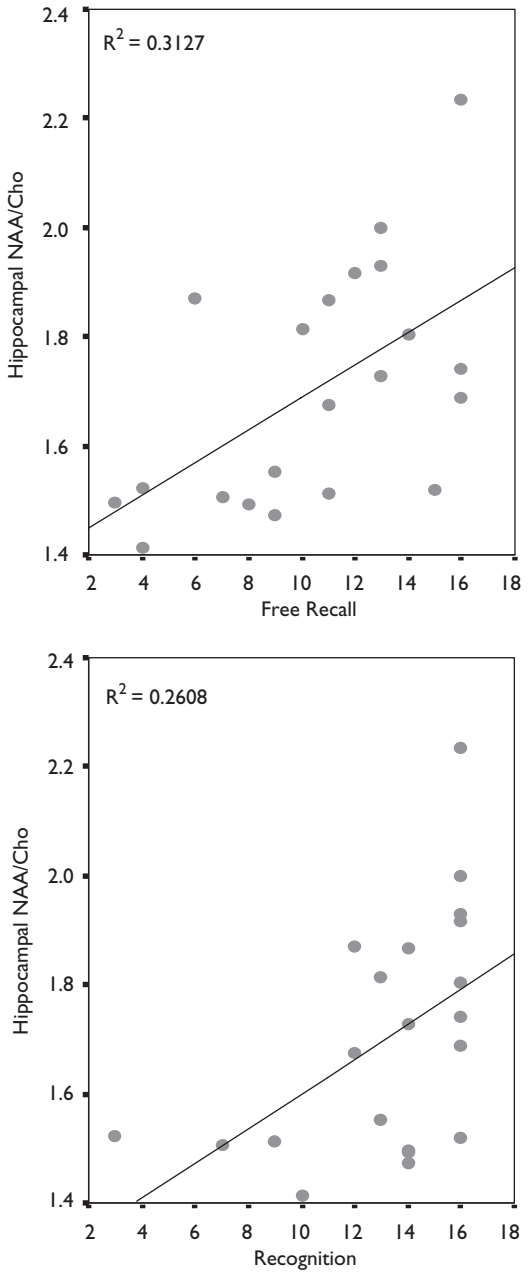

Fig. 3. Scatter plots showing the correlations between face–name learning task and NAA/Cho ratio.

DISCUSSION

Our results demonstrate a relationship between the medial temporal NAA/Cho ratio and memory performance in a normal adolescent sample. Simple correlation analysis indicated a positive relationship between performance on several memory variables (including immediate memory, learning, forgetting and face–name recognition) and NAA/Cho levels. Regression analysis showed that two memory variables (immediate memory and face–name recognition) explained half of the model's variance.

To our knowledge, this is the first study that relates memory capabilities in young people with NAA/Cho levels, although this relationship has been consistently reported in research on the neuropsychological correlates of memory impairment in epileptic subjects [4,5]. In other pathologies, such as traumatic brain injury, we also found correlations between temporal locations and memory performance, and between frontal locations and measures of attention and speed [18]. In schizophrenic patients we have found correlations between frontal MRS ROI and a task involving planning skills and procedural learning (Tower of Hanoi) [19]. Our paper corroborates previous reports that voxel location indicates the functional state of the corresponding cerebral region. This appears to be the case for both white and gray matter [15]. Although the definitive significance of NAA concentrations is still not known, it seems that NAA reductions may reflect mitochondrial function and myelin turnover [13]. Initially, NAA/Cho was proposed as a neuronal marker because NAA is present almost exclusively in neurons and Cho in all brain cells [20] but it was subsequently observed that NAA values change dramatically during infancy [21] and that NAA direct values or ratios change after pharmacological treatment [22,23]. It is possible, therefore, that NAA/Cho ratios reflect functional states more than structural substrates. Our results appear to disagree with those obtained in normal adult subjects, in whom significant positive correlations between the NAA/Cho ratio and intelligence have been reported [13–15]. We found no significant correlation between intelligence measures and the metabolite ratio values. It should be noted that we selected the medial temporal regions, focusing on the well-known relationships between the hippocampus and declarative memory. The studies by Jung *et al.* [13,14] and Valenzuela *et al.* [15] selected the posterior occipitoparietal regions, which are more likely to be related to high levels of cerebral functioning. One limitation of the present study was the relatively large size of the voxel, which covered other temporal medial regions in addition to the hippocampus. Another limitation is that in our design we did not contrast the midtemporal region metabolite changes with other cerebral regions, and were thus unable to demonstrate cerebral regional specificity. In summary, our main finding is the relationship between midtemporal metabolic NAA/Cho values and memory function, independent of general IQ, in an adolescent sample.

REFERENCES

1. Block W, Träber F, Flacke S, Jessen F, Pohl C and Schild H. *In-vivo* proton MR-spectroscopy of the human brain: assessment of N-acetylaspartate (NAA) reduction as a marker for neurodegeneration. *Amino Acids* **23**, 317–323 (2002).
2. Bertolino A and Weinberger DR. Proton magnetic resonance spectroscopy in schizophrenia. *Eur J Radiol* **30**, 132–141 (1999).
3. Farchione TR, Moore GJ and Rosenberg DR. Proton magnetic resonance spectroscopic imaging in pediatric major depression. *Biol Psychiatry* **52**, 86–92 (2002).
4. Sawrie SM, Martin RC, Knowlton R, Faugth E, Gilliam F and Kuzniecky R. Relationships among hippocampal volumetry, proton magnetic resonance spectroscopy, and verbal memory in temporal lobe epilepsy. *Epilepsia* **42**, 1403–1407 (2001).
5. Vermathen P, Laxer KD, Matson GB and Weiner MW. Hippocampal structures: anteroposterior N-acetylaspartate differences in patients with epilepsy and control subjects as shown with proton MR spectroscopic imaging. *Radiology* **214**, 403–410 (2000).
6. Ferrier CH, Alarcón G, Glover A, Koutroumanidis M, Morris RG, Simmons A *et al.* N-Acetylaspartate and creatine levels measured by (1)H-MRS relate to recognition memory. *Neurology* **55**, 1874–1883 (2000).

7. Martin RC, Sawrie S, Hugg J, Gilliam F, Faught E and Kuzniecky R. Cognitive correlates of ^{1}H MRSI-detected hippocampal abnormalities in temporal lobe epilepsy. *Neurology* **53**, 2052–2058 (1999).
8. Valenzuela MJ, Jones M, Wen W, Rae C, Graham S, Shnier R *et al*. Memory training alters hippocampal neurochemistry in healthy elderly. *Neuroreport* **14**, 1333–1337 (2003).
9. Schuff N, Amend DL, Knowlton R, Norman D, Fein G and Weiner MW. Age-related metabolite changes and volume loss in the hippocampus by magnetic resonance spectroscopy and imaging. *Neurobiol Aging* **20**, 279–285 (1999).
10. Angelie E, Bonmartin A, Boudraa A, Gonnaud PM, Mallet JJ and Sappey-Marinier D. Regional differences and metabolic changes in normal aging of the human brain: proton MR spectroscopic imaging study. *Am J Neuroradiol* **22**, 119–127 (2001).
11. Ferguson KJ, MacLullich AM, Marshall I, Deary IJ, Starr JM, Seckl JR *et al*. Magnetic resonance spectroscopy and cognitive function in healthy elderly men. *Brain* **125**, 2743–2749 (2002).
12. Bartrés-Faz D, Junqué C, Clemente IC, López-Alomar A, Bargalló N, Mercader JM *et al*. Relationship among ^{1}H-magnetic resonance spectroscopy, brain volumetry and genetic polymorphisms in humans with memory impairment. *Neurosci Lett* **327**, 177–180 (2002).
13. Jung RE, Brooks WM, Yeo RA, Chiulli SJ, Weers DC and Sibbitt WL. Biochemical markers of intelligence: a proton MR spectroscopy study of normal human brain. *Proc R Soc Lond B Biol* **266**, 1375–1379 (1999).
14. Jung RE, Yeo RA, Chiulli SJ, Sibbit WL, Weers DC, Hart BL *et al*. Biochemical markers of cognition: a proton MR spectroscopy study of normal human brain. *Neuroreport* **10**, 3327–3331 (1999).
15. Valenzuela MJ, Sachdev PS, Wen W, Shnier R, Brodaty H and Gillies D. Dual voxel proton magnetic resonance spectroscopy in the healthy elderly: subcortical-frontal axonal N-acetylaspartate levels are correlated with fluid cognitive abilities independent of structural brain changes. *Neuroimage* **12**, 747–756 (2000).
16. Hsu YY, Chen MC, Lim KE and Chang C. Reproductibility of hippocampal single-voxel proton MR spectroscopy and chemical shift imaging. *Am J Neuroradiol* **176**, 529–536 (2001).
17. Sperling R, Bates J, Cocchiarella A, Schacter DL, Rosen BR and Albert MS. Encoding novel face-name associations: a functional MRI study. *Hum Brain Mapp* **14**, 129–139 (2001).
18. Ariza M, Junqué C, Mataró M, Poca MA, Bargalló N, Olondo M *et al*. Neuropsychological correlations of basal ganglia and medial temporal lobe NAA/Cho reductions in traumatic brain injury. *Arch Neurol-Chicago* (in press) (2004).
19. Giménez M, Junqué C, Pérez M, Vendrell P, Baeza I, Salamero M *et al*. Basal ganglia N-acetylaspartate correlates with the performance in the procedural task Tower of Hanoi of neuroleptic-naive schizophrenic patients. *Neurosci Lett* **347**, 97–100 (2003).
20. Urenjak J, Williams SR, Gadian DG and Noble M. Specific expression of N-acetyl-aspartate in neurons, oligodendrocytetype-2 astrocyte progenitors, and immature oligodendrocytes *in vitro*. *J Neurochem* **59**, 55–61 (1992).
21. Horska A, Kaufmann WE, Brant LJ, Naidu S, Harris JC and Barker PB. *In vivo* quantitative proton MRSI study of brain development from childhood to adolescence. *J Magn Res Imaging* **15**, 137–143 (2002).
22. Heimberg C, Komoroski RA, Lawson WB, Cardwell D and Karson CN. Regional proton magnetic resonance spectroscopy in schizoprenia and exploration of drug effect. *Psychiatry Res* **83**, 105–115 (1998).
23. Bertolino A, Callicott JH, Mattay VS, Weidenhammer KM, Rakow R, Egan MF *et al*. The effect of treatment with antipsychotic drugs on brain N-acetylaspartate measures in patients with schizophrenia. *Biol Psychiatry* **49**, 39–46 (2001).

Acknowledgements: This study was supported by grants SAF2002-00836 (Ministerio de Ciencia y Tecnología), 200ISGR 00139 (Generalitat de Catalunya), a 2003FI00191 (Generalitat de Catalunya) to X.C., a research grant from the University of Barcelona to A.N. and the grant AP2002-0737 (Ministerio de Educación, Cultura y Deporte) to M.G.

Proton magnetic resonance spectroscopy reveals medial temporal metabolic abnormalities in adolescents with history of preterm birth

Prematurity and metabolic abnormalities
(Submitted)

Monica Gimenez MsC [1,2], *Carme Junque PhD [1,2], Francesc Botet MD, PhD [2,3], Nuria Bargallo PhD [4], Carles Falcon PhD [2,5], Josep Maria Mercader MD, PhD [2,4]

[1] Department of Psychiatry and Clinical Psychobiology, Faculty of Medicine, University of Barcelona, C/ Casanova 143, 08036 Barcelona, Spain
[2] Institut d'Investigacions Biomèdiques August Pi i Sunyer (IDIBAPS), C/ Villarroel 170, 08036 Barcelona, Spain
[3] Pediatrics Section, Department of Obstetrics & Gynecology, Pediatrics, Radiology & Physics Medicine, Hospital Clínic, C/ Sabino Arana 1, 08028 Barcelona, Spain
[4] Neuroradiology Section, Radiology Department, Centre de Diagnòstic per la Imatge (CDIC), Hospital Clínic, C/ Villarroel 170, 08036 Barcelona, Spain
[5] Biophysics & Bioengineering Unit. Department of Physiological Sciences, Faculty of Medicine, University of Barcelona, C/ Casanova 143, 08036 Barcelona, Spain

Prematurity is associated with volumetric reductions in specific brain areas such as the hippocampus and also with metabolic changes that can be detected by spectroscopy. Short echo time (35ms) Proton Magnetic Resonance Spectroscopy (^{1}H-MRS) was performed to assess possible medial temporal lobe metabolic abnormalities in 21adolescents with preterm birth (mean age: 14.8, SD: 1.3) compared to a control sample. ^{1}H-MRS spectra were analyzed with linear combination model fitting, obtaining the absolute metabolite concentrations for Creatine (Cr) and myo-inositol (Ins). In addition, the following metabolite sums were measured: total Ch (glycerophospho-choline+phosphocholine), total NA (N-acetyl-aspartate+N-acetyl-aspartylglutamate), and total Glx (glutamate+glutamine). A stereological analysis was performed to calculate hippocampal volume. Absolute Cr, Ins, and total NA values were decreased in the preterm group ($p=0.001$; $p=0.018$; $p<0.0001$, respectively). The preterm also showed a hippocampal reduction ($p<0.0001$). Significant relationships were found between gestational age and different metabolites and the hippocampal volume ($p<0.01$). Moreover, Cr and total NA correlated positively with the hippocampal volume in the whole sample ($p=0.001$ and $p<0.0001$, respectively). Results demonstrate that prematurity affects medial temporal lobe metabolites, and that the alteration is related to structural changes, suggesting that the cerebral changes associated with an interruption of neurodevelopment are not reversible.

ABBREVIATIONS

Ch, glycerophospho-choline+phosphocholine
Cho, Choline
Cr, Creatine
CSF, cerebral spinal fluid
GA, gestational age
Glx, glutamate+glutamine
^{1}H-MRS, proton magnetic resonance spectroscopy
ICV, intracranial volume
Ins, myo -inositol
MRI, magnetic resonance imaging
NA: N-acetyl-aspartate+N-acetyl-aspartylglutamate
NAA, N-acetyl-aspartate
TE, echo time

Acknowledgments of support
This work was supported by grants from the *Ministerio de Ciencia y Tecnología* (SAF2005-007340), and the *Generalitat de Catalunya* (2005 SGR 00855). M. Giménez holds a grant from the *Ministerio de Educación, Cultura y Deporte* (AP2002-0737).

*Corresponding author: Dr. Carme Junqué, Department of Psychiatry and Clinical Psychobiology, University of Barcelona. Institut d'Investigacions Biomèdiques August Pi i Sunyer (IDIBAPS), C/ Casanova, 143, CP: 08036 Barcelona, Spain.
Phone: +34 93 403 44 46; Fax: +34 93 403 52 94
e-mail: cjunque@ub.edu

Introduction

In vivo Proton Magnetic Resonance Spectroscopy (^{1}H-MRS) is a neurochemical technique used to investigate specific brain metabolites, which can expand on the structural and functional information obtained by other neuroimaging techniques. Volumetric magnetic resonance imaging (MRI) analyses of subjects with history of preterm birth showed temporal gray matter reductions (1) and also hippocampal changes that persist until the adolescence (2-3).

A previous study reported that preterms evaluated at 40 gestational weeks showed increased N-acetyl-aspartate (NAA) compared to the concentrations at birth, and that the levels at the second examination did not differ from those of the full-term control group (4). These data suggest that metabolic decreases in the immature brain may normalize. In contrast, there are other data that showed a NAA/Choline (Cho) reduction in preterm newborns (5). In addition, a study in adolescents with preterm birth (<30 weeks of gestation) found a NAA/Cho+Creatine (Cr) reduction in the right temporal lobe in a subsample of preterms (N=9) compared to full-term subjects, suggesting a persistent deficit (6).

No investigations to date have assessed abnormalities in the absolute metabolic concentrations by means of the user-independent frequency domain-fitting program LCModel in a healthy preterm sample at long term or their relationship with hippocampal volumetric atrophy. The goal of our study was to determine whether single-voxel ^{1}H-MRS is able to detect alterations in the medial temporal lobe region that would support the hypothesis of long-term neurofunctional abnormalities in adolescents with preterm birth and normal MRI.

Methods

Subjects

The sample comprised 21 healthy adolescents born prematurely (all $\leq$ 34 weeks' gestation) and without perinatal complications. Exclusion criteria were: a) history of focal traumatic brain injury, b) cerebral palsy or neurological diagnosis (including seizure and motor disorders), c) presence of global mental disabilities, and d) antecedents of intraventricular hemorrhages or hypoxic episodes. The preterm group was matched by age to 21 healthy normal gestation controls. All subjects attended normal school. Characteristics of the groups are summarized in Table 1. The study was approved by the ethics committee of the University of Barcelona and by a national research committee. All subjects or their family gave written informed consent prior to participation in the study. This investigation forms part of a larger project on the long-term consequences of prematurity underway at the University of Barcelona (3, 7-8).

Magnetic resonance imaging and spectroscopic acquisition

Data were obtained on a 1.5 Tesla whole body MR scanner (General Electric Signa System; Milwaukee, WI). A set of high-resolution T1-weighted images was acquired with fast spoiled gradient recalled acquisitions with the following parameters: repetition time / echo time (TE) = 12/5.2 ms, inversion time 300 ms 1 nex, field of view = 24x24 cm, and 256x256 matrix. The whole-brain data were acquired in an axial plane yielding contiguous slices with slice thickness of 1 mm.

^{1}H-MRS was obtained with a standard quadrature head coil. Proton spectra were obtained from a single 8 cm^3 voxel (2cmx2cmx2cm) in a coronal plane. In all subjects the voxel was placed on the T1-weighted image in the left medial temporal region, including mainly the hippocampus in all cases. The mid brain cistern was used as the landmark to locate the voxel in all subjects, although in some cases the voxel had to be moved to avoid bone and cerebral spinal fluid (CSF) contamination. This procedure was applied in the same manner in all subjects and care was taken to ensure standard placement. Spectra were acquired with the use of a double-spin echo point-resolved spectroscopy sequence with repetition time =1500 milliseconds and TE=35 milliseconds, data points 2048, number of scans 128, scan time 3 min 48 sec, with automatic shimming and water suppression. Point-resolved spectroscopy sequence is a good method for a no-loss sequence if false signals can be

Table 1. Characteristics of the sample

	Prematures ***Mean $\pm$ SD***	***Controls*** ***Mean $\pm$ SD***
Age (years)	14.8 $\pm$ 1.3	14.8 $\pm$ 1.6
Gender (Boys / Girls)	8 / 13	11 / 10
Gestational age (weeks)	30.0 $\pm$ 2.0	40.0 $\pm$ 1.8
Gestational weight (grams)	1,375 $\pm$ 348.1	3,453 $\pm$ 473.8

minimized at short TE (9). With short TE, metabolites with both short and long T2 relaxation times are observed. Apart from NAA, Cho, and Cr, additional signals can be observed of compounds such as glutamate/glutamine and myo -inositol (Ins) (10-11).

Absolute metabolite quantification: the Linear Combination Model-Fitting (LCModel)

For the quantification of the absolute concentrations in mmol/kg wet weight, we used the user-independent frequency domain-fitting program LCModel (12-13) version 6.1-4A, applying an eddy current correction (14) and using internal water signal reference to calculate absolute metabolite concentrations.

Certain metabolites are quite difficult to resolve from others (13) and the sum of the concentrations of metabolites with similar spectra is much more accurate than the individual concentrations. So, apart from the individual analysis of the Cr and the Ins compounds, we studied the sum of three pairs: NAA+N-acetyl-aspartylglutamate, referred to as 'total NA'; glycerophospho-choline+phosphocholine, referred to as 'total Ch'; and glutamate+glutamine, referred to as 'total Glx'. We only considered the metabolite values when the coefficient of variation for the LCModel concentrations was below 20%, indicating that these metabolites could be reliably estimated (13). For the total Glx, 3 subjects (2 preterm and 1 control) had a metabolic concentration with a SD >20%. So, in these cases the values for Glx were discarded. Figure 1 shows an example of the spectra analyzed with the LCModel.

Stereological volumetric analysis

To provide complementary volumetric analysis, we performed stereological measurements of the left hippocampus. Measures were carried out in a Linux workstation, using ANALYZE 6.0 software. First, images were interpolated from 1.5 mm slices to 0.5 mm slices in order to achieve better resolution; a voxel size of 0.5 mm^3 was generated. Afterwards, images were aligned in accordance with the anterior commissure-posterior commissure orientation. The hippocampal volume was measured using a 7 x 7 mm^2 rigid grid with random starting position and angle of deviation from horizontal. The grid was superimposed on every third coronal slice. The coronal orientation was chosen in order to work with slices oriented perpendicular to the long axis of the hippocampus, a procedure reported to improve measurements (15). The interslice increment and grid size chosen yielded a coefficient of error in the 0.01-0.03 range. The *orthogonals* tool provided by ANALYZE 6.0 makes it possible to view every grid point in three orthogonal views simultaneously,

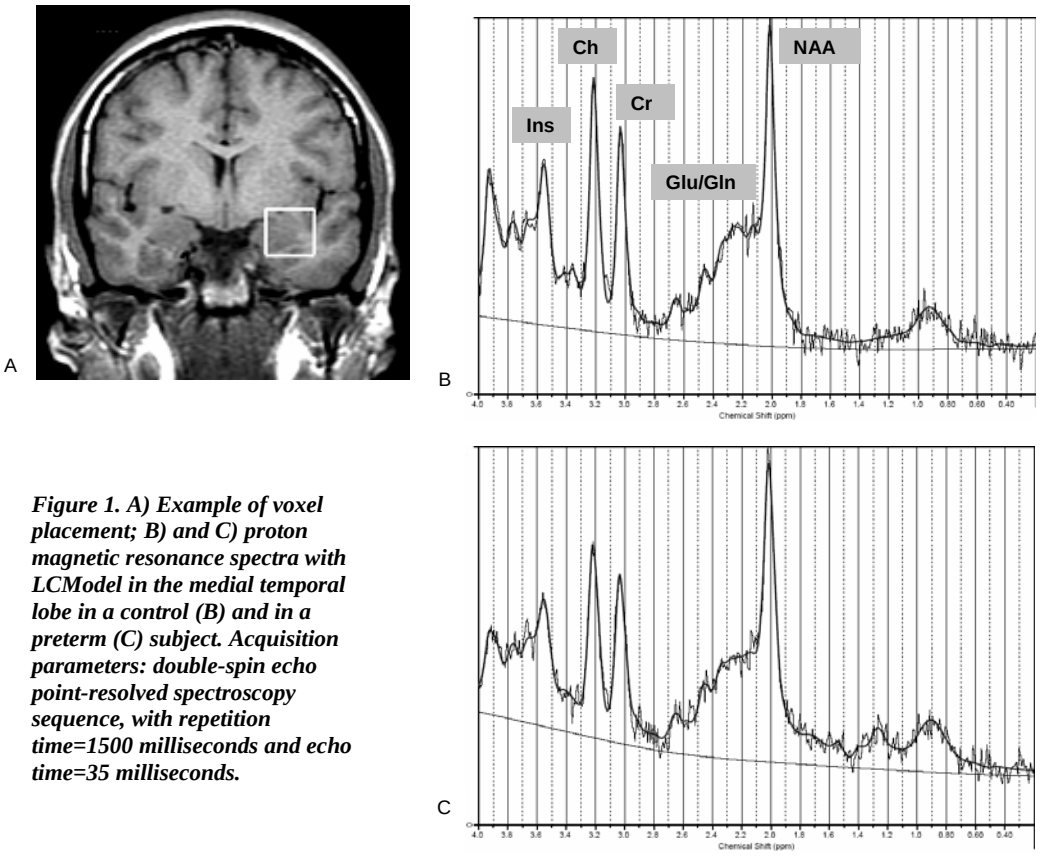

Figure 1. A) Example of voxel placement; B) and C) proton magnetic resonance spectra with LCModel in the medial temporal lobe in a control (B) and in a preterm (C) subject. Acquisition parameters: double-spin echo point-resolved spectroscopy sequence, with repetition time=1500 milliseconds and echo time=35 milliseconds.

which helps to decide whether a point is contained by the measured structure or not. With stereology we can exclude adjacent parahippocampal cortices (see Figure 2). We obtained direct values from the hippocampal volume in mm^3. All stereological measures were corrected by the intracranial volume (ICV)*100.

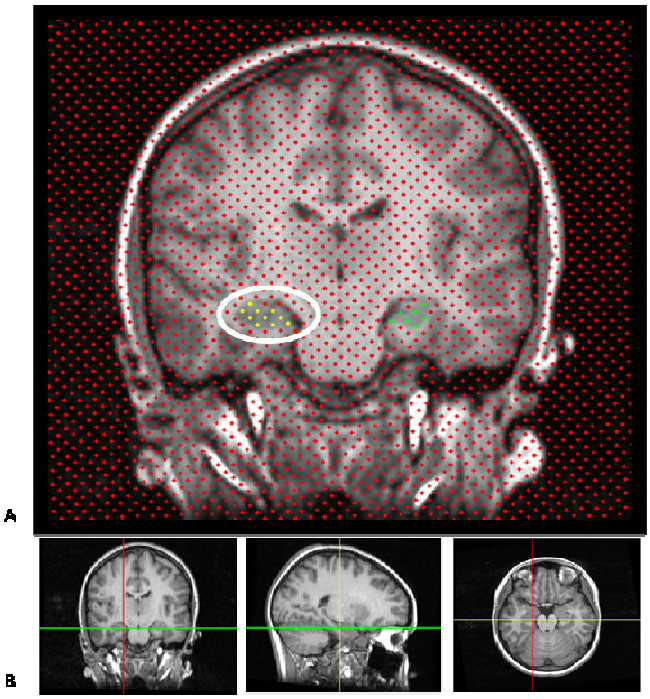

Figure 2. Illustrative stereological grid used for hippocampal measurements. Region Of Interest (ROI) is based on a point counting estimation. Only the points inside the structure are considered in the measurements. A) Circle showing hippocampal ROI. B) Orthogonal view option in stereology: coronal, sagittal and axial view of the same hippocampal point.

Statistical analysis

Metabolic and volumetric data were compared by the *Student's t test* or by the non-parametric *Mann-Whitney U test* in the variables that did not fulfill the requirement for parametrical statistical tests.

We performed correlation analyses to relate the gestational age (GA) and the metabolic and volumetric data for the whole sample (by Spearman, because the GA for the whole sample did not fulfill the normality conditions), and separately for patients and controls (by Pearson).

Finally, we performed a correlation analysis (Pearson) between the metabolic values and the hippocampal volume to evaluate the relationship between the reductions in hippocampal volume and changes in the brain metabolites in this region. All statistical analyses were carried out with the SPSS 12.0 version.

Results

Magnetic resonance imaging

T1 visual inspection carried out by two expert neuroradiologists (N.B., J.M.M.) revealed no brain MRI abnormalities in the whole sample. No visual differences were observed in cerebral development in either group.

Spectroscopy

^{1}H-MRS metabolite concentrations examined are shown in Table 2. The comparison between groups demonstrated that preterm subjects had significantly lower Ins, Cr and total NA levels than the control group. In contrast, no differences were found in the total Ch or total Glx.

Table 2. Metabolite concentrations (mmol/kg wet weight)

	Preterms ***Mean ± SD***	***Controls*** ***Mean ± SD***	***Statistics***
Metabolite			
Creatine	4.0 ± 0.6	4.5 ± 0.5	t = -3.46 (0.001)
Total Ch (Glycerophosphocholine+ Phosphocholine)	1.4 ± 0.3	1.5± 0.2	*U* = 193 (0.489)
Total NA (N-acetyl-aspartate+ N-acetyl-aspartylglutamate)	5.3 ± 0.8	6.3 ± 0.7	t = -4.09 (<0.0001)
Myo-inositol	4.3 ± 1.0	5.0 ± 0.8	t = -2.47 (0.018)
Total Glx (Glutamate+ Glutamine)*	10.2 ± 1.4	10.5 ± 1.1	*U* = 159 (0.396)

**N= 19 preterm vs 20 controls*

Hippocampal Stereology
We estimated the left hippocampal volume in premature and control groups, finding a significant volume loss in the premature group (volumes prior to standardization) compared to controls (t = - 5.807; p < 0.0001; preterm mean: 2,355.5 mm^3 ± 292.4; control mean: 2,848.1 mm^3 ± 256.2). After standardization of volumes by ICV, the hippocampal volume reduction remained statistically significant (t = - 4.074; p < 0.0001).

Correlation results
Correlations analyses between GA and the metabolic and volumetric data showed a significant positive correlation in the whole sample (N=42) between GA and Cr, total NA, Ins, and the volume of hippocampus (see Table 3 and Figure 3). In the preterm group, we also observed significant positive correlations between GA and Cr and total NA (see Table 3). No other correlations were observed either in the premature group and or in controls.

Table 3. Significant correlations between gestational age and metabolic and volumetric values

Whole sample	
	Rho Spearman (p)
Metabolites	
Creatine	0.46 (0.002)
Total NA (N-acetyl-aspartate+N-acetyl-aspartylglutamate)	0.51 (<0.0001)
Myo-inositol	0.46 (0.002)
Volumetric data	
Hippocampal volume (volume prior to standardization)	0.64 (<0.0001)
Hippocampal volume corrected by the Intracranial Volume*100	0.37 (0.018)
Preterm sample	
	Pearson (p)
Metabolites	
Creatine	0.54 (0.012)
Total NA (N-acetyl-aspartate+ N-acetyl-aspartylglutamate)	0.59 (0.005)

The study of the relationship between the volumetric data and the metabolic values revealed a significant positive correlation in the whole sample between total NA and hippocampal volume (both with volume prior to standardization and with the hippocampal volume corrected by the ICV): that is, the greater the volume of hippocampus, the higher the level of total NA (direct values: r = 0.53, p < 0.0001; values corrected by ICV: r = 0.34, p = 0.031). Moreover, we also found a relationship between Cr and hippocampal volume in direct values (r = 0.50, p = 0.001). For illustrative purposes, the Figure 4 shows the relationship between Cr and total NA and hippocampal volume (in direct values without standardization).

Discussion

In this ^{1}H-MRS study we found differences in absolute metabolite concentrations in the medial temporal lobe region between a group of adolescents with history of prematurity and a control group. Total NA, Cr, and Ins were lower in the preterm sample.

Metabolite concentrations of N-acetyl-containing compounds (NA) are thought to be localized mainly in mature neurons (16). NAA is a marker for either neuronal loss or cellular dysfunction (17). NAA values are decreased in several types of cerebral diseases (18-19), and depletion in total NA observed in this study can be interpreted as a reflection of neuronal dysfunction or significant neuronal damage (20). No previous studies in adolescent samples with preterm birth and without perinatal complications have been performed, but studies in child samples with hypoxic-ischemic insults show similar results (5, 21). One study reported no differences in NAA values in a group of preterms compared to controls (4), but the present study did not find a normalization of total NA values at adolescence in the preterm group.

Cr is a marker of cell energy in neurons and glial cells (22). It has been suggested that low Cr concentrations in an immature brain may increase susceptibility to brain damage (i.e., because of hypoxic episodes) (23). Cr depletion reported in this investigation agreed with other studies that demonstrated depletion of Cr in schizophrenic patients with hippocampal reductions (24) and in degenerative brain lesions (25). In addition, the loss of Cr may be secondary to a

Figure 3. Plots showing metabolic values and the volume of the hippocampus against gestational age. The lines indicate a linear fit to the data, with upper and lower confidence levels (95%).

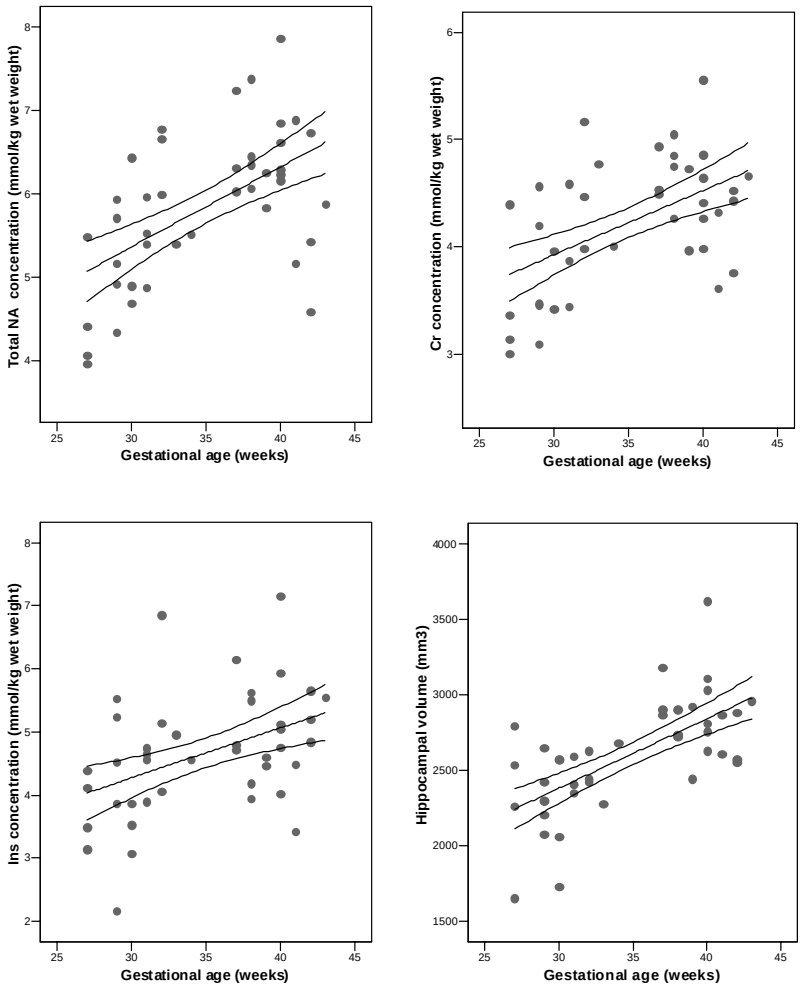

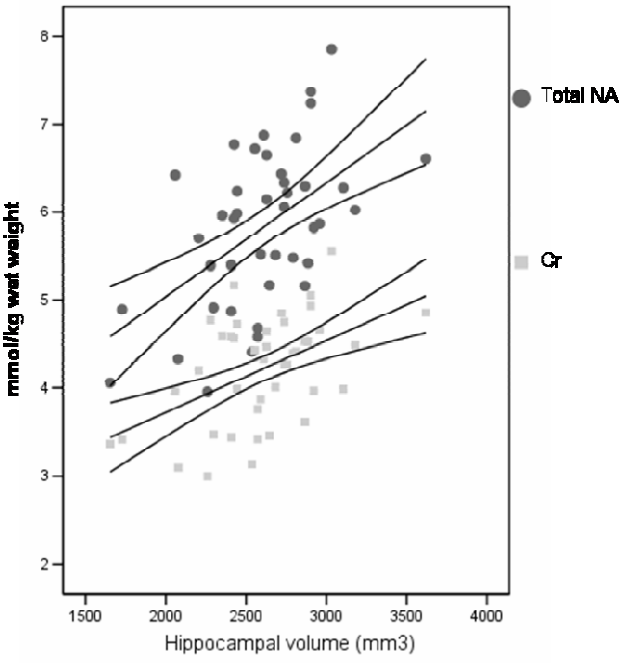

Figure 4. Plot showing metabolic values against the volume of the hippocampus. The lines indicate a linear fit to the data, with upper and lower confidence levels (95%).

reduction in glial proliferation because glial cells have higher Cr levels than neurons. A previous study (26) showed that Cr levels in the developing brain reached adolescent values at 4 months. In our case, the preterm sample did not reach control values at adolescence.

Ins was also significantly reduced in the preterm sample. This metabolite is a marker for glia (27) and is crucial for cell survival. A recent investigation in a depressive sample corroborated abnormal reductions in Ins as a response to glial loss (28). Previous studies in preterm infants showed a decrease in the Ins/Cho ratio at 41 weeks of postmenstrual age

compared to 32 weeks (29-30). The difference observed between groups may demonstrate a differentiation in the brain osmoregulation. Moreover, present results provide more evidence of the regional gray matter atrophy in the temporal region reported in preterm samples (1). Because of possible technical questions, Ins results in ^{1}H-MRS studies should be considered with caution. Although short TE can be used to minimize signal loss due to transverse relaxation, the signals may overlap with those of macromolecules (31-32).

In contrast to our results, a previous investigation found no differences in brain metabolites between a group of preterm infants and a control sample (33). Most subjects in the present sample (19 out of 21) have a GA $\leq$ 32 weeks, whereas they studied infants with a GA > 32 weeks. Moreover, they assessed the centrum semiovale for white matter, the thalamus, and the occipital gray matter.

Our preterm sample also showed a reduction in hippocampal volume compared to controls. This is in agreement with previous volumetric studies in adolescent samples (2-3). In the whole sample, the hippocampal volume reductions, like those of the three brain metabolites in the adolescents with preterm birth (total NA, Cr and Ins), varied significantly with GA. In the preterm group, total NA and Cr also showed a significant correlation. Our correlational results are partially in agreement with those of the previously mentioned study in preterm infants (33), who found positive relationships in infants between GA and total NA and Cr in different brain regions, but a negative correlation between GA and Ins. A very recent study about brain maturation in utero corroborates an increase of NAA and Ins decreases (34). This discrepancy is difficult to explain. As above, these authors studied brain metabolites in early development, whereas we analyzed brain metabolites at adolescence.

In addition, our finding of a correlation between total NA, Cr, and hippocampal volume suggests that extensive ^{1}H-MRS studies can be used to complementary determine certain degree of hippocampal injury. Other studies of temporal pathologies have demonstrated a relationship between metabolic and hippocampal volumetric data (35-36). Preterms are normally exposed to stressful situations, such as unpredictable handling and repeated painful procedures, and perinatal stress has been shown to change NAA concentrations (37). Moreover, Cr has been reported to protect immature brain from perinatal injury (38) and the fact we showed a relationship between Cr concentration levels and hippocampal atrophy (the loss of Cr, the reduction in the hippocampal volume) favors this hypothesis.

These differences in neuronal integrity between preterms and controls may be due to several factors, including a possible differential regional vulnerability and disruptions of brain maturation. The midtemporal region has been previously reported to be especially vulnerable in preterm children compared to controls (39).

Some technical aspects should be mentioned. Other studies have primarily used single-voxel approaches to obtain magnetic resonance spectra from the temporal lobe and recent investigations support the use of single-voxel spectroscopy for reproducibility in studies of the medial temporal lobe metabolic characteristics (41-42). Only the left medial temporal brain region was evaluated in this study, but it is possible that other regions, such as the thalamus (3, 8), may present biochemical evidence of neuronal damage at adolescence. Regarding the left-right question, an *in vivo* short echo time ^{1}H-MRS study demonstrated that there were no significant left-right differences in the study of the temporal lobe metabolites in normal subjects (42).

It should be mentioned a possible limitation of the present study related to the volume of tissue within the voxel placed in the temporal lobe. Some recent spectroscopic approaches consider the interest of assessing possible CSF contamination and the fraction of gray and white matter contained within the voxel to provide CSF correction and tissue type information for the analysis of proton MRI data (43-44). The present study did not, however, analyze the tissue content of the voxel. Though in all cases the voxel was located in a way to cover mainly the hippocampus, one must be cautious in the interpretation of the results, because possible mixtures in gray-white matter across the subjects may contribute to the metabolic differences. In addition, we cannot avoid the fact that the hippocampal volume reduction may suppose the increase of CSF in the voxel. In this sense, metabolic results cannot be considered specifically as a direct measure of regional hippocampal volume reduction, being more appropriate to talk in terms of metabolic medial temporal lobe abnormalities, rather than hippocampal metabolic differences.

This study is the first to demonstrate neurochemical alterations in adolescents with history of prematurity without perinatal complications and normal standard MRI. Consistent with previous spectroscopy findings in newborns, we found decreased total NA and Cr levels in the medial temporal lobe. These changes may provide support for either neuronal dysfunction or neuronal loss and may be associated with reduced neuronal integrity. In addition, these ^{1}H-MRS findings were related to the hippocampal volume.

This study suggests a possible abnormality in brain metabolism in the medial temporal lobe in preterm that persists until adolescence.

References

1. Kesler SR, Ment LR, Vohr B, Pajot SK, Schneider KC, Katz KH, Ebbitt TB, Duncan CC, Makuch RW, Reiss AL 2004 Volumetric analysis of regional cerebral development in preterm children. Pediatr Neurol 31:318-325

2. Nosarti C, Al-Asady MH, Frangou S, Stewart AL, Rifkin L, Murray RM 2002 Adolescents who were born very preterm have decreased brain volumes. Brain 125:1616-1623

3. Gimenez M, Junque C, Narberhaus A, Caldu X, Salgado-Pineda P, Bargallo N, Segarra D, Botet F 2004 Hippocampal gray matter reduction associates with memory deficits in adolescents with history of prematurity. Neuroimage 23:869-877

4. Huppi PS, Schuknecht B, Boesch C, Bossi E, Felblinger J, Fusch C, Herschkowitz N 1996 Structural and Neurobehavioral Delay in Postnatal Brain Development of Preterm Infants. Pedriatr Res 39:895-901

5. Penrice J, Cady EB, Lorek A, Wylezinska M, Amess PN, Aldridge RF, Stewart A, Wyatt JS, Reynolds EO 1996 Proton magnetic resonance spectroscopy of the brain in normal preterm and term infants, and early changes after perinatal hypoxia-ischemia. Pediatr Res 40:6-14

6. Isaacs EB, Lucas A, Chong WK, Wood SJ, Johnson CL, Marshall C, Vargha-Khadem F, Gadian DG 2000 Hippocampal Volume and Everyday Memory in Children of Very Low Birth Weight. Pediatr Res 47:713-720

7. Gimenez M, Junque C, Vendrell, P, Caldu X, Narberhaus A, Bargallo N, Falcon C, Botet F, Mercader JM 2005 Hippocampal functional magnetic resonance imaging during a face-name learning task in adolescents with antecedents of prematurity. NeuroImage 25:561-569

8. Gimenez M, Junque C, Narberhaus A, Botet F, Bargallo N, Mercader JM 2006 Correlations of thalamic reductions with verbal fluency impairment in prematures. Neuroreport 17:463-466

9. Hofmann L, Slotboom J, Jung B, Maloca P, Boesch C, Kreis R 2002 Quantitative 1H-magnetic resonance spectroscopy of human brain: Influence of composition and parameterization of the basis set in linear combination model-fitting. Magn Reson Med 48:440-453

10. Soher BJ, Young K, Govindaraju V, Maudsley AA 1998 Automated spectral analysis III: application to in vivo proton MR spectroscopy and spectroscopic imaging. Magn Reson Med 40:822-831

11. Zhong K, Ernst T 2004 Localized in vivo human 1H MRS at very short echo times. Magn Reson Med 52:898-901

12. Provencher SW 1993 Estimation of metabolite concentrations from localized in vivo proton NMR spectra. Magn Reson Med 30:672-679

13. Provencher SW 2001 Automatic quantitation of localized in vivo 1H spectra with LCModel. NMR Biomed 14:260-264

14. Klose U 1990 In vivo proton spectroscopy in presence of eddy currents. Magn Reson Med 14:26-30

15. Sheline YI, Wang PW, Gado MH, Csernansky JG, Vannier MW 1996 Hippocampal atrophy in recurrent major depression. Proc Natl Acad Sci 93:3908-3913

16. Urenjak J, Williams SR, Gadian DG, Noble M 1992 Specific expression of N-acetylaspartate in neurons, oligodendrocyte-type-2 astrocyte progenitors, and immature oligodendrocytes in vitro. J Neurochem 59:55-61

17. Demougeot C, Garnier P, Mossiat C, Bertrand N, Giroud M, Beley A, Marie C 2001 N-Acetylaspartate, a marker of both cellular dysfunction and neuronal loss: its relevance to studies of acute brain injury. J Neurochem 77:408-415

18. Bertolino A, Weinberger DR 1999 Proton magnetic resonance spectroscopy in schizophrenia. Euro J Radiol 30:132-141

19. Farchione TR, Moore GJ, Rosenberg DR 2002 Proton magnetic resonance spectroscopic imaging in pediatric major depression. Biol Psychiat 52:86-92

20. Block W, Träber F, Flacke S, Jessen F, Pohl C, Schild H 2002 In-vivo proton MR-spectroscopy of the human brain: Assessment of N-acetylaspartate (NAA) reduction as a marker for neurodegeneration. Amino Acids 23:317-323

21. Barkovich AJ, Baranski K, Vigneron D, Partridge JC, Hallam DK, Hajnal BL, Ferriero DM 1999 Proton

MR spectroscopy for the evaluation of brain injury in asphyxiated, term neonates. Am J Neuroradiol 20:1399-1405

22. Wyss M, Kaddurah-Daouk R 2000 Creatine and creatinine metabolism. Physiol Rev 80:1107–1213

23. Holtzman D, Togliatti A, Khait I, Jensen F 1998 Creatine increases survival and suppresses seizures in the hypoxic immature rat. Pediatr Res 44:410-414

24. Maier M, Ron MA, Barker GJ, Tofts PS 1995 Proton magnetic resonance spectroscopy: an in vivo method of estimating hippocampal neuronal depletion in schizophrenia. Psychol Med 25:1201-1209

25. Chang L, Ernst T, Tornatore C, Aronow H, Melchor R, Walot I, Singer E, Cornford M 1997 Metabolite abnormalities in progressive multifocal leukoencephalopathy by proton magnetic resonance spectroscopy. Neurology 48:836-845

26. Toft PB, Leth H, Lou HC, Pryds O, Henriksen O 1994 Metabolite concentrations in the developing brain estimated with proton MR spectroscopy. J Magn Reson Imaging 4:674-680

27. Griffin JL, Bollard M, Nicholson JK, Bhakoo K 2002 Spectral profiles of cultured neuronal and glial cells derived from HRMAS (1)HNMR spectroscopy. NMR Biomed 15:375–384

28. Coupland NJ, Ogilvie CJ, Hegadoren KM, Seres P, Hanstock CC, Allen PS 2005 Decreased prefrontal Myo-inositol in major depressive disorder. Biol Psychiatry 57:1526-1534

29. Kreis R, Ernst T, Ross BD 1993 Development of the human brain: in vivo quantification of metabolite and water content with proton magnetic resonance spectroscopy. Magn Reson Med 30:424-437

30. Roelants-van Rijn AM, van der Grond J, Stigter RH, de Vries LS, Groenendaal F 2004 Cerebral structure and metabolism and long-term outcome in small-for-gestational-age preterm neonates. Pediatr Res 56:285-290

31. Behar KL, Rothman DL, Spencer DD, Petroff OA 1994 Analysis of macromolecule resonances in ^{1}H-NMR spectra of human brain. Magn Reson Med 32:294–302

32. Hofmann L, Slotboom J, Boesch C, Kreis R 2001 Characterization of the macromolecule baseline in localized (1)H-MR spectra of human brain. Magn Reson Med 46:855–863

33. Kreis R, Hofmann L, Kuhlmann B, Boesch C, Bossi E, Huppi PS 2002 Brain metabolite composition during early human brain development as measured by quantitative in vivo 1H magnetic resonance spectroscopy. Magn Reson Med 48:949-958

34. Girard N, Fogliarini C, Viola A, Confort-Gouny S, Fur YL, Viout P, Chapon F, Levrier O, Cozzone P 2006 MRS of normal and impaired fetal brain development. Eur J Radiol 57:217-225

35. Sawrie SM, Martin RC, Knowlton R, Faugth E, Gilliam F, Kuzniecky R 2001 Relationships among hippocampal volumetry, proton magnetic resonance spectroscopy, and verbal memory in temporal lobe epilepsy. Epilepsia 42:1403-1407

36. Schuff N, Amend DL, Knowlton R, Norman D, Fein G, Weiner MW 1999 Age-related metabolite changes and volume loss in the hippocampus by magnetic resonance spectroscopy and imaging. Neurobiol Aging 20:279-285

37. Poland RE, Cloak C, Lutchmansingh PJ, McCracken JT, Chang L, Ernst T 1999 Brain N-acetyl aspartate concentrations measured by H MRS are reduced in adult male rats subjected to perinatal stress: preliminary observations and hypothetical implications for neurodevelopmental disorders. J Psychiatr Res 33:41-51

38. Berger R, Middelanis J, Vaihinger HM, Mies G, Wilken B, Jensen A 2004 Creatine protects the immature brain from hypoxic-ischemic injury. J Soc Gynecol Investig 11:9-15

39. Peterson BS, Vohr B, Staib LH, Cannistraci CJ, Dolberg A, Schneider KC, Katz KH, Westerveld M, Sparrow S, Anderson AW, Duncan CC, Makuch RW, Gore JC, Ment LR 2000 Regional brain volume abnormalities and long-term cognitive outcome in preterm infants. J Am Med Assoc 284:1939-1947

40. Traber F, Block W, Freymann N, Gur O, Kucinski T, Hammen T, Ende G, Pilatus U, Hampel H, Schild HH, Heun R, Jessen F 2006 A multicenter reproducibility study of single-voxel (1)H-MRS of the medial temporal lobe. Eur Radiol 17:1-8

41. Hammen T, Stadlbauer A, Tomandl B, Ganslandt O, Pauli E, Huk W, Neundorfer B, Stefan H 2005 Short TE single-voxel 1H-MR spectroscopy of hippocampal structures in healthy adults at 1.5 Tesla--how reproducible are the results? NMR Biomed 18:195-201

42. McLean MA, Woermann FG, Simister RJ, Barker

GJ, Duncan JS 2001 In vivo short echo time 1H-magnetic resonance spectroscopic imaging (MRSI) of the temporal lobes. Neuroimage 14:501-509

43. Bonekamp D, Horska A, Jacobs MA, Arslanoglu A, Barker PB 2005 Fast method for brain image segmentation: application to proton magnetic resonance spectroscopic imaging. Magn Reson Med 54:1268-1272

44. Jakary A, Vinogradov S, Feiwell R, Deicken RF 2005 N-acetylaspartate reductions in the mediodorsal and anterior thalamus in men with schizophrenia verified by tissue volume corrected proton MRSI. Schizophr Res 76:173-185

ELSEVIER

NeuroImage

www.elsevier.com/locate/ynimg
NeuroImage 25 (2005) 561–569

Hippocampal functional magnetic resonance imaging during a face–name learning task in adolescents with antecedents of prematurity

Mónica Giménez,[a,b] Carme Junqué,[a,b,*] Pere Vendrell,[a,b] Xavier Caldú,[a,b] Ana Narberhaus,[a] Núria Bargalló,[c] Carles Falcón,[d] Francesc Botet,[b,e] and Josep Maria Mercader[b,c]

[a]*Department of Psychiatry and Clinical Psychobiology, Faculty of Medicine, University of Barcelona, Spain*
[b]*Institut d'Investigacions Biomèdiques August Pi i Sunyer (IDIBAPS), Hospital Clínic, Faculty of Medicine, University of Barcelona, Spain*
[c]*Neuroradiology Section, Radiology Department, Centre de Diagnòstic per la Imatge (CDI), Hospital Clínic, Faculty of Medicine, University of Barcelona, Spain*
[d]*Functional Magnetic Resonance Unit-Hospital Clínic, Serveis de Suport a la Recerca (SSR-UB), Biophysics and Bioengineering Unit, Physiological Sciences Department, Faculty of Medicine, University of Barcelona, Spain*
[e]*Pediatrics Section, Department of Obstetrics and Gynecology, Pediatrics, Radiology and Physics Medicine, Hospital Clínic, Faculty of Medicine, University of Barcelona, Spain*

Received 9 July 2004; revised 8 September 2004; accepted 28 October 2004
Available online 27 January 2005

Functional magnetic resonance imaging (fMRI) was used to map hippocampal activation during a declarative memory task in a sample of 14 adolescents with antecedents of prematurity (AP). The sample with AP was matched by age, sex and handedness with 14 full-term controls with no history of neurological or psychiatric illness. The target task consisted in learning 16 novel face–name pairs, and the control task involved the examination of two repeated face–name pairs. Stereological methods were also used to quantify hippocampal volumes. In both groups, we observed increased activation in the learning condition compared to the control task in the right fusiform gyrus and the left inferior occipital gyrus, but only premature subjects activated the hippocampus. Group comparison of the activation versus control conditions showed that prematures had greater activity in the right hippocampus than controls during the encoding of the word–face association. Volumetric analyses showed a significant left hippocampal volume loss in adolescents with AP. In addition, we found a significant positive correlation in the premature group between right hippocampal activation and face–name recognition. Functional MRI data also correlated with structural MRI data: right hippocampal activation correlated positively with right hippocampal volume. Our findings are consistent with previous studies of brain plasticity after focal lesions. Left hippocampal tissue loss may be related to an increase in contralateral brain activity, probably reflecting a compensatory mechanism. Our data also suggest that this plasticity is not enough to achieve normal performance.

Keywords: Encoding memory task; Hippocampus; Brain activation; Neuroimaging; Preterm

Introduction

Prematurity has been associated with an increased risk of brain injury. Magnetic resonance volumetric studies have reported decreased hippocampal size in children and adolescents with history of very preterm delivery compared to subjects of similar age (Giménez et al., 2004; Isaacs et al., 2000; Nosarti et al., 2002; Peterson et al., 2000), and neuropsychological studies showed long-term memory deficits in these subjects (Briscoe and Gathercole, 2001).

Functional magnetic resonance imaging (fMRI) has been used to investigate regional brain plasticity after cerebral lesions, mainly in order to study motor functions. Cao et al. (1994) mapped the sensorimotor area of the hand in hemiparetic adolescents and young adults who had suffered unilateral brain damage in the perinatal period. Unlike normal subjects, who exhibit cortical activation primarily contralateral to voluntary finger movements, the intact hemispheres of hemiparetic patients were activated equally by contralateral and ipsilateral finger movements. Similar results were obtained in children with right congenital hemiplegia of cortical origin. The paretic finger

* Corresponding author. Department of Psychiatry and Clinical Psychobiology, Faculty of Medicine, University of Barcelona, C/Casanova, 143, 08036 Barcelona, Spain. Fax: +34 93 403 52 94.
E-mail address: cjunque@ub.edu (C. Junqué).
Available online on ScienceDirect (www.sciencedirect.com).

1053-8119/$ - see front matter © 2004 Elsevier Inc. All rights reserved.
doi:10.1016/j.neuroimage.2004.10.046

movements activated both hemispheres, with a strong ipsilateral predominance favoring the undamaged hemisphere. These activation patterns indicate an adaptive reorganization of the cortical motor networks with a prominent involvement of the undamaged hemisphere in the control of finger movements (Vandermeeren et al., 2003). In patients with multiple sclerosis, an increase in cortical activity was also observed in the ipsilateral, motor premotor and inferior parietal lobule during passive and active flexion–extension movement tasks (Reddy et al., 2002).

The plasticity of hippocampal damage has been investigated in samples of epileptic patients. Dupont et al. (2000) reported that patients exhibited consistent and extensive left prefrontal activations in all memory tasks (encoding and retrieval). These cortical activations were not observed in the control group, suggesting that verbal memory tasks did not involve the same functional patterns in patients and healthy controls. In a sample of nonamnesic patients with left medial temporal lobe pathology, Richardson et al. (2003) demonstrated a reorganization or reallocation of encoding processes to the right medial temporal lobe. In that study, subjects with left hippocampal sclerosis showed greater activity in the right hippocampus and parahippocampal gyrus than normal subjects during successful encoding of words. Moreover, subjects with left amygdalar sclerosis showed greater activity in the right amygdala than subjects without amygdalar sclerosis for successfully encoded emotional words.

In a previous study of premature subjects, Rushe et al. (2001) reported that subjects with radiological evidence of thinning of the corpus callosum showed abnormal lateralization of language function. During a task involving phonological processing (rhyming words) adults with AP showed significantly lower activation than controls in the left hemisphere, including the peristriate cortex and the cerebellum, and in the right parietal association area. Increased activation was seen in the right precentral gyrus and the right supplementary motor area. Peterson et al. (2002) found that preterm children have abnormal patterns of processing semantic contents. For semantic processing, the premature children engaged pathways that normal children used for phonological processing.

Maguire et al. (2001) studied the effects of bilateral hippocampal damage on fMRI regional activation in a single case with *antecedents of prematurity* (AP) and evidence of perinatal hypoxia. In spite of a bilateral hippocampal volume loss of 50%, retrieval in this subject was associated with an increased hippocampal activation compared to controls. In contrast, O'Carroll et al. (2004) reported that six preterm subjects showed bilateral reduced activation in the hippocampus, compared with five controls.

Hippocampal and medial temporal lobe activation during encoding and retrieval processes of declarative memory tasks has been widely and consistently reported in normal subjects using fMRI techniques (Dolan and Fletcher, 1999; Rombouts et al., 1997, 2001; Stark and Squire, 2000a,b; Stern et al., 1996; Sperling et al., 2001; Strange et al., 2002; Yonelinas et al., 2001). Learning the names of new faces is an essential aspect of everyday human memory and is known to engage the hippocampus (Small et al., 2001; Sperling et al., 2001; Zeineh et al., 2003).

The aim of this study was to investigate whether hippocampal damage alters the pattern of activation during declarative learning. We hypothesized that hippocampal reductions may result in increased activation.

Methods

Subjects

Subjects with AP were selected from the Archives of the Pediatric Service at the Hospital Clinic in Barcelona. The sample was selected from the population born between 1982 and 1994. During this period, the Service registered 857 cases of prematurity. Inclusion criteria for the present study were: (a) ages between 12 and 18, (b) gestational age equal or inferior to 34 weeks, and (c) no complications apart from intracranial hemorrhage, anoxia, or fetal suffering. After analyzing the database from the Service, two hundred and five subjects fulfilled these criteria. From these 205 subjects, 24 clinical histories were not available at the hospital archives (they were moved to other centers). Updated address or telephone number were not available in 16 cases. We tried to localize subjects by phone and mail and 68 subjects were not found. Two cases had died. Nineteen cases declined to enroll (or parents refused permission). Exclusion criteria applied in the screening were: (a) presence of mental deficiency (Full Intelligence Quotient [FIQ] inferior to 70), (b) history of focal traumatic brain injury, cerebral palsy or neurological diagnosis, (c) motor or sensitive impairment that precluded neuropsychological assessment, (d) metal orthodontic prosthesis, and (e) claustrophobia or anxiety levels high enough to require sedation. From the 76 subjects, eight cases presented a FIQ < 70; 12 cases did not meet the inclusion criteria because of the presence of neurological handicaps, three presented high anxiety levels, and 18 subjects were excluded because of metal orthodontic prosthesis. A group of 35 patients agreed to participate in the neuropsychological study and a group of 22 also agreed to undergo the MR study.

The final sample of subjects with AP comprised 14 adolescents (6 girls and 8 boys), chosen from an initial sample of 22 subjects. Eight subjects were excluded because they did not learn 25% of the 16 novel stimuli shown in the fMRI memory task. Gestational age ranged from 25 to 34 weeks (Mean = 29.43, SD = 2.98). All 14 subjects had perinatal complications (anoxia, periventricular hemorrhage or fetal suffering). Two subjects had low weight for their gestational age. The age at the time of neuropsychological and neuroimaging study ranged from 12 to 18 years (Mean = 14.71, SD = 2.05). Two subjects were left-handed. The mean of Full Intelligence Quotient of subjects with AP was 87.57 (SD = 13.36). All subjects currently receive normal schooling. A normal control group was matched to premature subjects by age, sex, handedness, and sociocultural status. The mean FIQ of the control sample was 115.79 (SD = 8.46). The study was approved by the ethics committee of the University of Barcelona and all the subjects or their family gave written informed consent prior to participating in the study.

Memory assessment

fMRI protocol: a declarative memory task

The task used during the fMRI acquisition consisted of a modified version of Sperling et al. design (2001), with four blocks of the control task alternating with four blocks of the memory activation task (see Fig. 1).

The memory activation task consisted of four 48-s presentation blocks of 16 novel face–name pairs (8 males and 8 females). Each pair was presented once per block. Each pair was presented for 2000 ms on a dark background followed by a blank screen period

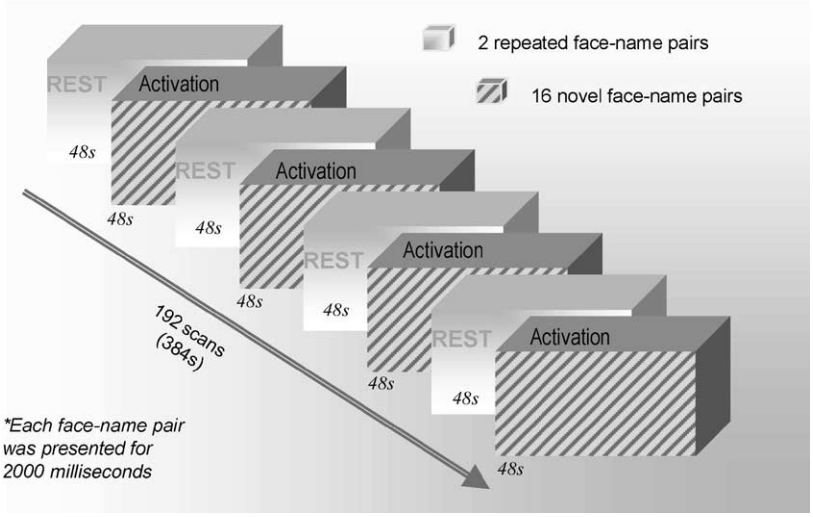

Fig. 1. Block design fMRI paradigm. The diagram shows two conditions (memory activation and control), each lasting 192 s. The memory activation condition consisted of 4 blocks showing 16 pairs of name–faces (8 males, 8 females) in each block. The four blocks in the control condition presented two previously learned face–name pairs (1 male and 1 female) in each block.

of 1000 ms. Subjects were instructed to learn the name of each face for later recall.

Like the memory activation task, the control task consisted of four 48 s presentation blocks of two repeated face–name pairs (1 male and 1 female). Both stimuli were memorized by the subjects before fMRI acquisition. During fMRI acquisition, four blocks of these two pairs were presented; in each block, the male appeared eight times, followed by the female image which also appeared eight times. Each pair appeared on the screen for 2000 ms on a dark background, followed by a blank screen period of 1000 ms.

The faces were digital color photographs of individuals between 18 and 25 years old. All the stimuli were back-projected (by a Sanyo Multimedia Prox-III) onto a screen which subjects viewed through a mirror located on the scanner's head coil. Stimuli were generated in a Hewlett Packard computer by the Presentation 0.76 version program (Neurobehavioral Systems, USA). Participants were administered a checked memory test to assess the number of the 16 novel face–name pairs remembered just after fMRI acquisition. Two measures were obtained: free recall (by asking the name of each face directly without any clues) and recognition (by providing the 16 names on independent cards).

Neuropsychological memory tests

We assessed verbal and visual memory. For verbal memory, we selected a modified version of the Auditory Verbal Learning Test (RAVLT), a test with well-known sensitivity for declarative memory impairment (Lezak, 1995). We obtained three measures: (a) learning: sum of the recall of the five 15-word list trials, (b) percentage of memory loss: percentage of words lost after 20 min of interference. The formula used to create this variable was "presentation of trial 6-presentation of trial 5/sum of words recalled across the five presentations * 100", and c) recognition: obtained by asking the respondent to indicate which words from a set of 30 were from the 15-word list and which were not. More details of this test are described in Mitrushina et al. (1999). We evaluated visual memory with the Rey's Complex Figure Test (Rey, 1980). The test was administered in two parts. Firstly, subjects were asked to copy the model on a blank piece of paper. After a 3-min interval, subjects were asked to draw the figure from memory, also to scale, on a blank sheet of paper. Participants were not forewarned of the retention requirement. We recorded the raw scores for visual retention.

MRI acquisition and processing

The MRI protocol was carried out with a 1.5-T MR unit (Signa-Lx, General Electric, Milwaukee, WI) using the blood–oxygen level-dependent (BOLD) fMRI signal. During the study, subjects reclined in a supine position on the bed of the scanner and a RF quadrature head coil was placed over their head. Care was taken to minimize the effect of movement by instructing subjects to remain still, and foam padding was placed around their head. After sagittal scout sequence, the functional images were acquired using a gradient echo single-shot ecoplanar imaging sequence (EPI): TR(repetition time) / TE(echo time) = 2000/35 ms; FOV (field of view) = 24 × 24 cm, 64 × 64 pixel matrix; flip angle = 90°; slice thickness 5 mm; gap 1.5 mm and 20 axial slices per scan. During fMRI, subjects performed the learning task series described above. Sequences of alternating periods of active (48 s) and control (48 s) conditions were repeated for a total of 6 min and 24 s, resulting in 192 volumes of 20 slices each. The series began with a control condition. Following fMRI scans, a set of high-resolution T1-weighted images was acquired with an axial inversion recovery three-dimensional fast spoiled gradient recalled acquisitions for anatomic localization (IRFSPGR) (TR/TE = 12/5.2; TI 300 1 nex; FOV = 24 × 24 cm; 256 × 25 6 pixel matrix).

The original MR images were registered in DICOM format (one two-dimensional file per slice). MRI data were processed in a SUN workstation provided by Solaris 8. The two-dimensional DICOM files were organized into volumetric three-dimensional files of each brain by means of the ANALYZE 5.0 software (Biomedical Resource, Mayo Foundation, Rochester, MN). The images were saved in ANALYZE 7.5 format, compatible with the SPM2 software (Statistical Parametric Mapping, Wellcome Department of Cognitive Neurology, University College London, UK).

The image pretreatment was: (1) movement correction, (2) normalization by non-linear functions; and (3) smoothing by the

use of an 8-mm full width at half-maximum (FWHM) isotropic Gaussian kernel.

Volumetric analysis by stereology

To obtain volumetric data for the hippocampus, we measured this structure using stereological procedures. Measures were carried out in a SUN workstation provided by Solaris 8, using ANALYZE 5.0 software. First, images were interpolated from 1.5 mm slices to 0.5 mm slices in order to achieve better resolution, generating a voxel size of 0.5 mm^3. Images were then aligned according to the anterior commissure-posterior commissure orientation. A 7×7 mm^2 rigid grid was used to measure the hippocampal volume with both random starting position and angle of deviation from horizontal plane. The grid was superimposed on every third coronal slice. The coronal orientation was chosen in order to work with slices perpendicular to the long axis of the hippocampus, a procedure reported to improve measures (Sheline et al., 1996). The interslice increment and grid size chosen yielded a coefficient error in the 0.01–0.03 range. The orthogonals tool provided by ANALYZE 5.0 allows simultaneous observation of every grid point in three orthogonal views, which helps to decide whether or not a point is contained in the structure measured. With stereology, we can exclude adjacent parahippocampal cortices. We obtained direct values from hippocampal volumes, and these values were corrected by the intracranial volume obtained by using the segmentation procedures from the SPM2, running in Matlab 6.5 (MathWorks, Natick, MA). The spatially normalized images were automatically partitioned into separate images representing probability maps for gray matter, white matter, and cerebrospinal fluid, using the combined pixel-intensity and the a priori knowledge approach integrated in SPM2.

Statistical analysis

fMRI data

All image processings were done using SPM2 (Wellcome Department of Imaging Neuroscience), running in Matlab 6.5 (MathWorks). The fMRI protocol was carried out as follows. In order to remove head movement effects, the 192 scans were first realigned. The realignment of subsequent slices in a time series used a least-square approach to the first scan as a reference. The criteria for rejecting data due to motion were movements in any axis superior to 1 mm and/or 1°. Following realignment, we resized the anatomical and functional images to avoid the interslice gap (volumes of 20 slices) in Z axis (1.3). Next, a single investigator determined the anterior commissure manually and reoriented all the images according to the anterior–posterior commissure line. This process was first done in the anatomical and functional images at the same time and later in the structural T1 image. All images were co-registered using mutual information defaults, and then transformed into a standardized coordinate system in two stages. First, the spatial transformation of structural T1 image was estimated, and then the parameter set produced by the above normalization procedure was applied to the fMRI EPI and anatomical images. For these steps, a trilinear interpolation was used. The normalized images were then smoothed with an isotropic Gaussian kernel (full width at half-maximum, FWHM = 8 mm) to create a local weighted average of the surrounding pixels. Smoothing in space enhances the signal-to-noise ratio of the data (Turner et al., 1998), increasing the validity of the subsequent statistical test and compensating for possibly inexact normalization (Ashburner and Friston, 1999).

Functional analyses were conducted to detect differences in cerebral activation between groups. The processed functional images were analyzed using a SPM2 group comparison.

We performed two one-sided comparisons of the "memory activation task > control task" contrast: a) prematures > controls; b) prematures < controls. First, focusing on our main objective, we checked for possible hippocampal differences, using the WFU-Pickatlas toolbox software for SPM, version 1.02 (Joseph Maldjian, Functional MRI Laboratory, Wake Forest University School of Medicine). We created an ROI including the hippocampus proper and both sides of the parahippocampal area. We used the convention that the ROI group comparison results should survive at FWE-corrected voxel P value ($P < 0.05$). Only clusters longer than 20 contiguous voxels were considered in the analysis. Moreover, after the ROI analysis, a whole-brain analysis was conducted to test for possible differences in other cerebral regions. For the whole-brain analysis, we only considered voxels at uncorrected $P < 0.0001$ and clusters of more than 20 contiguous voxels. The anatomical location of the cerebral activated areas was determined by the Talairach global maxima coordinates. Finally, for each group, we performed a separate analysis of the "memory activation task > control task" contrast.

We performed a "simple regression" SPM2 analysis to establish the relationship between hippocampal activations (by ROI analysis) and various neuropsychological memory measures separately for patients and controls. Only results at voxel uncorrected $P < 0.0001$ were considered.

Memory data

Memory performance in the two groups was compared by the non-parametric Mann–Whitney U test, given that the variables did not fulfill the requirement for parametrical statistical tests. All statistical analyses were carried out with the SPSS 11.0 version.

Volumetric data

Statistical analysis of data to compare the hippocampal volumes of the groups was carried out using Student's t test (SPSS 11.0 version). As a complementary analysis, we calculated the degree of deviation of the premature hippocampal volumes from the control mean.

We performed a "simple regression" SPM2 analysis to correlate hippocampal activation (by ROI analysis) with hippocampal volume, separately for patients and controls. Only results at voxel uncorrected $P < 0.0001$ were considered.

Finally, we performed ANCOVA analyses in the "prematures versus controls" group comparison to evaluate differences in hippocampal activation controlling for hippocampal volumes.

Results

Memory performance

Results of the memory fMRI task showed significant differences between groups in free recall and recognition (see Table 1).

Table 1
Memory performance

	Premature group Mean ± SD	Control group Mean ± SD	Mann–Whitney U (P value)
Face–name free recall	7.64 ± 3.82	11.64 ± 4.24	U = 43.00 (P = 0.011)
Face–name recognition	10.64 ± 4.31	13.93 ± 3.71	U = 50.50 (P = 0.027)
Learning (RAVLT)	49.50 ± 7.43	55.21 ± 7.84	U = 55.00 (P = 0.050)
% of memory loss (RAVLT)	14.15 ± 5.41	12.61 ± 3.63	U = 77.50 (P = 0.352)
Recognition (RAVLT)	13.64 ± 1.65	14.71 ± 0.73	U = 59.50 (P = 0.077)
Visual Retention (Rey's complex figure)	21.89 ± 5.70	25.46 ± 4.92	U = 54.50 (P = 0.044)

RAVLT = Rey's auditory verbal learning test.

Premature subjects recalled an average of 48% of the novel face–name pairs in the free recall test, whereas controls had a recall average of 73%.

RAVLT results indicated a significant difference between groups in learning. We also observed a trend towards statistical significance in recognition (P = 0.077). Visual memory, assessed by the Rey Complex Figure, showed a statistical significant difference between groups (Table 1).

fMRI results

Hippocampal ROI analysis showed a significant activation of this region in the premature sample compared to controls at the corrected level for multiple comparisons (cluster level FWE corrected P = 0.002; cluster size = 56 voxels) (see Fig. 2). The activated region comprised the right medial hippocampus (Z value = 4.60; Talairach global maxima coordinates: 36, −26, −10; voxel P value at these coordinates: FWE corrected P = 0.002). Fig. 3 shows the relative activation for each subject with respect to the mean of the entire sample (prematures and controls).

A complementary whole brain analysis comparison was conducted to evaluate possible differences in other cerebral regions. The group comparison (prematures > controls) of the values obtained from the "memory activation task > control task"

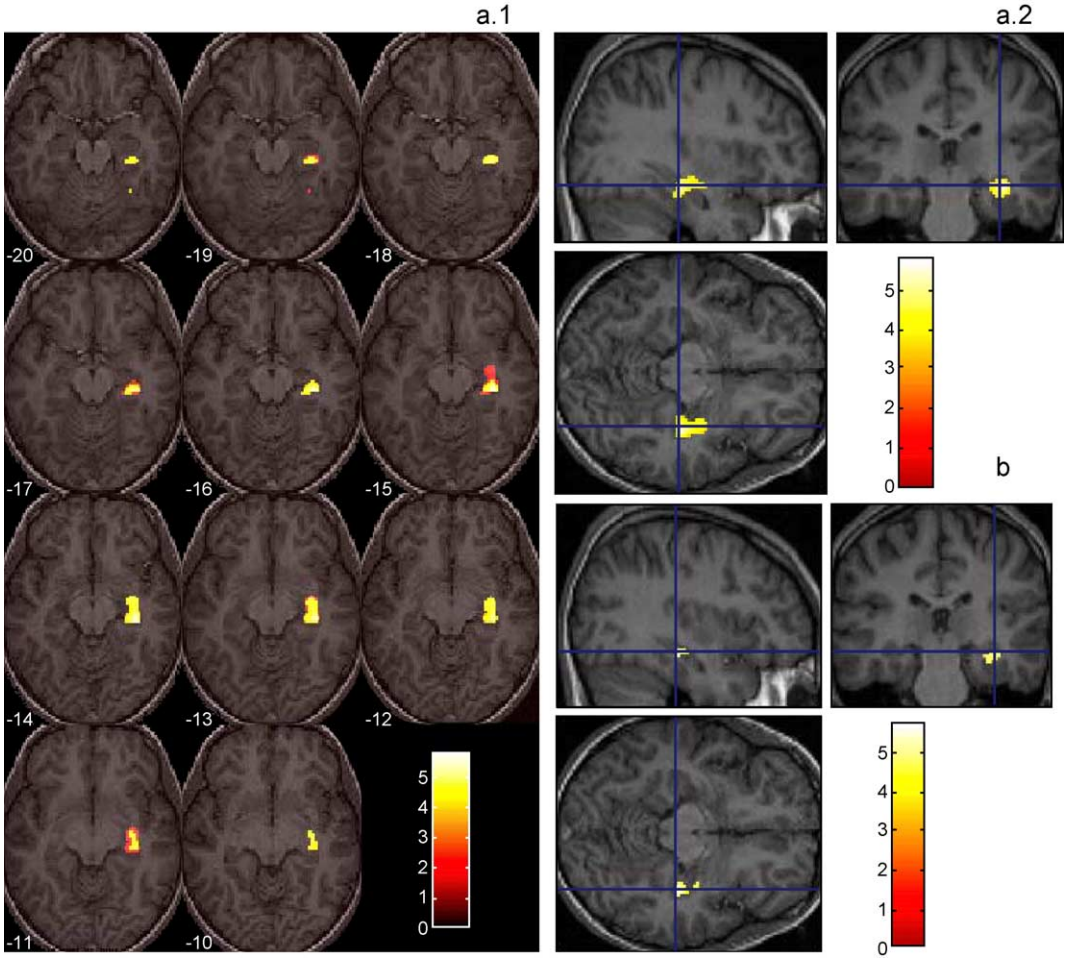

Fig. 2. Functional MRI results. Right hippocampal differences between prematures and controls (prematures > controls) in activation (memory activation task > control task contrast). Statistical Parametric Maps with left as left, according to neurological convention. Axial (a.1) and coronal (a.2) views showing the results of the whole brain analysis (voxel level P < 0.0001; clusters > 20 contiguous voxels) (b) hippocampal ROI analysis (FWE-corrected voxel level P < 0.05; clusters > 20 contiguous voxels). The global and ROI results are overlapped in a T1 standard control brain.

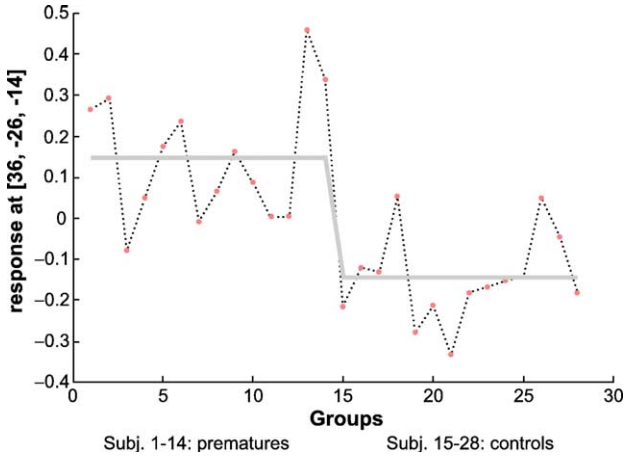

Fig. 3. Individual values relative to the mean (point 0) of all subjects (prematures and controls). *Y* axis: grade of activity in a right hippocampal voxel. *X* axis: premature group from 1 to 14; control group from 15 to 28.

contrast showed greater activation of the right hippocampus in prematures than in controls. The voxels significant at $P < 0.0001$ created a cluster of 213 voxels in the right hippocampus (cluster level $P = 0.009$; Z value = 4.60; Talairach global maxima coordinates: 36, −26, −10; voxel P value at these coordinates < 0.0001). (see Fig. 2 and Table 2). No other cerebral regions presented different levels of activation in the group comparison. With the reverse analysis (prematures < controls), no regions showed greater activity in controls than in prematures.

To further investigate the origin of the significant increase in right hippocampal activity in prematures, we performed a separate analysis of brain activation for both groups in the "memory activation task > control task" contrast. The results are summarized in Table 2: both prematures and controls activated the right fusiform gyrus and the left inferior occipital gyrus, but only the prematures activated the hippocampus.

fMRI and memory correlation analysis

Hippocampal ROI analysis revealed a positive significant correlation between fMRI recognition and right hippocampal activation at voxel level (Z value = 3.65; Talairach global maxima coordinates: 25, −14, −14; voxel level $P < 0.0001$) for the premature group. No other correlations were observed for memory measures in either group.

Volumetric data

Eight premature subjects had a 2 SD decrease in the left hippocampus compared with the control mean. Four other subjects had a decrease in the left hippocampus of 1 SD below the control mean. For the right hippocampus, the decrease of 2 SD was seen in only three subjects. Six premature subjects had a right hippocampus decrease of less than 1 SD (see Table 3).

The comparison of means showed that both left and right hippocampus direct values were significantly reduced in the premature sample (left: $P < 0.0001$; right: $P = 0.001$). After correcting direct values for intracranial volume, only the left hippocampal volume decrease remained statistically significant ($P = 0.013$) (see Table 4).

fMRI and volumetric correlation analysis

We found a positive significant correlation between right hippocampal activation and right hippocampal volume at voxel level (Z value = 3.63; Talairach global maxima coordinates: 26, −22, −18; voxel level $P < 0.0001$) for the premature group (see Fig. 4). No other correlations were observed for stereological volumes in either group.

Since hippocampal atrophy may be responsible for the increase in hippocampal activity in prematures compared to controls, we performed two analyses of covariance (ANCOVA). After removing the effects of right hippocampal volume, the comparison between prematures and controls showed that the statistical significance of hippocampal activation differences decreased (Z value = 3.89;

Table 2
Activation foci in prematures and controls in the contrast "activation memory task > control memory task" and comparison between both groups (prematures > controls)

	Region	*x*	*y*	*z*	*Z*	Cluster size
Controls	Right fusiform gyrus (BA 19)	44	−73	−13	4.27	73
	Left inferior occipital gyrus (BA 18)	−34	−88	−7	4.16	143
		−36	−85	1	4.08	
	Left lingual gyrus (BA 18)	−22	−90	−14	3.33	
	Left middle frontal gyrus (BA 8)	−44	13	25	3.78	72
	Left middle frontal gyrus (BA 6)	−46	6	33	3.33	70
		−46	12	38	3.32	
Prematures	Right fusiform gyrus (BA 37)	38	−52	−21	4.93	470
		42	−61	−9	4.19	
	Right fusiform gyrus (BA 19)	39	−74	−1	3.97	
	Right hippocampus	40	−28	−12	4.44	100
	Left inferior occipital gyrus (BA 18)	−30	−84	−3	3.76	36
	Left fusiform gyrus (BA 37)	−34	−46	−21	3.68	35
	Left fusiform gyrus (BA 19)	−34	−63	−15	3.55	73
		−34	−72	−10	3.35	
Prematures vs. Controls	Right hippocampus	36	−26	−10	4.60	213
		34	−12	−11	3.88	

Coordinates are according to the Talairach and Tournoux atlas.

Table 3
Standard deviations below the mean of controls for the premature sample (direct values)

Number of subject	Premature group					
	Left hippocampus			Right hippocampus		
	<1 SD	1 – 2 SD	>2 SD	<1 SD	1 – 2 SD	>2 SD
1			■		■	
2			■		■	
3			■		■	
4			■		■	
5			■	■		
6		■		■		
7		■		■		
8		■		■		
9			■			■
10			■			■
11			■			■
12		■			■	
13	■			■		
14	■			■		
% of subjects	14.28%	28.57%	57.14%	42.86%	35.71%	21.43%

Shaded box indicates the grade of deviation for each subject.

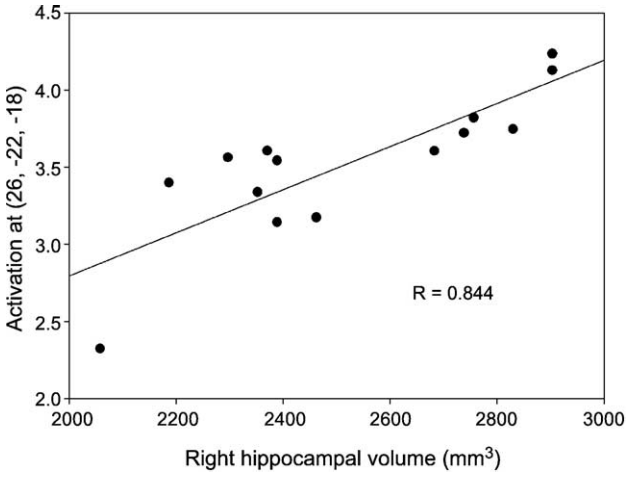

Fig. 4. Correlation between right hippocampal fMRI activation and hippocampal volume in premature subjects. These data correspond to the voxel with the highest value in the ROI correlation analysis.

Talairach global maxima coordinates: 34, −22, −12; voxel level $P < 0.0001$), and the cluster size (82 voxels) lost significance (cluster level $P = 0.091$). Similar effects were seen after removing the left hippocampal volume effect (Z value = 3.95; Talairach global maxima coordinates: 32, −22, −12; voxel level $P < 0.0001$), and the cluster size (57 voxels) showed a cluster level $P = 0.157$.

Discussion

In this fMRI study, we found a significant increase in right hippocampus activation in the premature group compared to controls during an encoding memory task. The left hippocampus in these subjects also presented a significant degree of atrophy, and significant positive correlations were found between right hippocampal activation and two variables—right hippocampal volume and face–name pair recognition—only in the premature group.

The increased activation in the right hippocampus in the premature sample during the encoding face–name memory task may reflect a contralateral reorganization of the impaired left hippocampus. These results are in agreement with previous studies on plasticity conducted with brain-damaged samples. Although our subjects had a bilateral hippocampal reduction, the left hemisphere was more impaired than the right, and so we obtained a higher activation for the more preserved hemisphere. Increased activation of the non-damaged hemisphere has previously been described for motor functions in patients with congenital hemiplegia (Cao et al., 1994; Vandermeeren et al., 2003). Moreover, our results agree with the findings of hippocampal structural and functional studies carried out in epileptic patients. Richardson et al. (2003) reported a functional reorganization of the hippocampus during a memory encoding task in patients with left hippocampal sclerosis: subjects with left hippocampal damage showed greater activity in the right hippocampus and parahippocampal gyrus during successful encoding of words than did controls.

Our results are not in agreement with recent data reported by O'Carroll et al. (2004). In that study, six prematures showed less hippocampal activation than controls. Unfortunately, we cannot compare the structural deficits because the abstract of that study does not provide such information, but in O'Carroll et al. sample, memory performance was similar to that of controls, indicating indirectly that the hippocampus was preserved. Another possible origin of the discrepancy may be the asymmetry in the hippocampal damage of our sample.

Analyzing separately the activation of each group during the memory activation task in contrast to the control task, we found that both groups showed a cortical activation increase in the right

Table 4
Volumetric differences between groups for the hippocampal measurements

	Premature group Mean ± SD	Control group Mean ± SD	Student's t test (P value)
Direct values			
Left hippocampus	2480.62 ± 278.86	3025.31 ± 246.17	$t = -5.479$ ($P < 0.0001$)
Right hippocampus	2522.63 ± 274.86	2971.50 ± 326.36	$t = -3.936$ ($P = 0.001$)
Corrected values by intracranial volume			
Left hippocampus	0.1684 ± 0.020	0.1894 ± 0.021	$t = -2.673$ ($P = 0.013$)
Right hippocampus	0.1713 ± 0.021	0.1857 ± 0.022	$t = -1.778$ ($P = 0.087$)

fusiform gyrus and the left inferior occipital gyrus. This is probably due to an increase in the activity of areas related to face perception and name reading. In addition, the controls activated the middle frontal gyrus while prematures did not. It may be that these additional frontal regions contribute to better memory performance; in this sense, Brodmann's area 8 has been found relevant for associative learning (Petrides et al., 1993).

Differential activation was also seen in the right hippocampus, which reached significance in prematures but not in controls. Indeed, this was the only region that remained statistically significant in the comparison between patients' and controls' activation patterns. The lack of hippocampal activation in the control group is difficult to explain. Using a face–name task, Sperling et al. (2001) showed strong hippocampal activation. However, in their design, there were 86 novel stimuli, whereas in our study, we had only 16 novel stimuli repeated four times. The lack of hippocampal activation in our study may also have been due to the small number of new stimuli or habituation over the successive repetitions. Using 17 words repeated four times, Dupont et al. (2000) found an activation of the hippocampus and of several cortical areas, but their baseline condition was the fixation of the letter A. In our study, the baseline condition and the target condition were quite similar, then the subtraction of both conditions necessarily should be small.

Like previous studies, we found a bilateral hippocampal reduction in prematures with left predominance (Giménez et al., 2004; Isaacs et al., 2000; Peterson et al., 2000). Since hippocampal reduction may be responsible for the increase of activation relative to controls, we performed an analysis of covariance. After removing the effects of hippocampal volumes in the group comparison, the cluster size of the activation in hippocampus was lower and lost statistical significance at cluster level. These results indicate that hippocampal atrophy plays a role in the differential activation pattern.

Despite the fact that premature subjects presented greater right hippocampal activation than controls, performance on the memory task was significantly poorer in the premature sample. This suggests that the right hemisphere's compensatory mechanism is not sufficient to obtain normal performance, and corroborates the learning deficits observed in different studies in premature samples (Anderson and Doyle, 2003; Isaacs et al., 2000).

We observed a positive correlation between fMRI right hippocampal activation and fMRI task recognition only in the premature group. The higher activation corresponded to better performance. The PET study of Alkire et al. (1998) observed that left hippocampal activity during encoding correlated with long-term free recall in a healthy adult sample. In our case, the correlation was between recognition and the contralateral side of the most atrophic hippocampus in the premature sample. Alkire et al. did not assess recognition. Moreover, our stimuli comprised both visual and verbal materials, whereas Alkire et al. examined only word learning. We obtained a positive correlation between the right hippocampal activation and right volumetric data in the premature sample. The study of Isaacs et al. (2000) reported verbal memory dysfunctions accompanied by bilateral hippocampal atrophy, but those authors did not find a brain–behavior correlation.

We should mention some methodological issues concerning the fMRI in our study. We cannot avoid the fact that the spatial normalization of pediatric brains was adapted to the SPM adult space. In fMRI studies, spatial normalization is an important tool for direct voxelwise comparison of data sets between subjects. This study uses an adult-derived template for spatial normalization of the adolescent brain. This condition is necessary to compare brains voxel by voxel. Some structural studies postulate that spatial normalization affects data. In the case of functional analysis, it has been shown that in voxelwise comparison images, functional differences are not significant when comparing adult and child brains, and that it is possible to use a common space and generate direct statistical comparisons between children and adults (Kang et al., 2003). So, in our case, the use of either an adult or a child template does not induce significant variability in the results. A second issue is the definition of the extent of activation. We used both the absolute number of activated voxels and the statistical significance threshold. The use of these restrictions allowed us to show specifically relevant activations related to the main finding of our study (the activation of the less damaged hippocampus in a significant cluster level), while suppressing artefact activations.

Despite the potential interest of our results regarding brain dysfunctions in subjects with antecedents of prematurity, the findings must be considered with caution because our sample is not representative of prematurity per se. All the premature subjects in this study suffered perinatal complications such as intraventricular hemorrhage, anoxia, or fetal suffering, and so the results are not generalizable to the premature population as a whole. It would be interesting to study premature subjects without these complications.

In summary, the present fMRI study provides evidence of contralateral compensatory activation mechanisms in the case of a volume decrease in left hippocampus in an encoding memory task. However, this reorganization does not seem to be sufficient to normalize neuropsychological outcomes in prematurity.

Acknowledgments

This study was supported by grants SAF2002-00836 (Ministerio de Ciencia y Tecnología), 2001SGR 00139 (Generalitat de Catalunya), a 2003F100191 (Generalitat de Catalunya) to X. Caldú, a research grant from the University of Barcelona to A. Narberhaus and the grant AP2002-0737 (Ministerio de Educación, Cultura y Deporte) to M. Giménez.

References

Alkire, M.T., Haier, R.J., Fallon, J.H., Cahill, L., 1998. Hippocampal, but not amygdala, activity at encoding correlates with long-term, free recall of non-emotional information. Proc. Natl. Acad. Sci. U. S. A. 95, 14506–14510.

Anderson, P., Doyle, L.W., 2003. Neurobehavioral outcomes of school-age children born extremely low birth weight or very preterm in the 1990s. J. Am. Med. Assoc. 289, 3264–3272.

Ashburner, J., Friston, K.J., 1999. Nonlinear spatial normalization using basis functions. Hum. Brain Mapp. 7, 254–266.

Briscoe, J., Gathercole, S.E., 2001. Everyday memory and cognitive ability in children born very prematurely. J. Child Psychol. Psychiatry 42, 749–754.

Cao, Y., Vikingstad, E.M., Huttenlocher, P.R., Towle, V.L., 1994. Functional magnetic resonance studies of the reorganization of the human hand sensorimotor area after unilateral brain injury in the perinatal period. Proc. Natl. Acad. Sci. U. S. A. 91, 9612–9616.

Dolan, R.J., Fletcher, P.C., 1999. Encoding and retrieval in human medial

temporal lobes: an empirical investigation using functional magnetic resonance imaging (fMRI). Hippocampus 9, 25–34.

Dupont, S., Van de Moortele, P.F., Samson, S., Hasboun, D., Poline, J.B., Adam, C., Lehéricy, S., Le Bihan, D., Samson, Y., Baulac, M., 2000. Episodic memory in left temporal lobe epilepsy: a functional MRI study. Brain 123, 1722–1732.

Giménez, M., Junqué, C., Narberhaus, A., Caldú, X., Salgado, P., Bargalló, N., Segarra, D., Botet, F., 2004. Hippocampal gray matter reduction associates with memory deficits in adolescents with history of prematurity. NeuroImage 23, 869–877.

Isaacs, E.B., Lucas, A., Chong, W.K., Wood, S.J., Johnson, C.L., Marshall, C., Vargha-Khadem, F., Gadian, D.G., 2000. Hippocampal volume and everyday memory in children of very low birth weight. Pediatr. Res. 47, 713–720.

Kang, H.C., Burgund, E.D., Lugar, H.M., Petersen, S.E., Schlaggar, B.L., 2003. Comparison of functional activation foci in children and adults using a common stereotactic space. NeuroImage 19, 16–28.

Lezak, M.D., 1995. Neuropsychological Assessment. Oxford Univ. Press, New York.

Maguire, E.A., Vargha-Khadem, F., Mishkin, M., 2001. The effects of bilateral hippocampal damage on fMRI regional activations and interactions during memory retrieval. Brain 124, 1156–1170.

Mitrushina, M.N., Boone, K.B., D'Elia, L.F., 1999. Handbook of Normative Data for Neuropsychological Assessment. Oxford Univ. Press, New York.

Nosarti, C., Al-Asady, M., Frangou, S., Stewart, A., Rifkin, L., Murray, R., 2002. Adolescents who were born very preterm have decreased brain volumes. Brain 125, 1616–1623.

O'Carroll, C., Nosarti, C., McGuire, P.K., Rifkin, L., Williams, S.C., Murray, R.M., 2004. Altered neuronal activation during processing of verbal episodic memory in preterm adolescents. Abstract of the 10th annual meeting of the organization for Human Brain Mapping, June 13–17, Budapest, Hungary.

Peterson, B.S., Vohr, B., Staib, L.H., Cannistraci, C.J., Dolberg, A., Schneider, K.C., Katz, K.H., Westerveld, M., Sparrow, S., Anderson, A.W., Duncan, C.C., Makuch, R.W., Gore, J.C., Ment, L.R., 2000. Regional brain volume abnormalities and long-term cognitive outcome in preterm infants. J. Am. Med. Assoc. 284, 1939–1947.

Peterson, B.S., Vohr, B., Jane, M., Whalen, D.H., Schneider, K.C., Katz, K.H., Zhang, H., Duncan, C.C., Makuch, R., Gore, J.C., Ment, L.R., 2002. A functional magnetic resonance imaging study of language processing and its cognitive correlates in prematurely born children. Pediatrics 110, 1153–1162.

Petrides, M., Alivisatos, B., Evans, A.C., Meyer, E., 1993. Dissociation of human mid-dorsolateral from posterior dorsolateral frontal cortex in memory processing. Proc. Natl. Acad. Sci. U. S. A. 90, 873–877.

Reddy, H., Narayanan, S., Woolrich, M., Mitsumori, T., Lapierre, Y., Arnold, D.L., Matthews, P.M., 2002. Functional brain reorganization for hand movement in patients with multiple sclerosis: defining distinct effects of injury and disability. Brain 125, 2646–2657.

Rey, A., 1980. Test de Copia de Una Figura Compleja: Manual. Tea, Barcelona.

Richardson, M.P., Strange, B.A., Duncan, J.S., Dolan, R.J., 2003. Preserved verbal memory function in left medial temporal pathology involves reorganisation of function to right medial temporal lobe. NeuroImage 20, S112–S119.

Rombouts, S.A.R.B., Barkhof, F., Witter, M.P., Machielsen, W.C.M., Scheltens, Ph., 2001. Anterior medial temporal lobe activation during attempted retrieval of encoded visuospatial scenes: an event-related fMRI study. NeuroImage 14, 67–76.

Rombouts, S.A.R.B., Machielsen, W.C.M., Witter, M.P., Barkhof, F., Lindeboom, J., Scheltens, P., 1997. Visual association encoding activates the medial temporal lobe: a functional magnetic resonance imaging study. Hippocampus 7, 594–601.

Rushe, T.M., Rifkin, L., Stewart, A.L., Townsend, J.P., Roth, S.C., Wyatt, J.S.W., Murria, R.M., 2001. Neuropsychological outcome at adolescence of very preterm birth and its relation to brain structure. Dev. Med. Child Neurol. 43, 226–233.

Sheline, Y.I., Wang, P.W., Gado, M.H., Csernansky, J.G., Vannier, M.W., 1996. Hippocampal atrophy in recurrent major depression. Proc. Natl. Acad. Sci. U. S. A. 93, 3908–3913.

Small, S.A., Nava, A.S., Perera, G.M., DeLaPaz, R., Mayeux, R., Stern, Y., 2001. Circuit mechanisms underlying memory encoding and retrieval in the long axis of the hippocampal formation. Nat. Neurosci. 4, 442–449.

Sperling, R.A., Bates, J.F., Cocchiarella, A.J., Schacter, D.L., Rosen, B.R., Albert, M.S., 2001. Encoding novel face–name associations: a functional MRI study. Hum. Brain Mapp. 14, 129–139.

Stark, C., Squire, L.R., 2000a. Functional Magnetic Resonance Imaging (fMRI) activity in the hippocampal region during recognition memory. J. Neurosci. 20, 7776–7778.

Stark, C., Squire, L.R., 2000b. fMRI activity in the medial temporal lobe during recognition memory as a function of study-test Interval. Hippocampus 10, 329–337.

Stern, C.E., Corkins, S., Gilberto González, R., Guimaraes, A.R., Baker, J.R., Jennings, P.J., Carr, C.A., Sugiura, R.M., Vendatham, V., Rosen, B.R., 1996. The hippocampal formation participates in novel picture encoding: evidence from functional magnetic resonance imaging. Proc. Natl. Acad. Sci. U. S. A. 93, 8660–8665.

Strange, B.A., Otten, L., Josephs, O., Rugg, M., Dolan, R., 2002. Dissociable human perirhinal, hippocampal, and parahippocampal roles during verbal encoding. J. Neurosci. 22, 523–528.

Turner, R., Howseman, A., Rees, G.E., Josephs, O., Friston, K., 1998. Functional magnetic resonance imaging of the human brain, data acquisition and analysis. Exp. Brain Res. 123, 5–12.

Vandermeeren, Y., Sébire, G., Grandin, C.B., Thonnard, J.L., Schlögel, X., De Volder, A.G., 2003. Functional reorganization of brain in children affected with congenital hemiplegia: fMRI study. NeuroImage 20, 289–301.

Yonelinas, A.P., Hopfinger, J.B., Buonocore, M.H., Kroll, N.E.A., Baynes, K., 2001. Hippocampal, parahippocampal and occipital–temporal contributions to associative and item recognition memory: an fMRI study. NeuroReport 12, 359–363.

Zeineh, M., Engel, S., Thompson, P., Bookheimer, S., 2003. Dynamics of the hippocampus during encoding and retrieval of face–name pairs. Science 299, 577–580.